Christian Rapp, BSc Bakk.phil.

# Whole-cell bioreductions of aromatic carbonyl substrates: Process intensification by cyclodextrins and water-immiscible co-solvents

## MASTER'S THESIS

to achieve the university degree of

Diplom-Ingenieur

Master's degree programme: Biotechnology

submitted to

**Graz University of Technology**

Supervisor

Ass.Prof. Dipl.-Ing. Dr.techn. Regina Kratzer

Institute of Biotechnology and Biochemical Engineering

Graz, May 2017

## AFFIDAVIT

I declare that I have authored this thesis independently, that I have not used other than the declared sources/resources, and that I have explicitly indicated all material which has been quoted either literally or by content from sources used. The text document uploaded to TUGRAZonline is identical to the present master’s thesis.

“What one generation finds ridiculous, the next accepts; and the third shudders when it looks back on what the first did.”

— **Peter Singer**

## Abstract

Effective reduction of *o*-chloroacetophenone to *(S)*-1-(2-chlorophenyl)ethanol by an *E. coli* whole-cell catalyst requires *in situ* substrate supply and product removal strategies. The most common method is the addition of water-immiscible organic solvents. However, cells and cell components that attach to the organic-aqueous interface lead to the formation of stable emulsions. Foci of the present thesis were put on microscopically analyzing emulsified reaction mixtures and on recovery of the product-containing, organic phase. Centrifugal separation of organic and aqueous phase was facilitated by adding primary or secondary alcohols. Addition of 1.5 v/v reaction volumes of isopropanol to reaction mixtures containing 20 % v/v hexane caused intermediate phases to completely collapse resulting in 90 % of isolated product. Further process intensification was achieved by deploying 2-hydroxypropyl-β-cyclodextrins (HBC) functioning as (1) enzyme stabilizing agents preventing protein aggregation, (2) aiding in cell permeabilization and (3) forming cyclodextrin/guest complexes enabling *in situ* substrate supply and product removal. The addition of 100 g/L HBC resulted in 98.1 % conversion of 1.9 M *o*-chloroacetophenone accompanied by an enantiomeric excess of > 99.9 %, a turnover number of 7.29 $g_{product}/g_{cdw}$ finally yielding 291 g/L of *(S)*-1-(2-chlorophenyl)ethanol. Moreover, an *E. coli* whole-cell catalyst was applied to establish a bioreductive dynamic kinetic resolution (DKR) of *rac*-2-phenylpropanal to *(S)*-2-phenylpropanol. Full conversion of 1 M substrate was accomplished reaching an enantiomeric excess > 93 % neither requiring cyclodextrins nor organic solvents. Increased $NAD^+$ concentrations enhanced the performance of biotransformations by overcoming mass transfer limitations in viscous reaction mixtures attributed to high catalyst and substrate loadings.

# Cyclodextrin-based process engineering in whole-cell biocatalysis

## Bioreduction of *o*-chloroacetophenone

Christian Rapp, Bernd Nidetzky*, Regina Kratzer*

Institute of Biotechnology and Biochemical Engineering, Graz University of Technology, Petersgasse 12/I, 8010 Graz/Austria

*Corresponding authors

RK: phone +43 316 873 8412
e-mail: regina.kratzer@tugraz.at

**Keywords:** Whole-cell biocatalysis, cyclodextrins, hydrophobic substrate, enzyme stabilization, *in situ* substrate supply and product removal

## Abstract

2-hydroxypropyl-β-cyclodextrins (HBC) proved to be a major driving force in intensifying the whole-cell bioreduction of *o*-chloroacetophenone. The cone-shaped structure of these cyclic oligosaccharides creates an inner hydrophobic cavity triggering the formation of cyclodextrin/guest complexes with aromatic compounds. This feature was exploited in several ways: (1) Establishment of an *in situ* substrate supply and product removal strategy (ISSS/ISPR), (2) enzyme stabilization by preventing aggregation (3) and permeabilization of cell membranes. The suitability of HBC for ISSS/ISPR was tested by performing phase solubility studies with *o*-chloroacetophenone (substrate) and *(S)*-1-(2-chlorophenyl)ethanol (product). The results obtained suggest 1:1 and 2:1 complexes for substrate and product with corresponding binding constants calculated to $K_{Substrate}$ = 532 $M^{-1}$ and $K_{Product}$ = 3 $M^{-2}$. Protein stabilizing effects by HBC were assayed by measuring enzyme activities of *Candida tenuis* xylose reductase (*Ct*XR) and *Candida boidinii* formate dehydrogenase (*Cb*FDH) in the presence of 50 % v/v hexane, hexanol or heptane. Addition of HBC counteracted enzyme precipitation at the organic/aqueous interface after 24 h of mixing thereby restoring and increasing volumetric or specific activities compared to mixtures not containing cyclodextrins. The extent of cell permeabilization was determined by whole-cell activity measurements resulting in the solubilization of insoluble enzyme fractions under certain conditions (75 mM HBC and 4 $g_{cell\ dry\ weight}$/L of *E. coli* whole-cell catalyst). Whole-cell biotransformations were intensified by increasing $NAD^+$ concentrations and changing *Ct*XR wild-type to *Ct*XR D51A. The addition of 100 g/L HBC (~ 62 mM) resulted in 98.1 % conversion of 1.9 M substrate accompanied by an enantiomeric excess of > 99.9 %, a turnover number of 7.29 $g_{product}/g_{cdw}$ finally yielding 291 g/L of *(S)*-1-(2-chlorophenyl)ethanol.

## 1. Introduction

The applicability of cyclodextrins in whole-cell biocatalysis has been reported in a modest number of studies so far[1,2,3,4,5]. Being characterized as cone-shaped cyclic oligosaccharides consisting of α-1,4 linked D-glucopyranose units, cyclodextrins are capable of forming non-rigid inclusion complexes with hydrophobic guest molecules thereby elevating their solubility in aqueous media[6,7]. Complexation itself is regarded as rapid chemical equilibrium enabling manipulation of complexation behaviour by altering the medium polarity. In recent years, the substantial drawback of natural β-cyclodextrins only displaying low water solubility was surmounted by synthesizing cyclodextrin-derivatives favouring gel-like structures over precipitation at high concentrations[8]. Among these derivatives frequently accompanied by high costs, 2-hydroxypropyl-β-cyclodextrins (HBC) not only offer the advantage of being affordable but also promoting improved interaction with aromatic guest molecules. Further benefits of cyclodextrins acting on cells arise from cell permeabilization[5,9] without crossing the membrane barrier therefore being considered less to non cell-toxic[10,11]. Moreover, by binding to hydrophobic amino acids thereby preventing protein coagulation[12], cyclodextrins also tend to stabilize formulated proteins and therefore enzymes under process conditions. Under the premise that deploying cyclodextrin-guest complexes in biocatalysis is limited by an increased viscosity of the reaction mixture concomitantly decreasing reaction rates, the establishment of cyclodextrin-shuttle systems might be preferred. An auxiliary water-immiscible organic phase functions as reservoir for substrate and product molecules in which cyclodextrins facilitate the transfer into the aqueous phase.[13] In this study, the whole-cell bioreduction of *o*-chloroacetophenone to *(S)*-1-(2-chlorophenyl)ethanol[14] applying *Candida tenuis* xylose reductase (*Ct*XR) sets the base in evaluating and optimizing reaction conditions under the influence of cyclodextrins. *(S)*-1-(2-chlorophenyl)ethanol constitutes a chiral

building block for L-clorprenaline[15], polo-like kinase 1 inhibitors, lysophosphatidic acid receptor agonists and cannabinoid receptor 2 agonists[16,17,18].

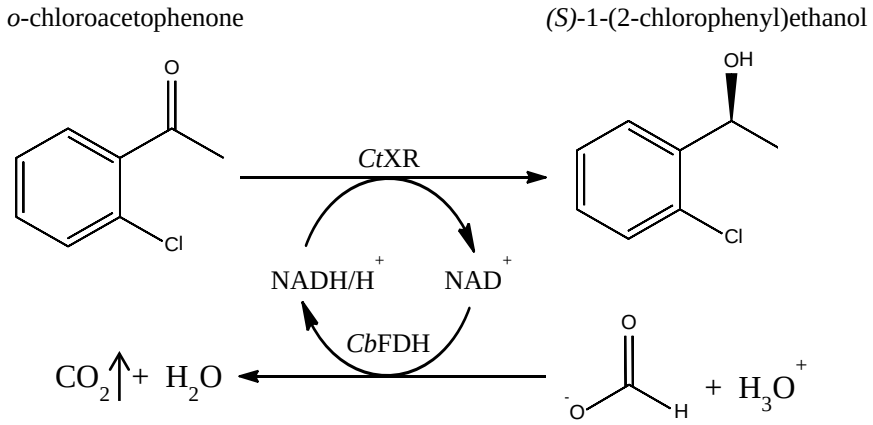


**Figure 1: Reaction scheme: Bioreduction of *o*-chloroacetophenone**. A recycling system was established by co-expressing *Candida boidinii* formate dehydrogenase (*Cb*FDH) and *Candida tenuis* xylose reductase (*Ct*XR).

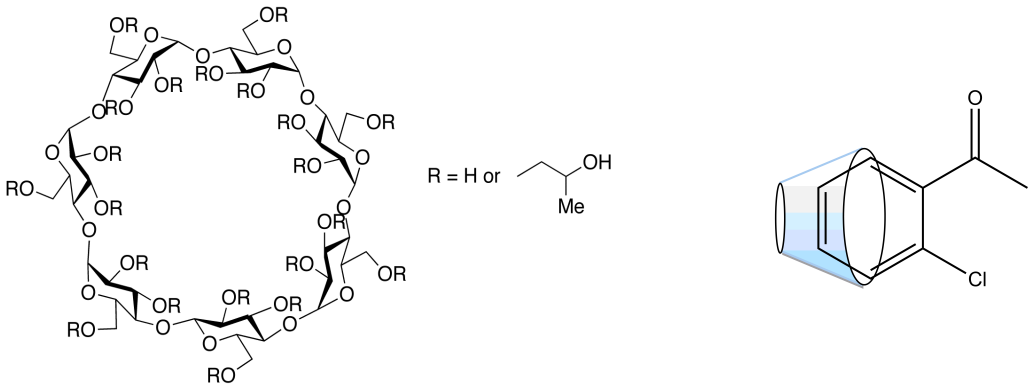


**Figure 2: Left image[19]: 2-Hydroxypropyl-β-cyclodextrin.** Inclusion complexes are preferably formed with aromatic compounds. Right image: Proposed complex formation with *o*-chloroacetophenone.

## 2. Materials and methods

### 2.1. Chemicals and strains

2-Hydroxypropyl-β-cyclodextrin (Carbosynth), *n*-hexane (Roth, ≥ 99 %), *n*-heptane (Roth, ≥ 99 %), 1-hexanol (Sigma-Aldrich, 98 %), sodium dodecyl sulfate (Serva), *o*-chloroacetophenone (Sigma-Aldrich), 1-(2-chlorophenyl)ethanol (Alfa Aesar), sodium chloride (Roth, ≥ 99.5 %), NADH-disodium salt (Roth, ≥ 98 %), NAD (Roth, ≈ 98 %), D-xylose (Roth, ≥ 98.5 %), sodium formate (Sigma, ≥ 99 %), B-PER© cell lysis buffer (Thermo Scientific), Pierce™ BCA Protein Assay Kit, peptone (Roth), yeast extract (Roth), polypropylene glycol (Aldrich), potassium hydroxide (Merck, p.a.), glucose (Sigma, Ultra), $K_2HPO_4$ (Roth, ≥ 99 %), $KH_2PO_4$ (Roth, ≥ 99 %), IPTG (Carbosynth), kanamycin (Roth), chloramphenicol (Fluka), ampicillin (Roth, ≥9 9.5 %), phosphorous acid (Roth, 85%), BSA (Roth), ethanol (AustrAlco, 99.9 %), 2-propanol (Roth, ≥ 99), acetonitrile (Roth, ≥ 99). Tubes (15 & 50 mL) were purchased at Sarstedt (Wr. Neudorf, Austria), 1.5 and 2 mL reaction tubes from Eppendorf (Wien, Austria).

Two *E. coli* strains co-expressing *Ct*XR variants and *Cb*FDH were used: *E. coli* Rosetta2 co-expressing *Ct*XR wild-type and *Cb*FDH reported by Mädje et al. 2012 (abbreviated XR_wild-type strain); *E. coli* Rosetta2 co-expressing *Ct*XR D51A and *Cb*FDH (abbreviated XR_D51A strain). The *Ct*XR D51A variant was previously described (Kratzer et al., 2006)[20]. Co-transformation of *E. coli* Rosetta2 with pET11a carrying the *Ct*XR D51A gene and pRSF-1b carrying the *Cb*FDH gene was accomplished by electroporation[21].

### 2.2. Cultivation

#### 2.2.1. Shake flask cultivation

*E. coli* strains were grown in 1000 mL baffled shake flasks containing 200 mL of LB media supplemented with ampicillin (115 mg/L), kanamycin (50 mg/L) and chloramphenicol

(34 mg/L). Cultures were shaken at 130 rpm and 37°C in a Certomat® BS-1 incubator (Sartorius) and cooled to 25 (XR_D51A strain) or 18°C (XR_wild-type strain) after reaching an optical density of 1.1 (± 10 %). Protein production was induced by adding 250 µM isopropyl-β-D-thiogalactopyranoside (IPTG) and further 115 mg/L ampicillin. After 20 h of cultivation, cells were harvested by centrifugation (Sorvall RC-5B). The biomass was frozen at -20°C, lyophilized (Christ α 1-4 lyophilizer from Braun Biotech International) and stored at -20°C.

### 2.2.2. Bioreactor cultivation (XR_wild-type strain)

The inoculum ($OD_{600}$ 8) was prepared using five 1000 mL baffled shaken flasks containing 150 mL of complex medium (Table 6, in the supporting information) supplemented with ampicillin (115 mg/L), kanamycin (50 mg/L), chloramphenicol (34 mg/L), thiamine (2 mg/mL) and glucose (5.5 g/L). The same medium was used for bioreactor cultivation only differing in glucose concentration (22 g/L). Large-scale fermentation was carried out in a Biostat CT 6.9-Liter BioReactor (B. Braun Biotech International GmbH, Melsungen, Germany) with a 5 L working volume, a vessel height to vessel diameter ratio of 2, provided with a twin 6-blade disc turbine stirrer (stirrer diameter to vessel diameter ratio of 0.4). Automated addition of 1 M $H_3PO_4$ and 2 M KOH ensured a pH of 7.0. $OD_{600}$ starting value was 0.5 and cultivation temperature was held constant at 37°C. Air supply was maintained at 45 % by an agitation and airflow cascade. The temperature was decreased to 18°C prior to induction with 1 mM IPTG at $OD_{600}$ 2.0. Additionally, ampicillin (115 mg/L) was added a second time after 24h. The biomass was harvested after 48 h of cultivation followed by centrifugation (Sorvall RC-5B), freezing at -20°C, lyophilisation (Christ α 1-4 lyophilizer from Braun Biotech International) and storage at -20°C.

2.3. Enzyme activity measurements

Xylose reductase and formate dehydrogenase activities were measured photometrically (Beckman Coulter DU 800® spectrophotometer) by observing oxidation or reduction rates of NADH/$NAD^+$ at 340 nm and 25°C for 5 min. 1 µmol of NADH formed or consumed per minute equals one unit of enzyme activity. B-PER© cell lysis reagent was used for soluble/insoluble protein extraction followed by adding up measured activities. Whole-cell activities of lyophilized cells were measured directly after 30 minutes of hydration at 25°C and 1400 rpm on a thermomixer (Eppendorf thermomixer comfort). For assaying *Ct*XR activity 700 mM (WT) or 1 M (D51A) D-xylose and 300 µM NADH were applied. *Cb*FDH-assay was carried out using 200 mM sodium formate and 2 mM $NAD^+$. Both assays were performed in 100 mM potassium phosphate buffer (pH 6.2) and started by adding NADH or $NAD^+$. Non-specific background oxidation/reduction was taken into account by measuring blank activities.

2.4. Determination of protein concentration

Protein concentrations were determined using Pierce™ BCA Protein Assay Kit from Thermo Fischer Scientific. Dilutions were made in potassium phosphate buffer (100 mM, pH 6.2).

2.5. Chiral HPLC analysis

HPLC analysis was performed using a Merck-Hitachi LaChrom HPLC system equipped with a Merck L-7490 RI detector, an L-7400 UV-detector, a reversed phase Chiralpak® AD-RH column (Daicel) and a thermo-stated column oven (40 °C). The mobile phase used contained 25 % acetonitrile in dd$H_2O$. A flowrate of 30 mL/min was applied. HPLC standards were prepared deploying substrate and racemic product in a range of 0.1, 0.5, 1, 5, 10 mM. Peak areas at corresponding retention times were used to calculate concentrations.

2.6. Phase solubility studies: Molar ratio determination of cyclodextrin/guest complex (complex stoichiometry)

HBC stock solutions were prepared in potassium phosphate buffer (100 mM, pH 6.2) and diluted to a final volume of 1 mL in 2 mL Eppendorf tubes. Dilutions covered concentrations from 25 - 421 mM HBC. The average molecular weight of HBC was calculated to 1453 g/mol, as the degree of 2-hydroxypropyl substitution ranges from 2-9 per cyclodextrin molecule. *o*-chloroacetophenone or *(S)*-1-(2-chlorophenyl)ethanol were added in excess amounts (170 µL, ~ 1.1 M) to 1 mL HBC containing solutions and equilibrated for 24 h on an end-over-end rotator at 30 rpm, RT. Samples were centrifuged for 10 min at 13.2k rpm. Defined aliquots were taken from the HBC/guest containing aqueous phase and diluted in 1:9 isopropanol/anhydrous ethanol accompanied by vigorous vortexing periods. Due to the decreased reaction medium polarity, HBC/guest interactions were lowered favouring de-complexation. Thus, reliable HPLC results were obtained owing to increased guest-accessibility for UV-detection. For calculations, final sample volumes of 1.17 mL were considered as dilutions, as HBC was found to additionally dissolve in and precipitate at the organic phase. All samples were prepared in triplicates. Phase solubility studies were carried out according to the method described by Higuchi and Connors (1965)[22].

2.7. HBC/*o*-chloroacetophenone complex preparation

Cyclodextrin/*o*-chloroacetophenone complexes were either prepared by microwave irradiation (MWI) or liquid complexation (LC). For LC, HBC was dissolved in potassium phosphate buffer followed by substrate addition. The mixture was vortexed for 10 s. Alternatively, cyclodextrins were directly mixed with substrate molecules in case of high substrate loading (1 to 2 M) accompanied by adding 50 µL potassium phosphate buffer (100 mM, pH 6.2). Microwave irradiation[23] was applied for preparing 1:2 HBC/substrate complexes.

Components listed in Table 1 were transferred into a glass beaker, mixed using a glass rod and reacted for 20-25 s at 750 W in a microwave oven. Obtained crystals were crushed.

**Table 1: MWI complex preparation.**

| Component | Amount |
|---|---|
| HBC | HBC (mg) |
| *o*-chloroacetophenone | *o*-chloroacetophenone (mM) = (HBC*2) (mM) |
| Ethanol (96 %) | EtOH (µL) = HBC (mg) / 1.875 (mg) |
| $dH_2O$ | $H_2O$ (µL) = HBC (mg) / 7.5 (mg) |

e.g.: 600 mg HBC (370 mM) + 99.1µL (740mM) substrate + 320µL EtOH + 80µL $dH_2O$

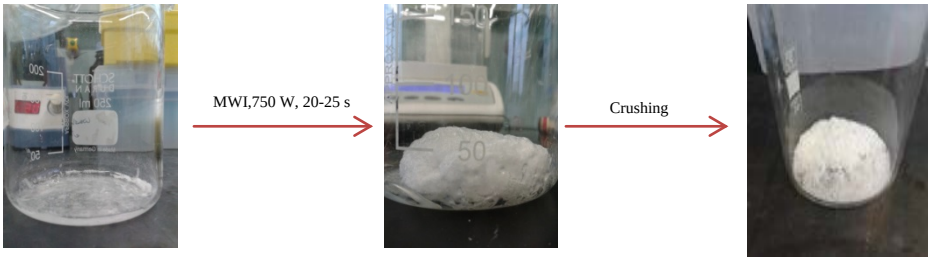


2.8. Whole-cell activities of xylose reduction & formate oxidation in the presence of HBC

Lyophilized cells (4 mg) were re-hydrated for 30 min in 150 µL potassium phosphate buffer (100 mM, pH 6.2) at 1400 rpm and 25°C on a thermomixer. HBC was pre-dissolved in the same buffer and combined with the re-hydrated cells followed by adjusting the volume to 1 mL. The mixtures were placed on an end-over-end rotator (30 rpm). After re-suspending, samples (10 µL) were taken over time and directly subjected to the enzyme assay described prior. Experiments were performed in triplicates.

2.9. Cyclodextrin-cell adsorption studies

In order to evaluate the amount of cyclodextrins adsorbed to cells, both linear equations obtained from the phase solubility studies were rearranged. These linear equations reflect the concentration (y) of *o*-chloroacetophenone or *(S)*-1-(2-chlorophenyl)ethanol in aqueous solution in the presence of a distinct concentration of HBC denoted (x).

For *o*-chloroacetophenone, y = 11.2652 + 0.8569 x and for *(S)*-1-(2-chlorophenyl)ethanol, y = 23.5445 + 1.2359 x. After rearranging to x = [HBC]:

[HBC] = ([*o*-chloroacetophenone] - 11.2652)/0.8569

[HBC] = ([*(S)*-1-(2-chlorophenyl)ethanol] - 23.5445)/1.2359

This enables the indirect calculation of the HBC concentration in the supernatant of a reaction mixture after centrifugation by simply measuring substrate and product concentrations, inserting these values in the equations above and summing up the results for HBC/substrate and HBC/product. The sum was subtracted from the HBC concentration applied in the beginning (e.g. 337 mM) reflecting the amount of HBC adsorbed to cells (pellet).

Example: The reaction mixture containing 1.5 $g_{cdw}$/L cells, 337 mM HBC and 300 mM *o*-chloroacetophenone was centrifuged after 48 h. Substrate and product concentrations were measured in the supernatant (171.47 mM and 109.28 mM) and inserted into the equations resulting in the amount of HBC necessary to keep e.g. 171.47 mM of substrate in aqueous solution, which is 186.95 mM HBC or 69.37 mM HBC for 109.28 mM of product. Summing up these results gives 256.32 mM HBC. As 337 mM HBC were applied originally, 337 - 256.32 = 80.68 mM HBC are adsorbed to cells. After dividing 80.68 mM HBC by 1.5 $g_{cdw}$/L cells, 53.79 mmol/$g_{cdw}$ of HBC will be found pelletized.

### 2.9.1. Adsorption study 1

The linear equation for HBC/*o*-chloroacetophenone complexation was rearranged to calculate the HBC concentration necessary to fully solubilize 300 mM *o*-chloroacetophenone, which results in 337 mM HBC. For the actual reaction, concentrations of *o*-chloroacetophenone (300 mM), HBC (337 mM), $NAD^+$ (0.5 mM) and sodium formate (350 mM) were kept constant, while the concentration of lyophilized cells was varied. The reaction was carried out for 48 h followed by centrifugation (10 min, 25°C, 13.2 k rpm). The supernatant was isolated, properly diluted in 7:3 ethanol/d$H_2O$, vortexed vigorously and subjected to HPLC analysis.

2.9.2. Adsorption study 2

A series of reaction mixtures either with or without 300 mM *o*-chloroacetophenone was prepared. Therefore, lyophilized cells (4 mg) were re-hydrated in potassium phosphate buffer (100 mM, pH 6.2) in the presence of 0.5 mM $NAD^+$ and 350 mM sodium formate. HBC (150 mM, 242 mg)) was either complexed with 300 mM *o*-chloroacetophenone or added directly to the re-hydrated cells without substrate (final volume 1 mL). Reactions were stopped at distinct time points by centrifugation (10 min, 25°C, 13.2 k rpm) followed by isolating the supernatant. Supernatants resulting from reaction mixtures containing substrate were diluted in 7:3 ethanol/$dH_2O$, vortexed vigorously and subjected to HPLC analysis. For supernatants from reaction mixtures not containing substrate, excess amounts of *o*-chloroacetophenone (100 µL) were added and complexed with HBC present in the supernatant by simply vortexing (1 min). Samples were centrifuged (10 min, 25°C, 13.2 k rpm) and the upper aqueous phase analysed with HPLC.

2.10. Enzyme stabilization by HBC in the presence of organic solvents by measuring XR and FDH activities

Experiments were performed with purified XR wild-type and partially purified FDH. Hexane, hexanol or heptane (50 % v/v, 0.5 mL) were added to 2 mL Eppendorf tubes containing 0.5 mL of XR (0.11 g/L, 1-1.37 U/mL) or FDH (~1.6 g/L, 0.9 U/mL) dissolved in potassium phosphate buffer (100 mM, pH 6.2). FDH activity/stability was only tested in the presence of heptane. Measured activities were referenced to those obtained after 1 h in unmodified mixtures. Enzyme assays were performed as described prior.

2.11. Enzyme purification

Lyophilized cells (80 mg) were re-hydrated in 2 mL potassium phosphate buffer (100 mM, pH 6.2), centrifuged for 10 min at 13.2k rpm followed by isolating the supernatant (soluble

enzyme fraction). The supernatant was loaded onto the Red31 dye-ligand column (6×2.6 cm, approximately 6-8 mg protein/mL of gel) equilibrated with 50 mM potassium phosphate buffer (pH 7.0) at RT. Adsorbed XR (wild-type) and FDH were eluted with a step gradient (Table 2). Fractions were collected and pooled according to activity measurements. Pooled fractions (10 mL) were concentrated and desalted in Vivaspin 20 mL Concentrator tubes (10.000 MWCO) to approx. 1 mg/mL. The buffer was changed to 100 mM potassium phosphate buffer (pH 6.2) by applying 3x10 mL in the final concentration steps. Enzymes were stored at -20°C. Enzyme purification for both enzymes at once was not further optimized.

**Table 2: FPLC step gradient.**
Buffer A: 50 mM potassium phosphate buffer (pH 7).
Buffer B: 50 mM potassium phosphate buffer (pH 7), 2 M NaCl.

| Vol (mL) | Buffer B (%) | Flow (mL) | Fraction size (mL) |
|---|---|---|---|
| 0 | 0 | 3 | 0 |
| 10 | 0 | 3 | 10 |
| 20 | 0 | 3 | 10 |
| 50 | 0 | 3 | 10 |
| 50.1 | 10 | 3 | 10 |
| 90 | 10 | 3 | 10 |
| 90.1 | 40 | 3 | 10 |
| 130 | 40 | 3 | 10 |
| 130.1 | 70 | 3 | 10 |
| 170 | 70 | 3 | 10 |
| 170.1 | 100 | 3 | 10 |
| 210 | 100 | 3 | 10 |

### 2.12. Whole-cell biotransformation and HPLC-sample preparation

Cells (lyophilized) were re-hydrated in potassium phosphate buffer (100 mM, pH 6.2, volume ≤ 50 % v/v) in the presence of $NAD^+$ (0.5-6 mM) and sodium formate (50 mM excess on [substrate]) using 2 mL Eppendorf tubes. The tubes were placed on a thermomixer for 30 min at 25°C and 1400 rpm. Afterwards, re-hydrated cells were combined with HBC/substrate complexes and filled up to a total working volume of 1 mL. The mixtures were incubated for 24 – 48 h on an end-over-end rotator (30rpm) at room temperature. Prior to HPLC analysis, reaction mixtures were vortexed vigorously to loosen up emulsified structures. Aliquots (100 - 500 µL) were taken and diluted stepwise in 7:3 ethanol/$dH_2O$ accompanied by extensive

vortexing periods. Alternatively, the work up was performed by transferring the whole reaction mixture (1 mL) into 15 mL Sarstedt tubes followed by adding 4 mL isopropanol. The mixture was vortexed and centrifuged for 10 min, 25°C and 3220 g. The resulting supernatant was isolated, syringe-filtered and properly diluted using isopropanol. All samples were prepared in duplicates or triplicates. Deviations from above mentioned reaction mixture preparations are described in the respective section.

### 2.13. Cell-free biotransformation

Lyophilized cells (40 mg) were re-hydrated for 30 min in 1 mL potassium phosphate buffer (100 mM, pH 6.2) at 1400 rpm and 25°C on a thermomixer followed by centrifugation (13.2k rpm, 10 min, 25°C). The supernatant was isolated. *o*-chloroacetophenone (300 mM), sodium formate (350 mM), HBC (100 mg) and $NAD^+$ (0.5 mM) were added to 400 µL of isolated supernatant. All mixtures were adjusted to 1 mL and placed on an end-over-end rotator (30rpm) for 24 h.

# 3. Results

## 3.1. Phase solubility studies

A linear increase in solubilities for *o*-chloroacetophenone (substrate) and *(S)*-1-(2-chlorophenyl)ethanol (product) was measured by HPLC at stepwise elevated HBC concentrations (Figure 3). Intersects reflect the intrinsic solubilities, which are 11.8 mM (*o*-chloroacetophenone) and 23.4 mM (*(S)*-1-(2-chlorophenyl)ethanol) in 100 mM phosphate buffer (pH 6.2). Binding constants were calculated using the formulas given below[6,24].

$$K_{s,1:1} = \frac{k}{S_0 \cdot (1-k)} = 532\ M^{-1}$$

$$K_{P,2:1} = \frac{k}{(P_0^2 \cdot (2-k))} = 3\ M^{-2}$$

K: Binding constant ($M^{-1}$)
k: Linear slope (mM/mM)
$S_o$: Intrinsic solubility of substrate (mM)
$P_o$: Intrinsic solubility of product (mM)

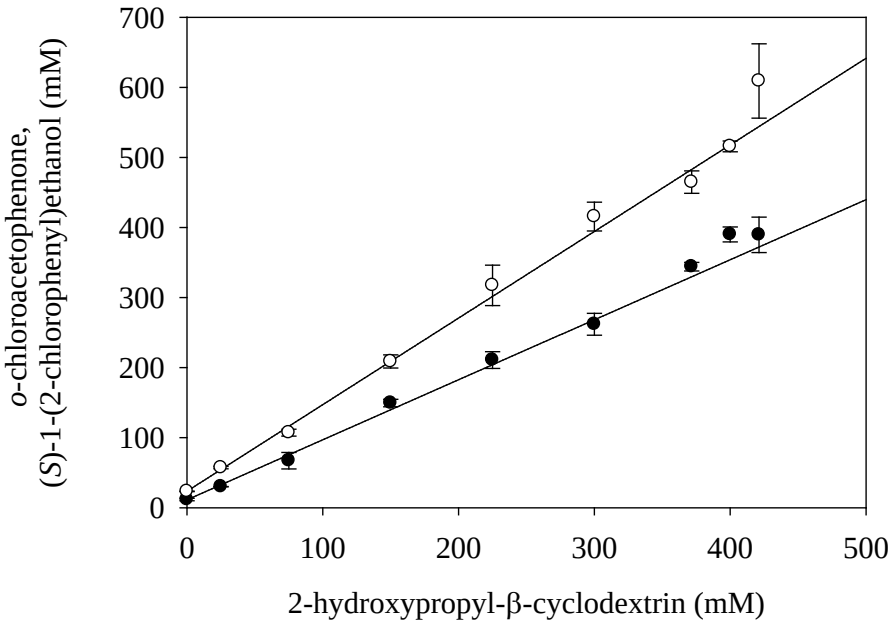


**Figure 3: Phase solubility study.** Increasing solubility of *o*-chloroacetophenone (black dots) and *(S)*-1-(2-chlorophenyl)ethanol (open circles) with increased HBC concentrations. Linear fit for *o*-chloroacetophenone (substrate): y=11.265+0.857x; ($R^2$=0.9922). Linear fit for *(S)*-1-(2-chlorophenyl)ethanol (product): y=23.545+1.236x; ($R^2$=0.9967).

3.2. Gibbs energies of complex formation

Gibbs energies were calculated based on the data obtained from the solubility studies representing an alternative approach of estimating complexation efficiency[25] (Figure 4). Negative Gibbs energies indicate that complex formation occurs spontaneously. At higher HBC concentrations, Gibbs energies for both, *o*-chloroacetophenone and *(S)*-1-(2-chlorophenyl)ethanol, still remain negative but seem to approach a maximum beyond which complexation efficiencies will not be further enhanced.

$\Delta G_S = -RT \ln [(HBC:S)/S_0]$

$\Delta G_P = -RT \ln [(HBC:P)/P_0]$

ΔG: Gibbs energy (kJ/mol)
R: Gas constant = 8.314 J/(mol K)
T: Temperature = 298.15 K
$S_o$: Intrinsic solubility of substrate (mM)
$P_o$: Intrinsic solubility of product (mM)
HBC:S & HBC:P = Solubilities of complexed substrate or product with increasing [HBC]

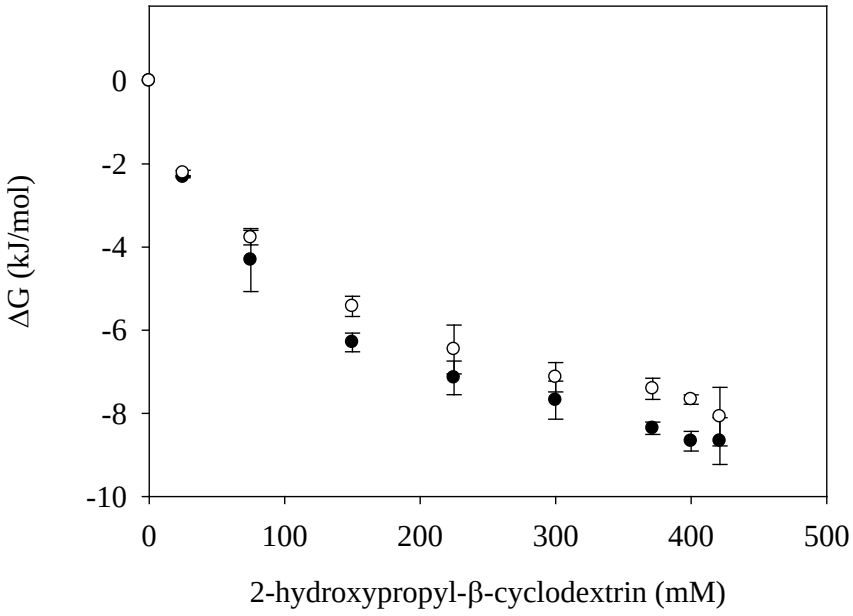


**Figure 4: Gibbs energy of substrate- and product-complexation**. Decreasing complexation efficiency of *o*-chloroacetophenone (black dots) and *(S)*-1-(2-chlorophenyl)ethanol (open circles) with increased HBC concentrations.

3.3.Whole-cell activities of xylose reduction & formate oxidation in the presence of HBC

*CtXR activities.* Measurements performed immediately after cell re-hydration already reveal the impact of HBC on whole-cell activities as compared to unmodified mixtures (Figure 5). Activities further increase after 2 h, except for 320 mM HBC. High HBC concentrations (300 - 320 mM) are counteracting effective xylose reduction. Outstanding results were obtained for 75 mM HBC reaching 2670 U/$g_{cdw}$ after 6 h of rotation followed by a drop to approximately its initial value after 24 h. Apart from fluctuations, the overall trend shows a decrease in activity after 24 h for all conditions tested, with unmodified mixtures displaying almost no activity at this point.

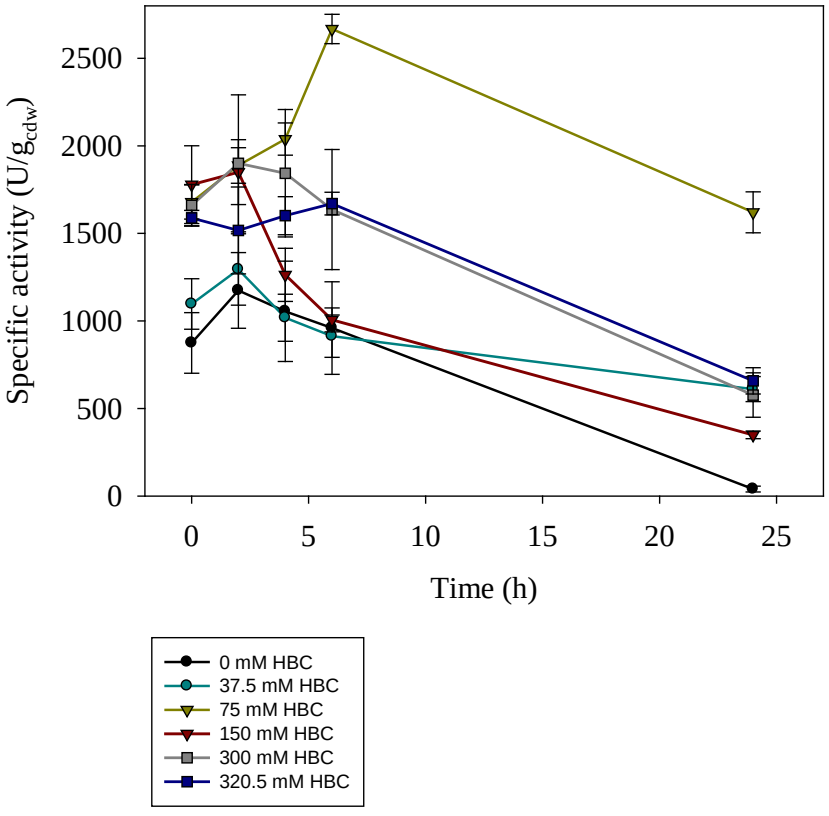


**Figure 5: Specific activity (U/gcdw) of xylose reductase (WT).** Activities refer to measurements applying 4$g_{cdw}$/L whole-cells.

*CbFDH activities*. Immediately after cell rehydration, HBC increases FDH activities in each case, except for 300 mM (Figure 6). Activities are further increased and drop after 6 h. Compared to the results obtained for xylose reductase, even unmodified mixtures display elevated activities similar to HBC containing mixtures. After 24 h, only the presence of 37.5 and 150 mM HBC keeps FDH activities significantly higher while others drop. As measurements were aggravated by cell clump formation, calculated errors are depicted in Table 3 in order to distinguish curves in Figure 6 more clearly.

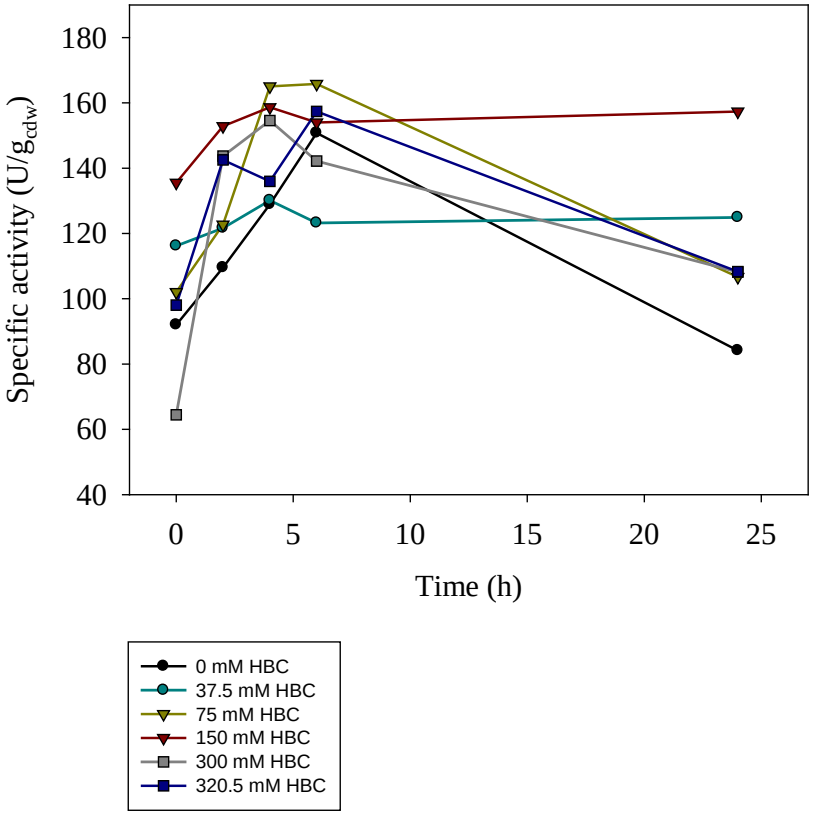


**Figure 6: Specific activity (U/gcdw) of formate dehydrogenase**. Activities refer to measurements applying 4$g_{cdw}$/L whole-cells.

**Table 3: Calculated errors for FDH whole-cell activity measurements.** Top row: HBC (mM) applied. Left column: Sampling time. Grey and white rows: Errors (mM) calculated for respective sampling time and HBC concentrations.

| HBC | 0 mM | 37.5 mM | 75 mM | 150 mM | 300 mM | 320.5 mM |
|---|---|---|---|---|---|---|
| 0 h | 6.6 | 12.2 | 4.8 | 13.4 | 19.7 | 14.9 |
| 2 h | 13.2 | 14.4 | 5.2 | 10.6 | 15.4 | 10.3 |
| 4 h | 12.8 | 17.5 | 8.0 | 26.7 | 14.9 | 4.7 |
| 6 h | 11.7 | 15.2 | 8.0 | 9.5 | 17.7 | 12.0 |
| 24 h | 15.4 | 26.3 | 6.4 | 17.9 | 3.0 | 12.6 |

### 3.4. Cyclodextrin-cell adsorption studies

#### 3.4.1. Adsorption study 1

As cyclodextrins are capable of interacting with cell membranes[9], adsorption studies aiming at elucidating theses interactions were performed. Not surprisingly, increased catalyst concentrations result in higher conversions and lower specific activities in the presence of 337 mM HBC and 300 mM substrate (Figure 7). A full conversion is achieved applying 20 $g_{cdw}$/L cells. As described prior, substrate and product concentrations were measured in the supernatant after centrifuging the reaction mixtures to determine HBC concentrations in the pellet. Calculated HBC concentrations were further divided by the amount of catalyst applied. HBC found in pellets was interpreted as being adsorbed to cells. In absolutes, 24 % of HBC was adsorbed to cells at a catalyst loading of 1.5 $g_{cdw}$/L and up to 59 % of HBC at 40 $g_{cdw}$/L. Pelletized HBC correlates with the specific activities calculated: A high degree of adsorption results in high specific activities and vice versa relative to the amount of catalyst used.

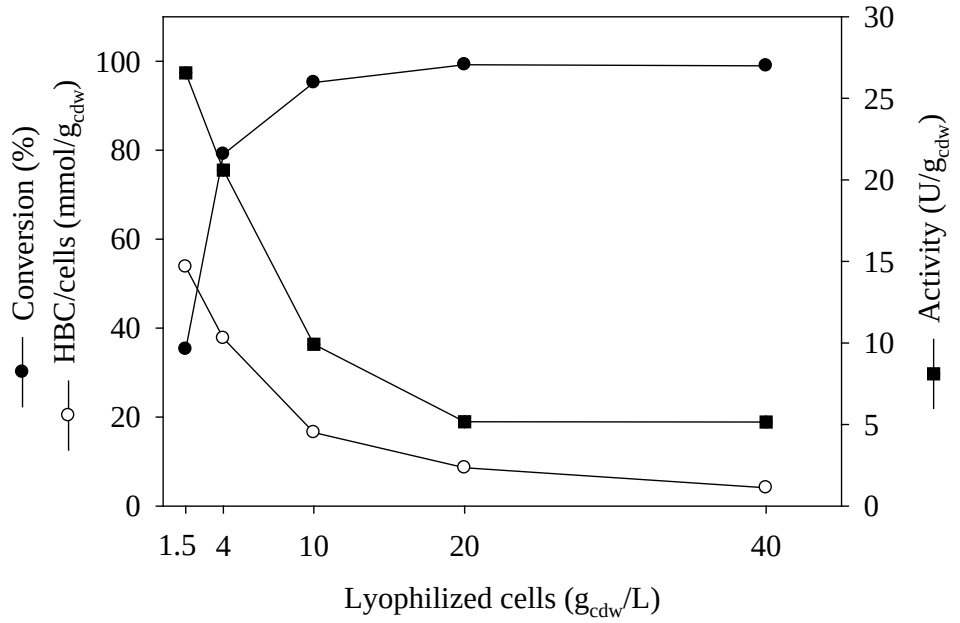


**Figure 7: Adsorption study 1:** Concentrations of *o*-chloroacetophenone (300 mM), HBC (337 mM), $NAD^+$ (0.5 mM) and sodium formate (350 mM) were kept constant, while the concentration of lyophilized cells was varied. Substrate and product concentrations were measured in supernatants after 48 h reaction time. Black dots: Conversion results (%). Open circles: HBC adsorbed to cells (mmol/$g_{cdw}$). Black squares: Specific activity for 4-40 $g_{cdw}$/L on 300 mM substrate over 48 h (U/$g_{cdw}$).

### 3.4.2. Adsorption study 2

In order to compare the dynamics of HBC adsorbing to cells over 24 h of rotation/reaction, mixtures with and without 300 mM substrate present were prepared (Figure 8). The results obtained suggest that adsorption is favoured in the presence of substrate.

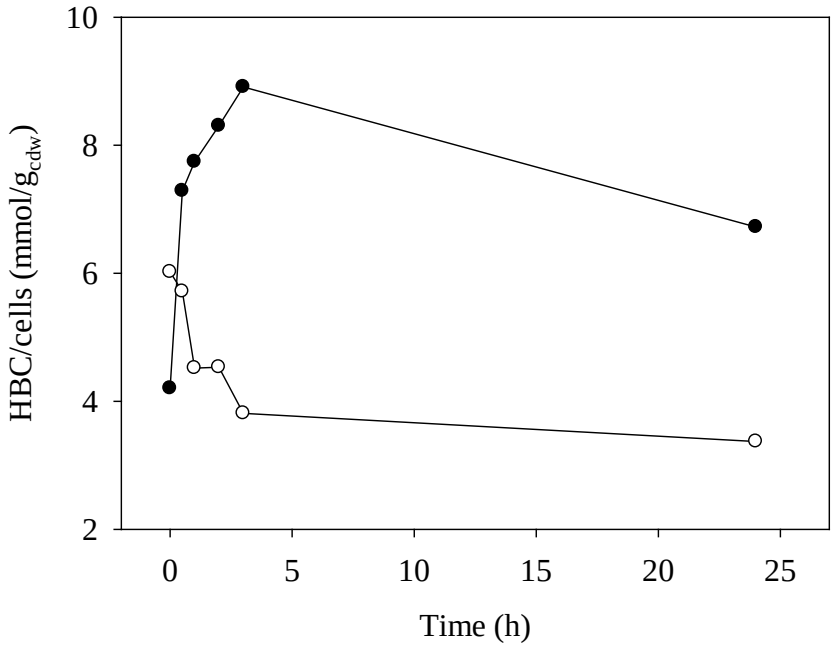


**Figure 8: Adsorption study 2:** Conditions: 4 $g_{cdw}$/L cells, 0.5 mM $NAD^+$, 350 mM sodium formate and 150 mM HBC. Black dots: HBC adsorbed to cells in the presence of 300 mM substrate (mmol/$g_{cdw}$). Open circles: HBC adsorbed to cells with no substrate present (mmol/$g_{cdw}$)

3.5. Enzyme stabilization by HBC in the presence of organic solvents

*Hexane.* As can be seen in Figure 9, XR activities decrease in the presence of 50 % v/v hexane after 24 h to ~50 % (black bars). However, by comparing reference activities (dotted and straight lines) corresponding to XR activities in plain phosphate buffer after 1 h (= 8.9 U/mg) and 24 h to activities with hexane present, stabilization effects by hexane can be observed manifesting in higher activities after 24 h. HBC positively affects XR activities in hexane/buffer two-phase systems. Highest stabilizing effects occur at 100 g/L HBC resulting in ~13.8 U/mg, which might be considered as enzyme hyperactivation compared to 12.4 U/mg representing the average specific activity in phosphate buffer (100 mM, pH 6.2). At higher HBC concentrations (300 g/L), stabilizing effects tend to vanish.

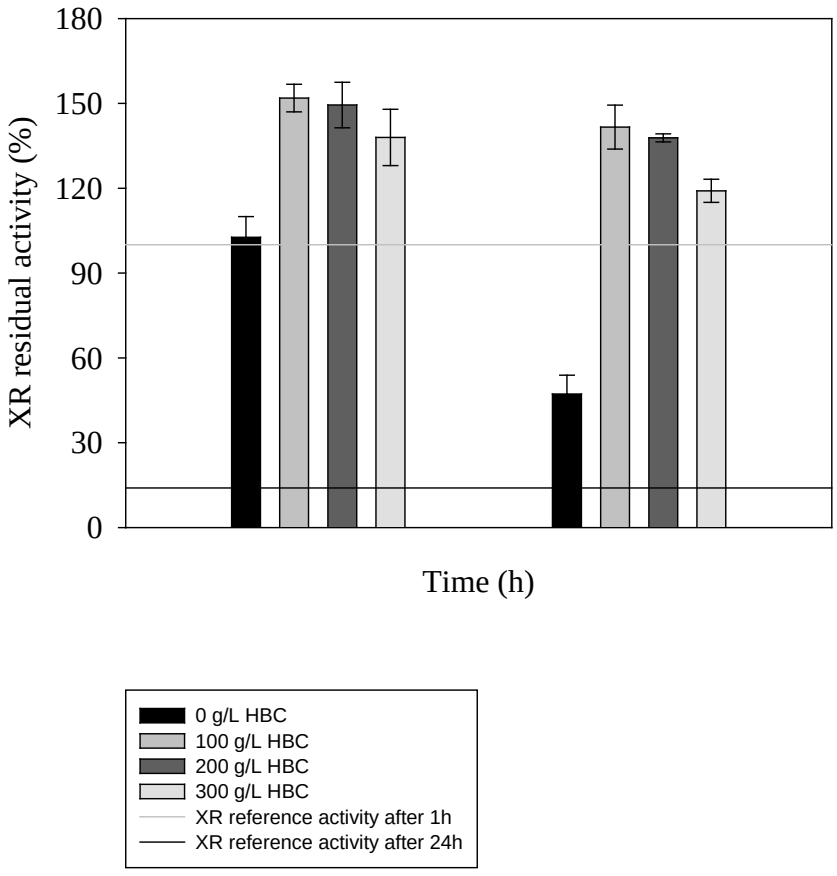


**Figure 9: XR wild-type in hexane (50 % v/v):** Enzyme stabilization in the presence of HBC. Reference activity after 1 h: 8.9 U/mg. XR concentration: 0.1 g/L (2.78 µM).

*Hexanol.* Compared to studies performed with 50 % v/v hexane, hexanol largely contributes to XR inactivation (Figure 11). In mixtures only containing XR in buffer and 50 % v/v hexanol, activities decrease to 60 % after 1 h and to 0 after 24 h. As described prior, HBC again stabilizes XR in hexanol/buffer two-phase systems, although these effects are less pronounced in contrast to hexane.

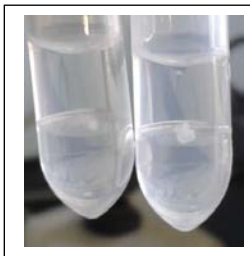

**Figure 10:** Precipitation of XR at hexanol/buffer interface.

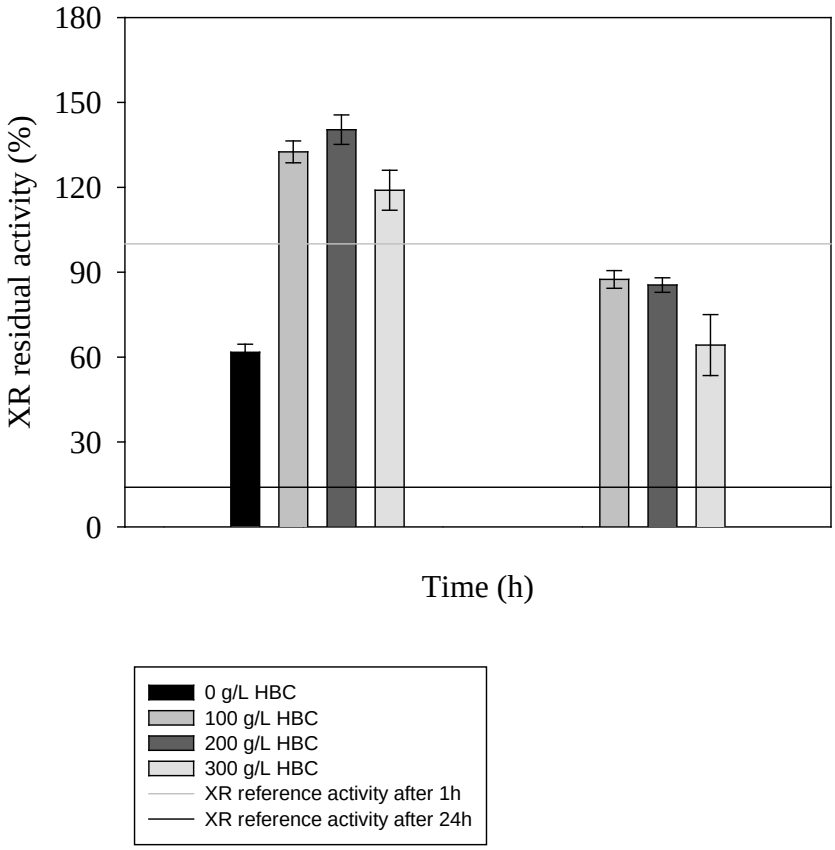


**Figure 11: XR wild-type in hexanol (50 % v/v):** Enzyme stabilization in the presence of HBC. Reference activity after 1 h: 8.9 U/mg. XR concentration: 0.1 g/L (2.78 µM).

*Heptane.* FDH activity decreases tremendously after 24 h in plain heptane/buffer two-phase systems (black bars, Figure 12) but remains ~ 80 % in the presence of 100 g/L HBC. As XR displayed full activity in experiments performed with 50 % v/v heptane, stabilizing effects by HBC mainly result in restoring the original activity of 12.4 U/mg (Figure 13). 100-300 g/L HBC do not significantly change outcomes. After 24 h, XR displays residual activities of > 90 %, while almost no activity was detectable in reaction mixtures not containing HBC.

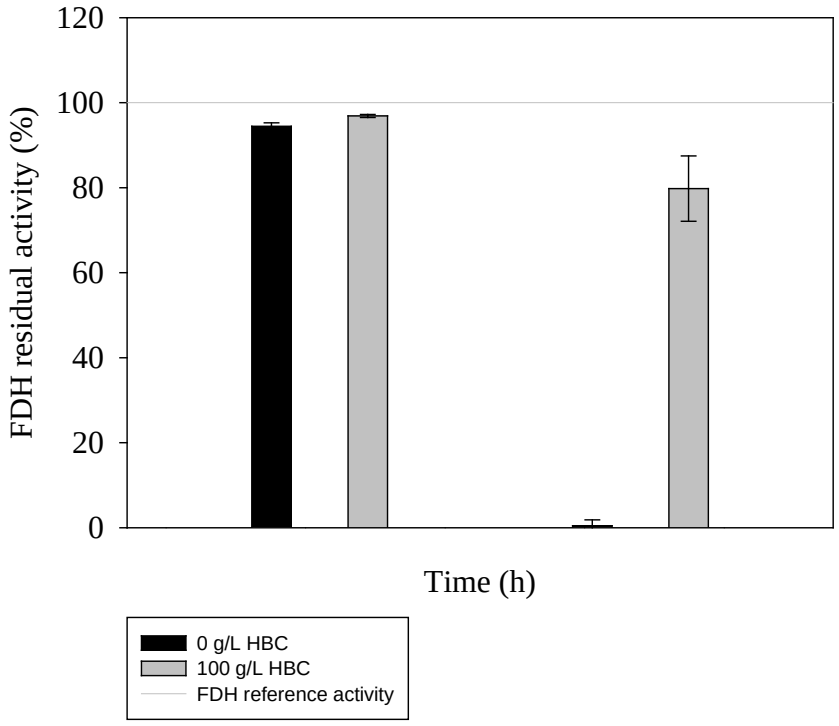


**Figure 12: FDH in heptane (50 % v/v).** Enzyme stabilization in the presence of HBC. Reference activity after 1 h: 0.9 U/mL. Enzyme concentration: 1.5 g/L

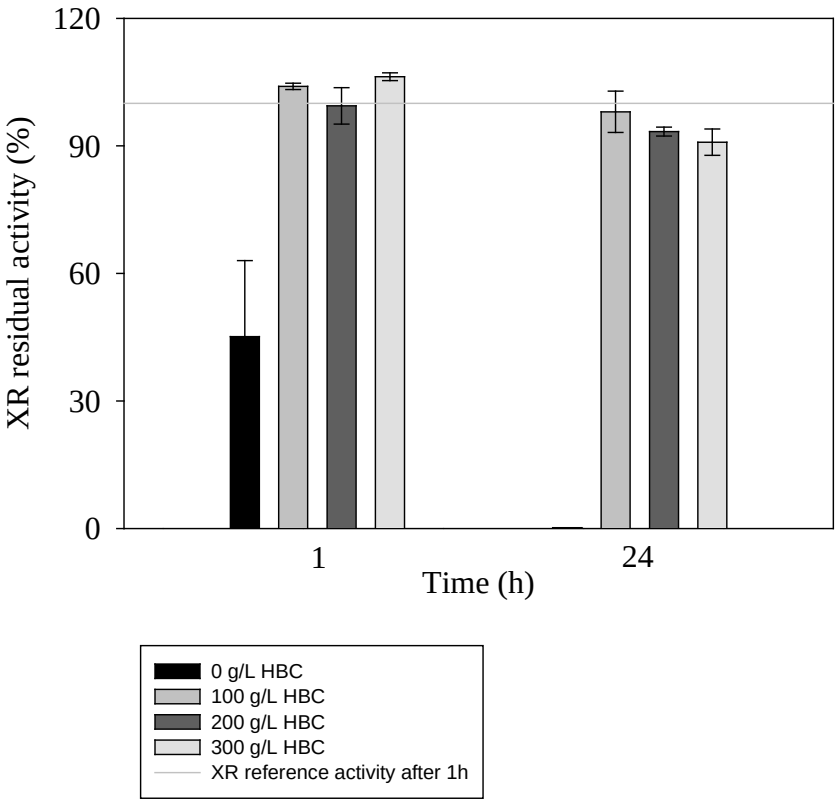


**Figure 13: XR wild-type in heptane (50 % v/v):** Enzyme stabilization in the presence of HBC. Reference activity after 1 h: 12.4 U/mg. XR concentration: 0.1 g/L (2.78 µM).

## 3.6. Biotransformations of *o*-chloroacetophenone

### 3.6.1. Complex preparation: Comparison by whole-cell biotransformation

Figure 14 reveals that no significant changes in conversions occur when preparing HBC/substrate complexes either by microwave irradiation or liquid complexation. Conditions were only tested for 150 mM HBC and 300 mM substrate resulting in 1:2 HBC/substrate complexes. As can be seen further, differences in conversion are insignificant comparing 4 and 10 $g_{cdw}$/L whole-cell catalyst.

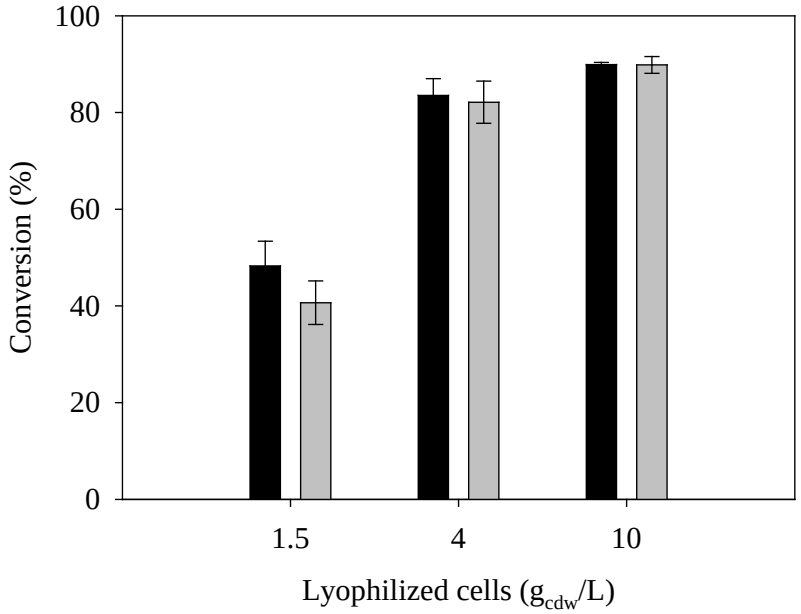


**Figure 14: Comparison between liquid and microwave assisted complexation.** Reaction conditions: 300 mM *o*-chloroacetophenone, 150 mM HBC, 0.5 mM $NAD^+$, 350 mM sodium formate, 24 h. Black bars: Microwave irradiation assisted complexation. Grey bars: Liquid complexation.

### 3.6.2. Cell-free biotransformation

Cell-free conversions (300 mM substrate) were performed applying supernatants from lyophilized cells after re-hydration and centrifugation (Figure 15). The volumetric activities correspond to XR (WT) ~ 12.8 U/mL (xylose) and FDH ~ 1.8 U/mL (sodium formate). Conversions applying solely supernatants resulted in 80 %, whereas full conversion of 300 mM substrate was achieved by additionally applying 100 g/L HBC. These findings support enzyme leakage from lyophilized cells verified prior by enzyme purification (see section 3.6.3).

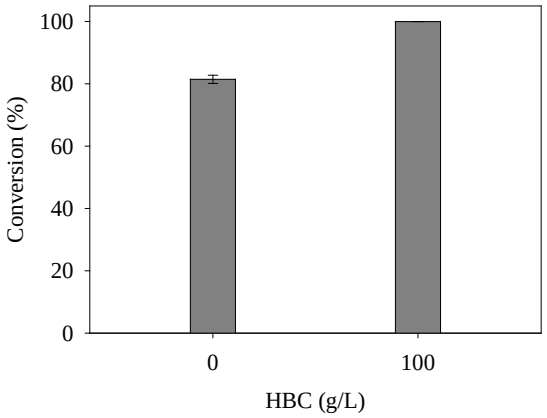


**Figure 15: Cell-free conversion.** Reaction conditions: 40 $g_{cdw}$/L, 300 mM *o*-chloroacetophenone, 0 & 100 mg HBC, 0.5 mM $NAD^+$, 350 mM sodium formate, 24 h. Recovery: 90 - 93 %.

### 3.6.3. Enzyme purification

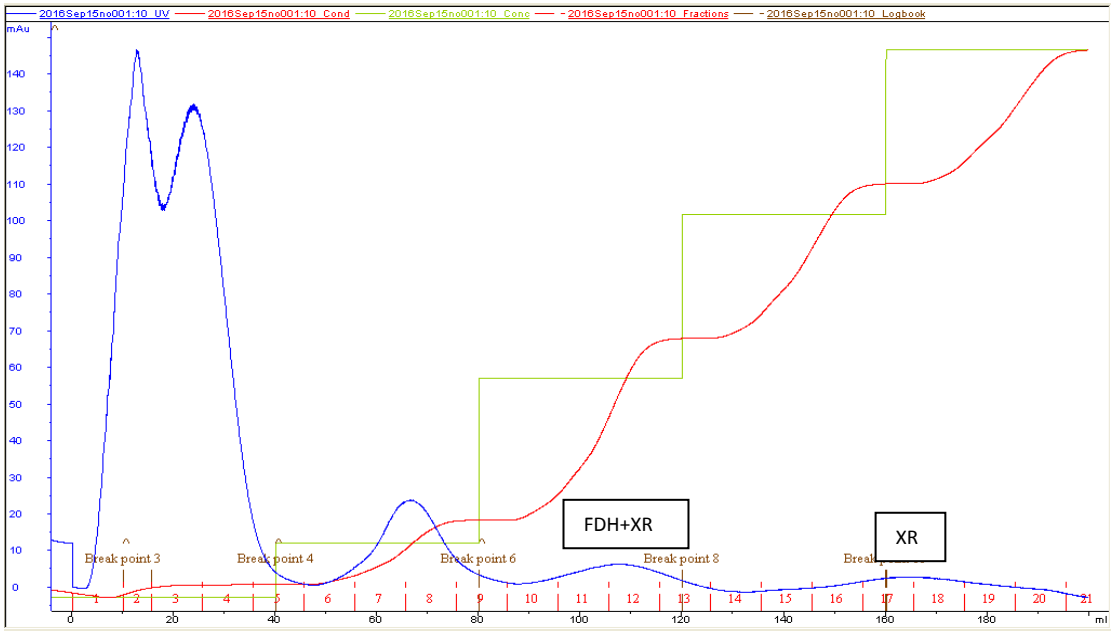


**Figure 16: Results for enzyme purification**: XR wild-type and FDH fractions are marked in the chromatogram.

In order to confirm protein leakage, lyophilized cells (40$g_{cdw}$/L) were re-hydrated and centrifuged followed by subjecting the supernatant to affinity chromatography (Figure 16). Double-purification of XR wild-type and FDH resulted in XR fractions obtained purely, while FDH fractions remained contaminated with XR. Although yields after purification were fairly

moderate (~ 1 g/L XR), the specific activity for XR wild-type was calculated to 12.4 U/mg confirming both, intactness and leakage. Following that, XR and FDH were subjected to enzyme stability assays.

### 3.6.4. Whole-cell biotransformation: 300 - 400 mM *o*-chloroacetophenone

*300 mM o-chloroacetophenone*. We varied concentrations of lyophilized cells from 1.5 to 10 $g_{cdw}$/L and HBC from 0 to 337 mM. 337 mM HBC corresponds to the amount of HBC necessary to fully dissolve 300 mM *o*-chloroacetophenone. In each case, addition of HBC increases conversions compared to unmodified mixtures. 4 $g_{cdw}$/L catalyst in combination with 75 mM HBC resulted in ~ 90 % conversion. At higher cyclodextrin concentrations, conversions drop again and positive effects of HBC are diminished. 10 $g_{cdw}$/L catalyst without HBC led to a conversion of 30 % and addition of HBC led to conversions of 82 - 97 % almost irrespective of the HBC amount (Figure 18).

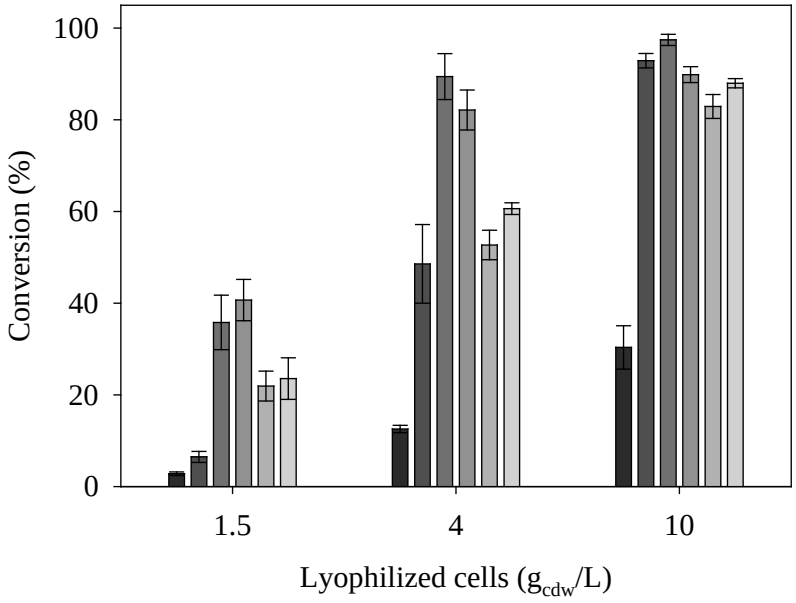


**Figure 17:** Turbidity-decrease and demulsification of reaction mixtures with increased [HBC].

**Figure 18: Whole-cell biotransformation (300 mM):** Reaction conditions: 300 mM *o*-chloroacetophenone, 0.5 mM $NAD^+$, 350 mM sodium formate, 24 h. Black to light grey bars correspond to increased HBC concentrations: 0, 37.5, 75, 150, 320.5, 337 mM. Recovery: 65 - 88 %.

*400 mM o-chloroacetophenone.* We varied concentrations of lyophilized cells from 4 to 10 $g_{cdw}$/L and HBC from 75 to 250 mM (Figure 19). Results obtained for conversions of 400 mM *o*-chloroacetophenone support findings from 300 mM conversions. HBC concentrations $\geq 200$ mM do not contribute to higher conversions and even counteract increased catalyst concentrations. Furthermore, no significant differences in conversions occur by changing catalyst loadings from 4 to 10 $g_{cdw}$/L indicating that HBC largely controls the outcome of reactions. The combination of 8 $g_{cdw}$/L and 200 mM HBC results in ~90 % conversion, which also represents the maximum. On the other hand, halving the amount of cells and cyclodextrins to 4 $g_{cdw}$/L and 100 mM HBC yields ~82 %, clearly demonstrating a dependency of catalyst and HBC concentrations in terms of conversion.

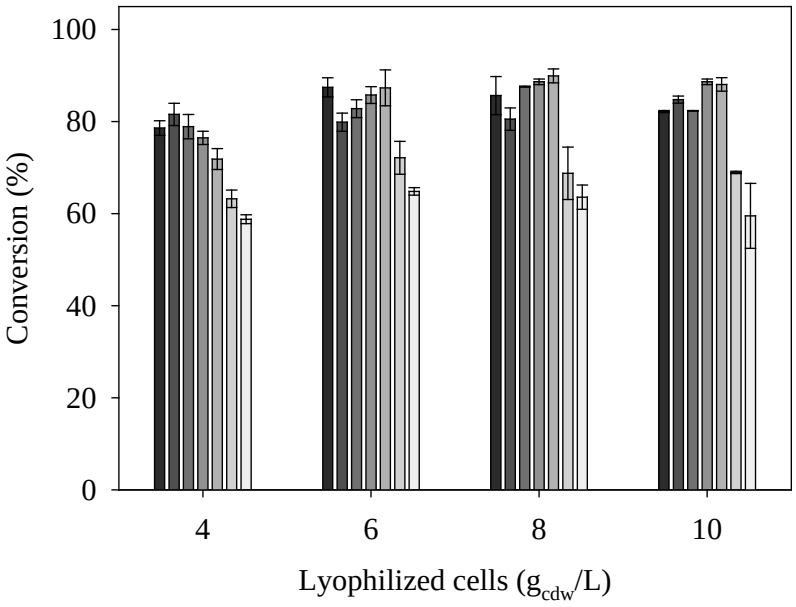


**Figure 19: Whole-cell biotransformation (400 mM):** Reaction conditions: 400 mM *o*-chloroacetophenone, 0.5 mM $NAD^+$, 450 mM sodium formate, 48 h. Dark to light grey bars correspond to increased HBC concentrations: 75, 100, 125, 150, 200, 225, 250 mM. Recovery: 83 - 96 %.

*Effect of additives to alter reaction medium polarity*. The polarity of the reaction medium was altered intending to strengthen (hydrophobic) interactions between substrate and HBC by applying potassium chloride[26] (Table 4). Vice versa, isopropanol was used to decrease the

polarity aiming at weakening substrate/HBC interactions (Figure 20) and simultaneously increase the solubility of substrate and product[27]. Compared to unmodified reaction mixtures, no positive effects are observable. Highest conversions (~80 %) at 400 mM substrate loading are reached applying 0.5 % v/v isopropanol combined with 8 $g_{cdw}$/L and 150 mM HBC. Increased isopropanol concentrations are accompanied by lower conversions. Addition of 50 mM KCL to 8 $g_{cdw}$/L cells and 150 mM HBC results in 79.5 % conversion over 48 h of reaction time, while 100 mM KCL cause a drop of ~ 4%.

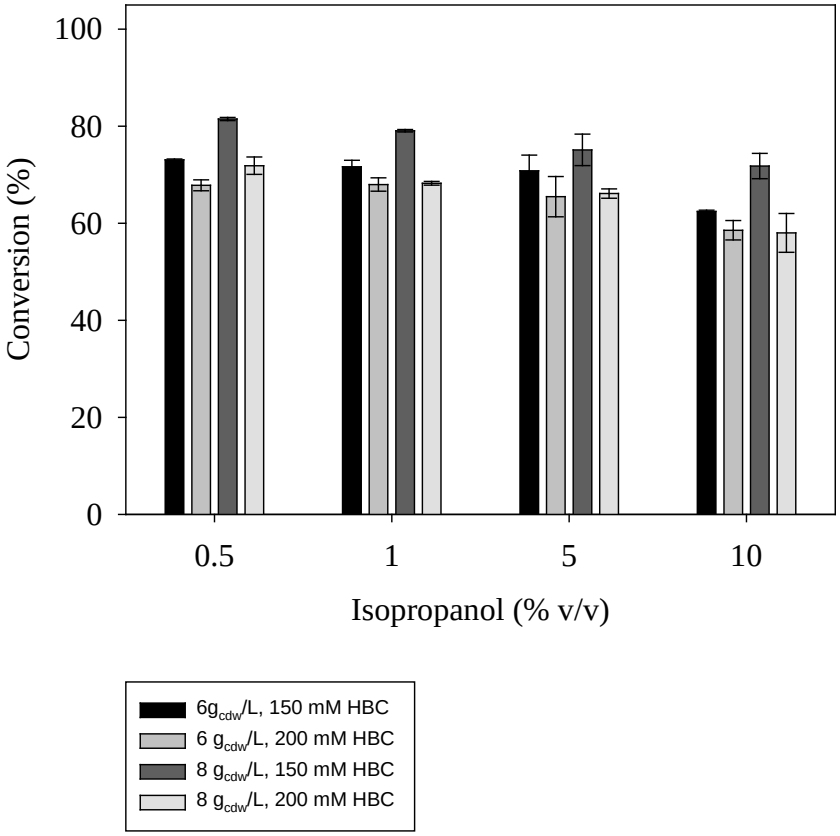


**Figure 20:** D**ecrease of reaction medium polarity by adding isopropanol.** Reaction conditions: 400 mM *o*-chloroacetophenone, 0.5-10 % v/v isopropanol, 0.5 mM $NAD^+$, 450 mM sodium formate, 48 h. Recovery: 65 – 88 %.

**Table 4: Increase of reaction medium polarity by adding KCl.**

| Reaction time (h) | Lyophilized cells ($g_{cdw}$/L) | HBC (mM) | KCl (mM) | Conversion (%) | Std. dev. (%) |
|---|---|---|---|---|---|
| 24 | 8 | 150 | 50 | 76.2 | 2.7 |
| 24 | 8 | 150 | 100 | 72.0 | 1.8 |
| 48 | 8 | 150 | 50 | 79.5 | 3.3 |
| 48 | 8 | 150 | 100 | 76.0 | 2.1 |

3.6.5. Maximizing product concentrations in whole-cell biotransformations

*Effects of $NAD^+$ concentration and XR variant.* Figure 21 displays the impact of increasing $NAD^+$ concentrations and changing XR wild-type to XR D51A. Higher $NAD^+$ loadings contribute to high conversions as well as XR D51A. A full conversion of 1.5 M substrate is reached applying 40 $g_{cdw}$/L XR D51A, 6 mM $NAD^+$ all accompanied by no further reaction mixture modifications.

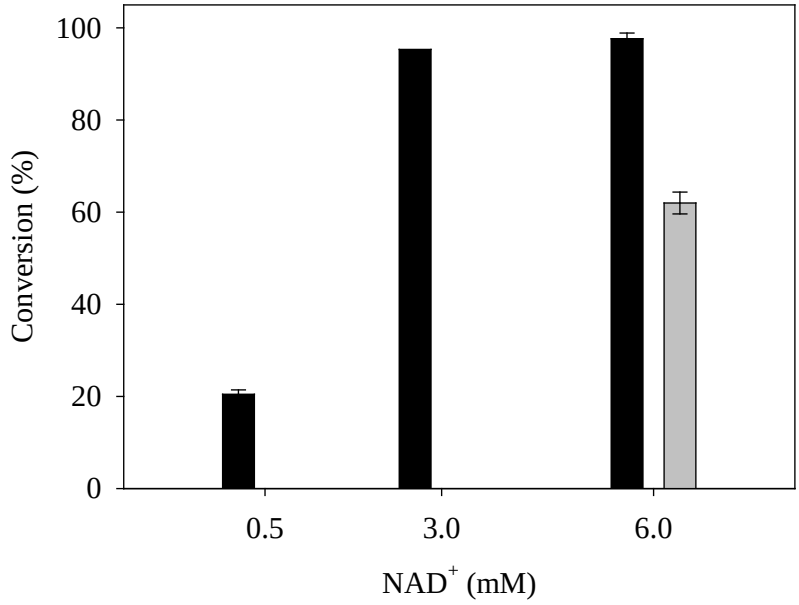


**Figure 21: Whole-cell biotransformation (1.5 M)**: Comparison of XR (WT) and XR (D51A) combined with increased [$NAD^+$]. Reaction conditions: 1.5 M *o*-chloroacetophenone, 40 $g_{cdw}$/L, 0.5-6 mM $NAD^+$, 1550 mM sodium formate, 48 h. Recovery: 80 - 96 %.

*HBC concentration.* Substrate loadings were increased to 2 M keeping catalyst concentrations constant at 40 $g_{cdw}$/L (Figure 22). The addition of 50 to 200 g/L HBC supports the trend observed for biotransformations of 300 and 400 mM substrate. Positive effects on conversions were observed up to 100 g/L HBC while conversions decreased at HBC concentrations ≥ 125 g/L. At 100 g/L HBC, ~88 % of substrate was converted while at 125 g/L cyclodextrins only ~ 50 % are converted over 48 h of reaction time.

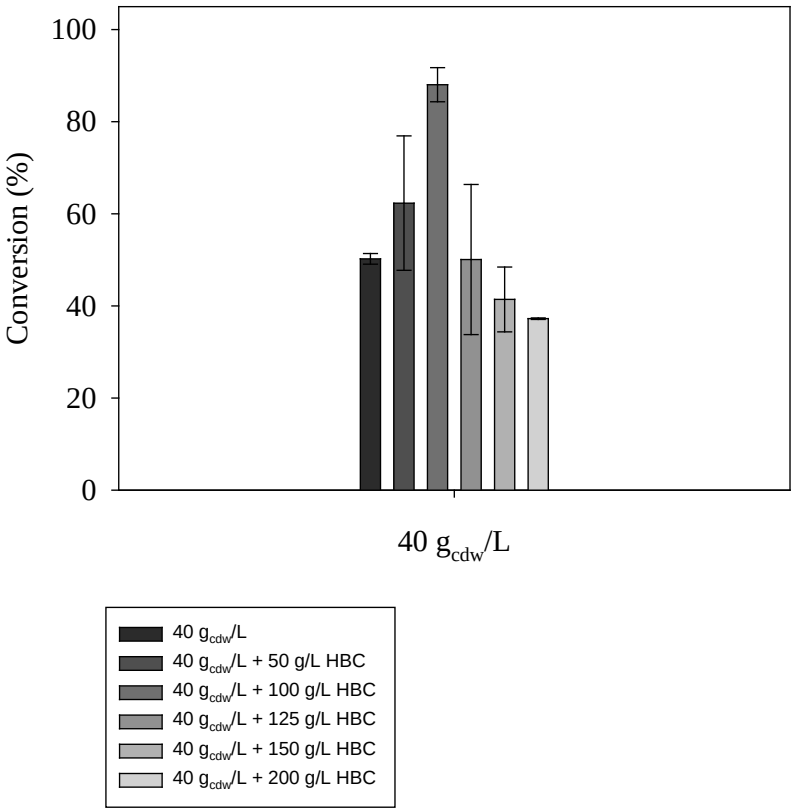


**Figure 22: Whole-cell biotransformation (2 M):** Reaction conditions: 2 M *o*-chloroacetophenone, 40 $g_{cdw}$/L, 0-200 g/L HBC, 6 mM $NAD^+$, 2050 mM sodium formate, 48 h. Recovery: 87 – 95 %.

*Addition of hexane*. Addition of 5-10 % v/v hexane to 50-200 g/L HBC at 40 $g_{cdw}$/L catalyst concentration slightly alters the conversion of 2 M *o*-chloroacetophenone compared to reaction mixtures without hexane (Figure 23, Figure 22). Although most deviations for reaction mixtures containing hexane overlap with solely HBC-modified reactions, a faint increase in conversion is achieved applying 5 % v/v hexane and 100 g/L HBC leading to ~ 92 % (288 g/L product). By choosing 10 % v/v hexane over 5 % v/v while keeping HBC at 100 g/L, outcomes massively change manifesting in a decrease of almost 30 %. Reaction mixtures containing 50, 125, 150, 200 g/L HBC with either 5 or 10 % v/v hexane are comparable in terms of overall conversions.

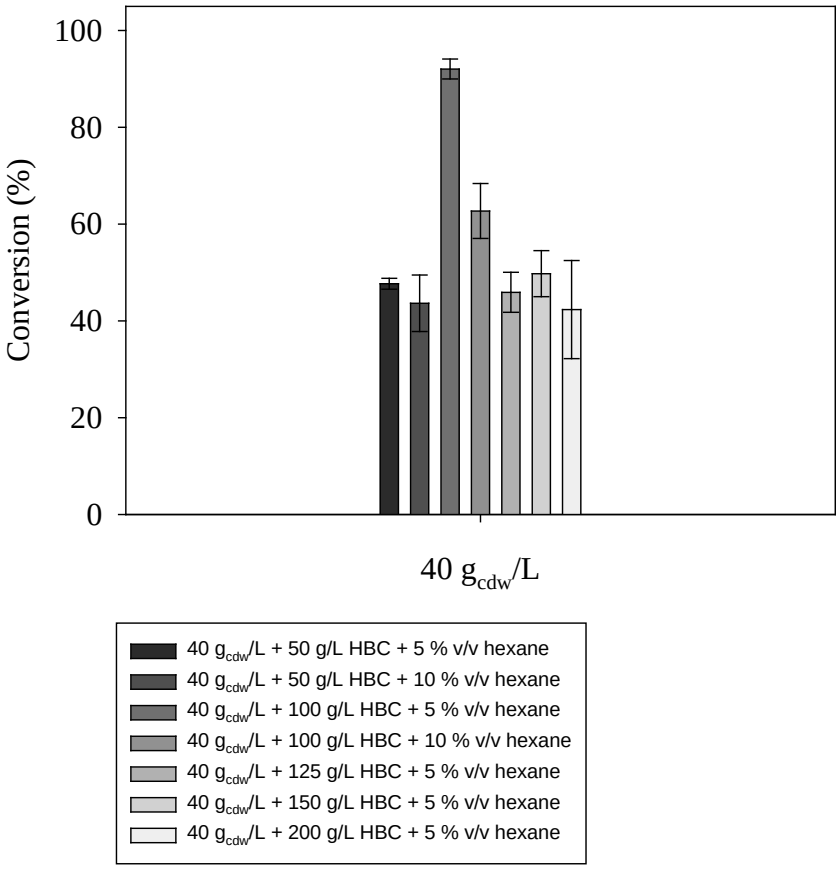


**Figure 23: Whole-cell biotransformation (2 M):** Reaction conditions: 2 M *o*-chloroacetophenone, 40 $g_{cdw}$/L, 50-200 g/L HBC, 5-10 % v/v hexane, 6 mM $NAD^+$, 2050 mM sodium formate, 48 h. Recovery: 93 - 99 %.

Increased amounts of hexane and heptane were applied intending to establish a second organic phase protecting the whole-cell catalyst. The first organic phase is constituted by *o*-chloroacetophenone itself making up ~27 % v/v (2 M) of the reaction mixture. As can be seen in Figure 24, conversions are limited to ~25 %. Further, reaction mixtures containing hexane or heptane were modified by adding 100 g/L HBC thereby exploiting features of cyclodextrins acting as 'shuttles' thus increasing substrate/product transfer from organic to the aqueous phase and vice versa. No significant effects are observable. On the other hand, cell-free biotransformations result in conversions $\geq$ 50 %, but displaying a weaker performance in the presence of HBC/hexane.

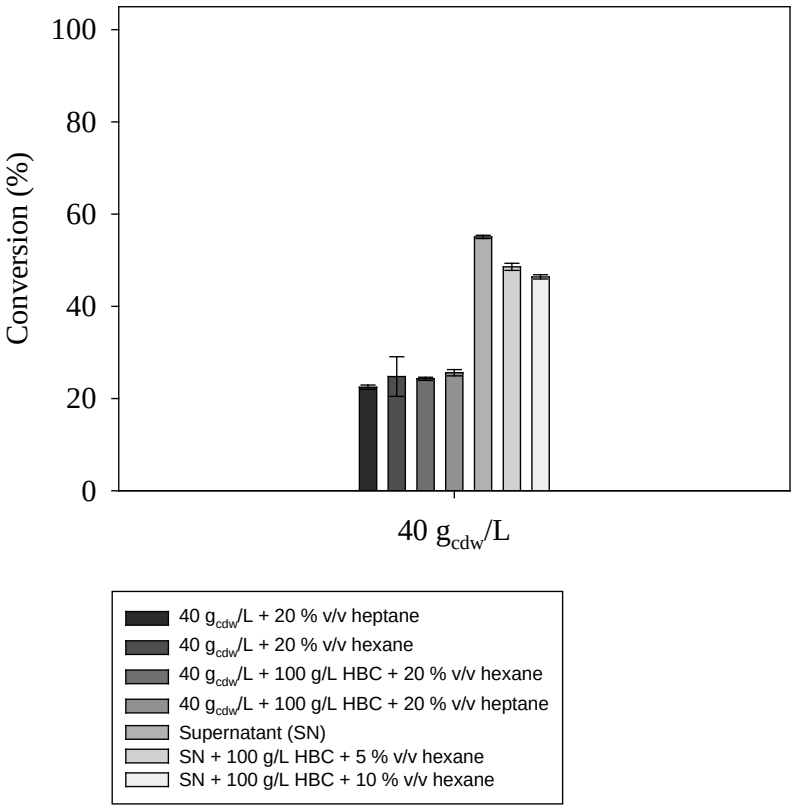


**Figure 24: Whole-cell biotransformation (2 M):** Reaction conditions: 2 M *o*-chloroacetophenone, 40 $g_{cdw}$/L, 10-100 g/L HBC, 5-20 % v/v hexane or heptane, 6 mM $NAD^+$, 2050 mM sodium formate, 48 h.* [1] Recovery: 87 – 97.5 %.

Figure 25 displays the effects of lowering the catalyst concentration to 20 $g_{cdw}$/L at 2 M substrate loading accompanied by increased amounts of HBC/hexane. 50-100 g/L HBC are capable of more than doubling conversions to > 50 %, whereas further addition of 5 % v/v hexane are not significantly contributing to any change.

[1] *Conversion performed using supernatant: 40 mg lyophilized cells were re-hydrated in 0.5 mL potassium phosphate buffer, centrifuged (10 min, 13.2 k rpm, 25°C) followed by isolating the supernatant and adding $NAD^+$, sodium formate, HBC and substrate.

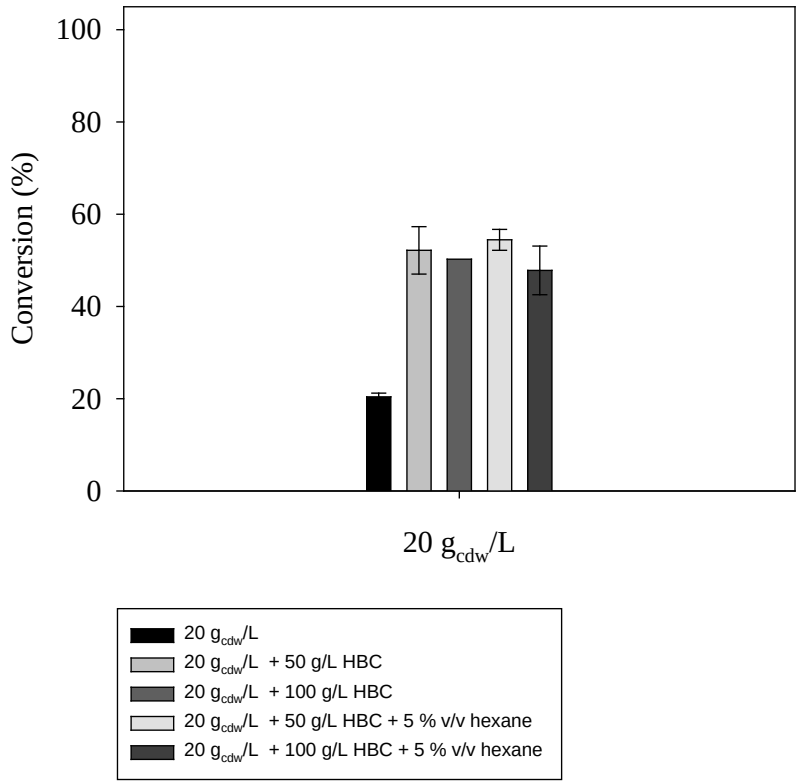


**Figure 25: Whole-cell biotransformation (2 M):** Reaction conditions: 2 M *o*-chloroacetophenone, 20 $g_{cdw}$/L, 0-100 g/L HBC, 5 % v/v hexane, 6 mM $NAD^+$, 2050 mM sodium formate, 48 h. Recovery: 88 – 99 %.

*Conversion of 1.9 M o-chloroacetophenone under optimized conditions.*

**Table 5: Whole-cell biotransformation (1.9 M):** Reaction conditions: 1.9 M *o*-chloroacetophenone, 40 $g_{cdw}$/L, 100 g/L HBC, 6 mM $NAD^+$, 1950 mM sodium formate, 48h.

| **Conversion (%)** | **Std. Dev. Conversion (%)** | **e.e. Product (%)** | **Std. Dev. e.e (%)** | **Product (g/L)** | **TON $g_{product}/g_{cdw}$** |
|---|---|---|---|---|---|
| 98.1 | 2.3 | 99.97 | 0.05 | **291** | **7.3** |

## 4. Discussion

*Phase solubility study and Gibbs energy calculations.* Strong enzyme inactivation by *(S)*-1-(2-chlorophenyl)ethanol and *o*-chloroacetophenone impelled the establishment of *in situ* substrate supply and product removal strategies[28]. Following that, the suitability of HBC for ISSS/ISPR was tested by performing a phase solubility study. The data obtained was used to calculate binding constants which are regarded as beneficial in comparing complexation efficiencies of different cyclodextrin/guest species and therefore ISSS/ISPR aptness. Binding constants (*K*) can be calculated by rearranging the chemical equilibrium for cyclodextrin/guest molecules where solely the slope (k) and the intrinsic solubility are needed for determination[6]. According to the literature, a 1:1 complex is assumed if the slope $k \leq 1$, a 2:1 complex if $k > 1$. In the latter case, two guest molecules bind to one cyclodextrin molecule. For *o*-chloroacetophenone k = 0.86, representing a 1:1 complex, while k = 1.24 for *(S)*-1-(2-chlorophenyl)ethanol suggesting a 2:1 complex. For *o*-chloroacetophenone $K_S$ was calculated to 532 $M^{-1}$ reflecting a moderately strong binding constant, while $K_P$ for *(S)*-1-(2-chlorophenyl)ethanol equals 3 $M^{-2}$. The higher the constants are the more effective complexation is. Keeping in mind that this deceptively low value for $K_P$ accounts for a 2:1 complex, it still can be regarded as highly favourable as *(S)*-1-(2-chlorophenyl)ethanol is showing higher enzyme inactivating effects[28,29]. Both binding constants therefore suggest effective protection of the whole-cell catalyst. Gibbs energy values might be used alternatively to estimate complexation efficiencies for various and individual cyclodextrin concentrations[6]. As can be seen in the respective section, Gibbs energy values flatten at higher HBC concentrations, which can be ascribed to increased viscosities[30] and self-aggregation of HBC with the latter causing less binding sites to be available for complexation[24]. Further, as both, substrate and product are hydrophobic liquids, oil-in-water emulsions generally form at concentrations exceeding the intrinsic solubility. With HBC increasing the viscosity of the

mixture, fine dispersion of substrate/product molecules is less favourable thereby decreasing efficient HBC/guest molecule interactions. Thus, working at elevated HBC concentrations should be considered not recommendable in terms of complexation efficiency as well as mixing behaviour.

*Complex preparation.* Although phase solubility studies are generally performed over stretched time periods, no extended equilibration time is necessary for efficient complexation of HBC/substrate to happen. As can be seen in Figure 14, microwave irradiation or liquid complexation carried out immediately before starting the reactions do not differ largely in terms of conversion and further suggest efficient catalyst protection. This assessment seems justified when comparing HBC-aided whole-cell biotransformations with those performed without protective agents and even higher catalyst concentrations (Figure 18, Figure 28). If storage of HBC/substrate complexes is preferred, MWI represents a fast method in terms of preparing crystallized complexes, while liquid complexation can be considered a method of choice to quickly test different HBC/substrate ratios in follow-up biotransformations.

*Cyclodextrin-cell adsorption studies.* In the first adsorption study, an HBC concentration of 337 mM was chosen to entirely dissolve 300 mM substrate. Following that, liquid substrate molecules are unable to form oil-in-water emulsions and are unlikely to attach to cells immediately after starting the reaction. Due to full encapsulation, substrate-mediated effects of enzyme inactivation were thought to be minimized. As can be seen in Figure 17, HBC concentrations near or at the point of full substrate solubilization result in demulsification of reaction mixtures. In addition, HBC/substrate complexes have to undergo cycles of de-complexation/re-complexation for efficient biotransformation to happen. As already described in the respective section, a high degree of pelletized/adsorbed HBC results in high specific activities of the whole-cell catalyst, whereas increased catalyst concentration causes less HBC

to be pelletized relative to the amount of catalyst. These findings could be simply ascribed to the elevated viscosity of the reaction mixture at high HBC and catalyst concentrations. However, it should be stated that substrate/product concentrations actually measured in supernatants are covering a range of 215 - 280 mM for 40 - 1.5 $g_{cdw}$/L. This indicates that recoveries for substrate/product molecules increase at lower whole-cell catalyst concentrations and are allegedly contradictive to the conclusion drawn prior. A second adsorption study was carried out aiming at further clarifying the fate of HBC/substrate or product complexes and non-complexed HBC molecules, which was not taken into account in the first study. The conditions tested only included 4 $g_{cdw}$/L lyophilized cells and 150 mM HBC with or without 300 mM substrate. As it can be seen in Figure 8, HBC is desorbing from cells over time without substrate present, but is adsorbing when 300 mM substrate are added. One explanation for the adsorption of HBC/substrate over time lies within the affinity of substrate (or product) molecules towards hydrophobic cell membranes being present additionally to the hydrophobic cavity of HBC. As 1:2 HBC/substrate complexes were prepared, substrate molecules outnumber HBC by a factor of two causing HBC to be brought into the vicinity of cell membranes more likely. This process occurs over several hours and reverses up to a certain extent after 24 h of rotation, probably due to cell disintegration. These results elucidate the findings of adsorption study 1: Protective effects of HBC vanish in combination with increased catalyst concentration due to the decreased polarity of the reaction medium causing substrate molecules to continuously dissolve in cell membranes rather than forming complexes with HBC. This is further supported by diminished complexation efficiencies at higher amounts of HBC leading to an oversupply of substrate delivered to the whole-cell catalyst ending up in inactivation. Vice versa, at lower whole-cell catalyst loadings less substrate will dissolve in membranes leading to a higher degree of HBC/substrate complexes offering expanded protection combined with increased specific activities. The phenomenon of HBC/substrate complexes tending to desorb at elevated

catalyst concentrations is now explicable by re-complexation of HBC and substrate/product molecules after being delivered to the whole-cell catalyst. In this case, re-complexation can be considered more favourable due to the decreased reaction medium polarity compared to low catalyst loadings. On the other hand, desorption of HBC over time without substrate present is explicable by a high degree of cell membrane permeability resulting in enzyme leakage followed by enzyme/HBC interactions releasing adsorbed HBC (see next sections).

*Whole-cell activity and enzyme leakage.* The cell-free biotransformations carried out and described in section 3.6.2 suggest rethinking the term 'whole-cell' biotransformation – at least in this case. Theoretically, when applying whole-cell catalysts reactions are thought to take place in the cytosol or periplasma. However, lyophilisation increases the permeability of the cell membrane (compare Figure 27 and Figure 28). This might not only lead to increased substrate uptake but also trigger protein release. Enzyme leakage from lyophilized cells was proven by means of affinity chromatography and cell-free biotransformations, where solely supernatants of re-hydrated and centrifuged cells were applied. Full conversion of 300 mM substrate was achieved by additionally deploying 100 g/L HBC. Centrifugation promotes protein release of lyophilized cells, and so does HBC supported by the results presented in section 3.3. The activity of XR (WT) expressed in the whole-cell catalyst used was determined to ~ 1730 $U/g_{cdw}$ for the soluble fraction and ~ 590 $U/g_{cdw}$ for the insoluble fraction (B-Per lysis), with 2320 $U/g_{cdw}$ representing the sum. Measurements of whole-cell activities applying 4 $g_{cdw}/L$ lyophilized cells in combination with e.g. 75 mM HBC resulted in 2670 $U/g_{cdw}$ maximally thereby exceeding 2320 $U/g_{cdw}$ obtained after B-Per lysis. The conclusion to be drawn here has to include cell membrane permeabilization and enzyme leakage promoted by HBC. Interactions of cyclodextrins and cell membranes are well known phenomena, especially in terms of disordering membrane components like cholesterol, phospholipids and protein extraction from membranes[9,31]. In the case of 4 $g_{cdw}/L$ cells and

75 mM cyclodextrins, HBC-aided enzyme release results in the soluble enzyme fraction to be found outside the cells, which increases substrate availability and activity. The results obtained also suggest solubilisation of the insoluble enzyme fraction in the presence of HBC (under certain conditions) and enzyme stabilization (next section). At higher HBC concentrations enzyme destabilization prevails and decreases whole-cell activities. Further, intrinsic enzyme inactivation can be observed for XR under all conditions tested, while FDH partially displays a higher stability. For XR being expressed to a higher degree, coagulation is more likely to occur compared to FDH contributing to intrinsic enzyme inactivation. Stabilizing and solubilizing effects of HBC on FDH are not that pronounced compared to XR, as already a large fraction of FDH is released without the aid of HBC.

*Enzyme stabilization by HBC.* One of the major prerequisites for protein aggregation to happen includes partially unfolded proteins exposing their hydrophobic structures. Derivatives of β-cyclodextrins (like HBC) are capable of forming complexes with phenylalanine, tyrosine, histidine and tryptophane thereby inhibiting hydrophobic protein–protein interaction and aggregation[12].

In section 3.5, activities of isolated XR as well as partially purified FDH were measured after being incubated with 50 % v/v hexane, hexanol or heptane. In these experiments, the main reason for enzyme inactivation is protein precipitation at the organic/aqueous interface, which can be clearly seen in Figure 10. Although visible enzyme precipitation in mixtures containing hexanol, hexane or heptane set in after 24 h, XR activities were already reduced after 1 h in the presence of hexanol. This is explicable by the liquid water interfacial tension of hexanol (0.0068 N/m at 20°C) being lower than that of hexane or heptane (0.0511 N/m at 20°C), which additionally leads to hexanol intercalating in XR. In each case, the presence of HBC boosted enzyme activities. However, at higher HBC concentrations activities decrease. Possible reasons for this phenomenon might be found in the homodimeric enzyme structures

of both, XR and FDH. Elevated HBC concentrations might contribute to enzyme distortion by binding to hydrophobic amino acids and finally lead to the dissociation of the homodimers. As described prior, the combination of hexane and 100 g/L HBC (~62 mM) resulted in enzyme hyperactivation (~13.8 U/mg). These results suggest that XR activities can be influenced positively in hydrophobic surroundings, making it more likely to handle increased substrate concentrations.

*Whole-cell biotransformation (300 - 400 mM).* The addition of HBC to reaction mixtures containing lower amounts of catalyst results in overall positive effects regarding conversions (Figure 18, Figure 19). This is attributed to HBC forming catalyst-protective non-rigid inclusion complexes with substrate/product molecules and stabilizing effects of XR and FDH. One should keep in mind that a major part of these reactions will take place outside the whole-cell catalyst due to enzyme leakage. Therefore, enzyme stabilization has to be taken into account particularly at low HBC concentrations. 4 $g_{cdw}$/L cells and 75 mM HBC result in ~90 % conversion of 300 mM substrate, which corresponds to a HBC/substrate stoichiometry of 1:4. This ratio cannot guarantee for effective catalyst protection and ISSS/ISPR. Following that, 75 mM HBC on 4 $g_{cdw}$/L catalyst should be considered the most effective HBC/catalyst stabilizing ratio, at least under these conditions, which drives successful conversion. Vice versa, higher HBC concentrations not only increase viscosities but contribute to enzyme destabilizing effects at lower catalyst concentrations and self-aggregation of HBC accompanied by substrate inclusion decreasing conversions. At higher catalyst amounts, HBC-aided conversion diminishes. Not surprisingly, at increased catalyst concentrations there is no need for adding stabilizing or protecting agents, as the amount of substrate applied can be readily converted. Moreover, concurring equilibria between HBC/substrate and HBC/enzyme seem to be shifted towards HBC/enzyme causing, if not balanced, enzyme destabilization and more substrate or product to be uncomplexed thereby inactivating the

catalyst. Mass transfer problems have to be considered as well, which are further contributing to results not being highly divergent, even when doubling catalyst concentrations (Figure 19). Changing reaction medium polarity (Figure 20, Table 4) influenced outcomes negatively, especially when increased amounts of isopropanol were applied. Isopropanol itself was found to be XR inactivating[32].

*Whole-cell biotransformation (1.5 – 2M).* As mentioned prior, limitations in mass transfer will inevitably result at higher catalyst, HBC or substrate loadings. One crucial element in this regard is constituted by sufficient $NAD^+$ supply. Figure 21 displays the impact of increasing $NAD^+$ concentrations contributing to higher conversions. As both, XR and FDH undergo inactivation (intrinsic or precipitation at organic/aqueous interface) in the course of biotransformation, increased amounts of $NAD^+$ will guarantee for higher reactions rates over the first several hours. $NAD^+$ limitations further explain all too similar outcomes of conversions at 400 mM substrate loading mentioned before. Moreover, the original whole-cell catalyst expressing XR wild-type was replaced by a catalyst co-expressing XR D51A and FDH. The major difference lies within the higher catalytic efficiency of the XR D51A variant compared to XR wild-type, which were calculated to $k_{cat}/K_m$ = 1500 ($M^{-1}s^{-1}$)[32] for D51A and $k_{cat}/K_m$ = 340 ($M^{-1}$ $s^{-1}$) for the wild-type, respectively. As the enantiomeric excess for both enzyme variants is quite similar (> 99 %), XR D51A proved to be the enzyme of choice, which was demonstrated in the full conversion of 1.5 M substrate (Figure 21). The specific activities on D-xylose and sodium formate are significantly lower for the novel whole-cell catalyst (XR D51A ~ 1105 $U/g_{cdw}$, FDH ~ 37 $U/g_{cdw}$) compared to the XR wild-type containing strain (XR wild-type ~ 2319 $U/g_{cdw}$, FDH ~ 180 $U/g_{cdw}$). FDH activities were thought to be the overall limiting factor for efficient whole-cell conversion. This assumption does not hold any longer, as 37 $U/g_{cdw}$ are sufficient. This further leads to the conclusion that XR inactivation is way more pronounced than FDH inactivation in the presence of *o*-

chloroacetophenone and *(S)*-1-(2-chlorophenyl)ethanol. XR was found to be the major bottleneck besides limited $NAD^+$ supply. Substrate loadings were further increased to 2 M keeping $NAD^+$ concentrations constant at 6 mM but varying amounts of catalyst and HBC. Under the assumption that XR might show increased activities in hydrophobic surroundings (see enzyme stability study), attempts to establish cyclodextrin-shuttle systems[13] in the presence of 20 % v/v hexane or heptane were made. Alas, 27 % v/v substrate and 20 % v/v hexane or heptane ended up in catalyst inactivation (precipitation) and high reaction mixture viscosity prohibiting this approach. These findings at least indicate an upper limit for the tolerance of organic phase volumes and might be optimizable. Decent results (~ 88 %) were achieved applying 40 $g_{cdw}$/L (Figure 22) and HBC concentrations up to 100 g/L, where again enzyme destabilization prevailed beyond this concentration. The combination of hexane (5 % v/v) and 100 g/L HBC visibly decreases the viscosity of the reaction mixture, which might have been the reason why a higher conversion of ~ 92 % was achieved. By comparing cell-free and whole-cell biotransformations (Figure 22, Figure 24) at catalyst loadings of 40 $g_{cdw}$/L - either applying the whole-cell catalyst or its respective supernatant - results suggest that only soluble enzyme fractions are active without HBC present. These findings are compelling insofar as it has to be assumed that mass transfer limitations by cell membranes are either non-existent, or the soluble enzyme fraction is found outside the cells even without HBC present. This further emphasizes the findings that HBC is capable of solubilizing the insoluble enzyme fraction under certain conditions. Not surprisingly, decreasing catalyst concentrations to 20 $g_{cdw}$/L (Figure 25) resulted in conversions of approximately half of those obtained with 40 $g_{cdw}$/L.

The final optimization applying 40 $g_{cdw}$/L lyophilized cells, 1.9 M substrate and 100 g/L HBC resulted in 98.09 % conversion with an e.e. value of 99.97 %. The turnover number was calculated to 7.29 $g_{product}/g_{cdw}$ yielding 291 g/L product over 48 h.

## 5. Conclusion

Enzyme stabilizing effects as well as the establishment of ISSS/ISPR by HBC are major driving forces contributing to high substrate conversions. Mass transfer limitations at increased catalyst and substrate loadings necessitate elevated $NAD^+$ concentrations. By further changing XR wild-type to XR D51A, 291 g/L *(S)*-1-(2-chlorophenyl)ethanol could be produced.

## 6. Literature


1. Shukla, V. B. & Kulkarni, P. R. Biotransformation of benzaldehyde to L-phenylacetylcarbinol (L-PAC) by free cells of Torulaspora delbrueckii in presence of beta-cyclodextrin. *Brazilian Arch. Biol. Technol.* **45,** 265–268 (2002).
2. Wang, W. & Yu, L. Preparation, characterization, and biotransformation of the inclusion complex of phytosterols and hydroxypropyl-β-cyclodextrin by Mycobacterium neoaurum. *Zeitschrift fur Naturforsch. - Sect. C J. Biosci.* **66 C,** 277–282 (2011).
3. Zhang, X.-Y. *et al.* Optimization of biotransformation from phytosterol to androstenedione by a mutant Mycobacterium neoaurum ZJUVN-08 *. *J Zhejiang Univ-Sci B (Biomed Biotechnol)* **14,** 132–143 (2013).
4. Kang, D.-J., Im, J.-H., Kang, J.-H. & Kim, K. H. Whole cell bioconversion of vitamin D3 to calcitriol using Pseudonocardia sp. KCTC 1029BP. *Bioprocess Biosyst. Eng.* **38,** 1281–90 (2015).
5. Kiss, F. M., Lundemo, M. T., Zapp, J., Woodley, J. M. & Bernhardt, R. Process development for the production of 15β-hydroxycyproterone acetate using Bacillus megaterium expressing CYP106A2 as whole-cell biocatalyst. *Microb. Cell Fact.* **14,** 1–13 (2015).
6. Del Valle, E. M. M. Cyclodextrins and their uses: A review. *Process Biochem.* **39,** 1033–1046 (2004).
7. Stella, V. J. & He, Q. Cyclodextrins. *Toxicol. Pathol.* **30,** 30–42 (2008).
8. Szejtli, J. Past, Present, and Future of Cyclodextrin Research. *Pure Appl. Chem.* **76,** 1825–1845 (2004).
9. Zidovetzki, R. & Levitan, I. Use of cyclodextrins to manipulate plasma membrane cholesterol content: Evidence, misconceptions and control strategies. *Biochim. Biophys. Acta - Biomembr.* **1768,** 1311–1324 (2007).

10. European Medicines Agency. Background review for cyclodextrins used as excipients - In the context of the revision of the guideline on ‘ Excipients in the label and package leaflet of medicinal products for human use’ (CPMP/463/00 Rev. 1). **44,** (2014).

11. Malanga, M. *et al.* ‘Back to the Future’: A New Look at Hydroxypropyl Beta-Cyclodextrins. *J. Pharm. Sci.* **105,** 2921–31 (2016).

12. Serno, T., Geidobler, R. & Winter, G. Protein stabilization by cyclodextrins in the liquid and dried state. *Adv. Drug Deliv. Rev.* **63,** 1086–1106 (2011).

13. Bricout, H., Hapiot, F., Ponchel, A., Tilloy, S. & Monflier, E. Chemically modified cyclodextrins: An attractive class of supramolecular hosts for the development of aqueous biphasic catalytic processes. *Sustainability* **1,** 924–945 (2009).

14. Kratzer, R., Woodley, J. M. & Nidetzky, B. Rules for biocatalyst and reaction engineering to implement effective, NAD(P)H-dependent, whole cell bioreductions. *Biotechnol. Adv.* (2015). doi:10.1016/j.biotechadv.2015.08.006

15. Kurbanoglu, E. B., Taskin, M., Zilbeyaz, K. & Hasenekoglu, I. Efficient Synthesis of (S)-1-(2-chlorophenyl)ethanol in the Submerged Culture of Alternaria alternata Isolate. *Chinese J. Catal.* **30,** 370–374 (2009).

16. Sato Y, Onozaki Y, Sugimoto T, Kurihara H, Kamijo K, Kadowaki C, Tsujino T, Watanabe A, Otsuki S, Mitsuya M, Iida M, Haze K, Machida T, Nakatsuru Y, Komatani H, Kotani H, I. Y. Imidazopyridine derivatives as potent and selective polo-like kinase (PLK) inhibitors. *Bioorg Med Chem Lett* **19,** 4673–4678 (2009).

17. Sato T, Sugimoto K, Inoue A, Okudaira S, Aoki J, T. H. Synthesis and biological evaluation of optically active Ki16425. *Bioorg Med Chem Lett* **22,** 4323–4326 (2012).

18. Bissantz C, Grether U, Kimbara A, Nettekoven M, Roever S, R.-E. M. 1,2,3-Triazolo[4,5-d]pyrimidine derivatives as agonists of the cannabinoid receptor 2 agonists. *WO 2013076182 A1* (2013).

19. https://www.clearsynth.com/en/CST56406.html.

20. Kratzer, R., Leitgeb, S., Wilson, D. K. & Nidetzky, B. Probing the substrate binding site of Candida tenuis xylose reductase (AKR2B5) with site-directed mutagenesis. *Biochem. J.* **393,** 51–58 (2006).

21. Gonzales, M. F., Brooks, T., Pukatzki, S. U. & Provenzano, D. Rapid Protocol for Preparation of Electrocompetent Escherichia coli and Vibrio cholerae. 6–11 (2013). doi:10.3791/50684

22. Higuchi, T. & Connors, K. A. Phase solubility techniques, advances in analytical chemistry and instrumentation. *Interscience* **4,** 117–212 (1965).

23. Badr-Eldin, S. M., Ahmed, T. A. & Ismail, H. R. Aripiprazole-cyclodextrin binary systems for dissolution enhancement: Effect of preparation technique, cyclodextrin type and molar ratio. *Iran. J. Basic Med. Sci.* **16,** 1223–1231 (2013).

24. Loftsson, T., Másson, M. & Brewster, M. Self-association of cyclodextrins and cyclodextrin complexes. *J Pharm Sci.* 1091–1099 (2004).

25. Pandit, V., Gorantla, R., Devi, K., Pai, R. & Sarasija, S. Preparation and

characterization of pioglitazone cyclodextrin inclusion complexes. *J. Young Pharm.* **3,** 267–74 (2011).

26. Mochida, K., Kagita, A. & Matsui, Y. Effects of Inorganic Salts on the Dissociation of b-Cyclodextrin with an Azo Dye in an Aqueous Solution. *Bull. Chem. Soc. Jpn.* **46,** 3703–3707 (1973).

27. Loftsson, T. & Brewster, M. E. Cyclodextrins as functional excipients: Methods to enhance complexation efficiency. *J. Pharm. Sci.* **101,** 3019–3032 (2012).

28. Schmölzer, K., Mädje, K., Nidetzky, B. & Kratzer, R. Bioprocess design guided by in situ substrate supply and product removal: process intensification for synthesis of (S)-1-(2-chlorophenyl)ethanol. *Bioresour. Technol.* **108,** 216–23 (2012).

29. Mädje, K., Schmölzer, K., Nidetzky, B. & Kratzer, R. Host cell and expression engineering for development of an E. coli ketoreductase catalyst: enhancement of formate dehydrogenase activity for regeneration of NADH. *Microb. Cell Fact.* **11,** 7 (2012).

30. www.roquette.com.

31. Mahammad, S. & Parmryd, I. Cholesterol depletion using methyl-β-cyclodextrin. *Methods Mol. Biol.* **1232,** 91–102 (2015).

32. Kratzer, R. Unpublished results. (2005).

# 7. Supporting information

## Bioreactor cultivation

**Table 6: *E.coli* Rosetta2 pre-culture growth medium.**

| Solution | Component | Concentration (g/L) |
|---|---|---|
| A | Glucose·$H_2O$ | 5.5 |
| B | Peptone (Casein) | 10 |
| | Yeast extract | 5 |
| | NaCl | 5 |
| | $NH_4Cl$ | 1 |
| | $MgSO_4$·7 $H_2O$ | 0.25 |
| | Trace element solution | 1× |
| | Polypropylene glycol | 0.1× |
| C | $K_2HPO_4$ | 3 |
| | $KH_2PO_4$ | 6 |

× mL/L

**Table 7: Trace element solution.** All components were dissolved in 5 M HCl.

| Component | Concentration (g/L) |
|---|---|
| $FeSO_4$·7 $H_2O$ | 4 |
| $MnSO_4$·$H_2O$ | 1 |
| AlCl·6 $H_2O$ | 0.55 |
| $CoCl_2$ | 0.4 |
| $H_3BO_3$ | 0.1 |
| $CuSO_4$·5 $H_2O$ | 0.15 |
| $ZnSO_4$·7 $H_2O$ | 0.2 |
| $Na_2MoO_4$·2 $H_2O$ | 0.2 |

**Table 8: Bioreactor growth medium (5 L).**

| Solution | Substance | Concentration (g/L) |
|---|---|---|
| A | Glucose·$H_2O$ | 22 |
| B | Peptone (Casein) | 10 |
| | Yeast extract | 5 |
| | NaCl | 5 |
| | $NH_4Cl$ | 1 |
| | $MgSO_4$·7 $H_2O$ | 0.25 |
| | Trace element solution | 1× |
| | Polypropylene glycol | 0.1× |
| C | $K_2HPO_4$ | 3 |
| | $KH_2PO_4$ | 6 |

× mL/L

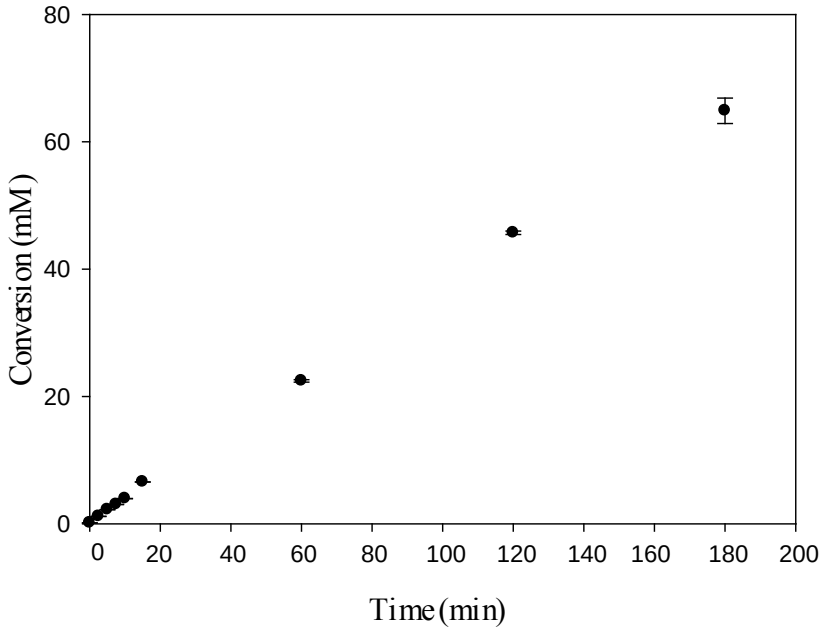


**Figure 26: Time course.** Reaction conditions: 4 $g_{cdw}$/L lyophilized cells, 75 mM HBC, 300 mM substrate, 350 mM sodium formate. Whole-cell activity calculated out of linear slope: 102 U/$g_{cdw.}$

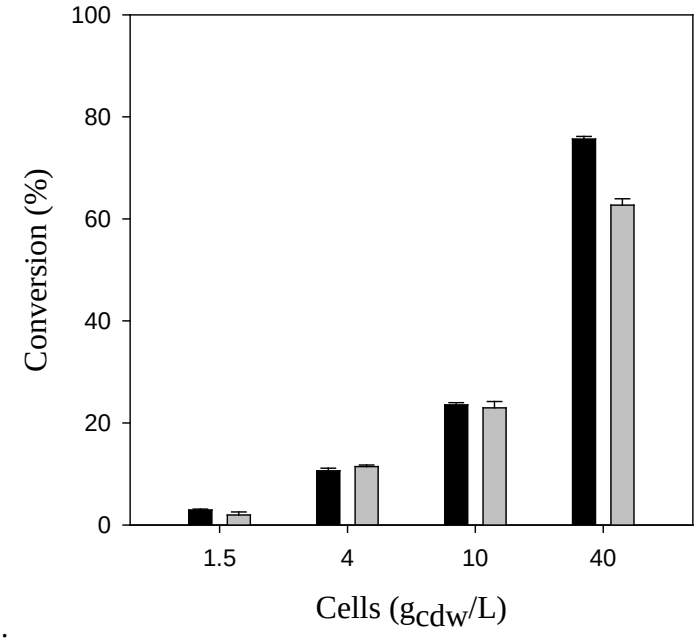


.

**Figure 27: Whole-cell biotransformation (300mM) with frozen cells:** Performance of cells frozen for 2 days at -20°C or -70°C after cell-harvest. Reaction conditions: 1.5-40 $g_{cdw}$/L cells, 300 mM substrate, 350 mM sodium formate, 24 h.

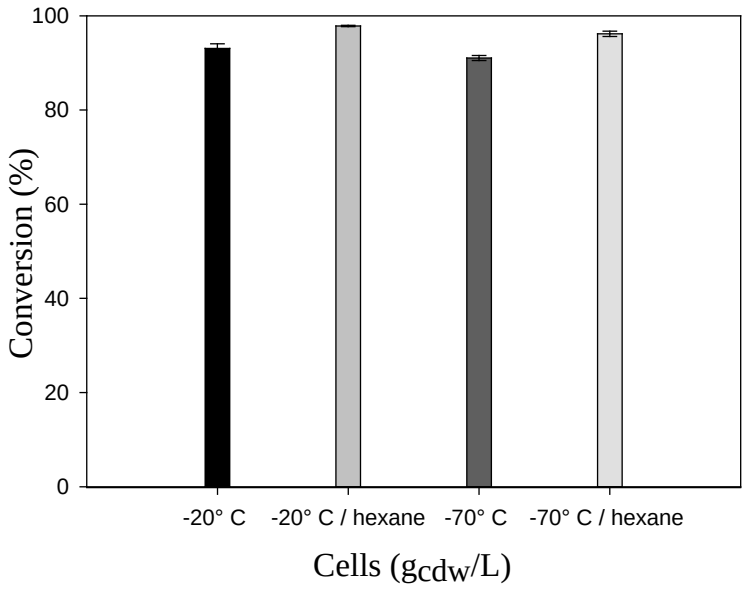


**Figure 28: Whole-cell biotransformation (300mM) with lyophilized cells:** Cells frozen prior at -20°C or -70°C (black & dark grey bars) were lyophilized and subjected to whole-cell biotransformations. Effects of 20 % v/v hexane on conversions were tested further (light grey bars). Reaction conditions: 40 $g_{cdw}$/L cells, 300 mM substrate, 350 mM sodium formate, 24 h, +/- 20 % v/v hexane.

# Separation behavior and microstructure of *E. coli* stabilized Pickering emulsions derived from two-phasic whole-cell bioreductions

Bernhard Lauss[1], Christian Rapp[1], Dorothea Leis, Bernd Nidetzky*, Regina Kratzer*

Institute of Biotechnology and Biochemical Engineering, Graz University of Technology, Petersgasse 12/I, 8010 Graz/Austria

[1]Equally contributing
*Corresponding authors

RK: phone +43 316 873 8412
e-mail: regina.kratzer@tugraz.at

**Keywords:** Whole cell bioreaction mixture, phase separation quality, settling behavior, crud phase, droplet size, microscopy

## Abstract

Constraints in downstream processing attributed to cell-stabilized emulsions gave rise to scrutinize factors triggering emulsion formation and stability in the whole-cell bioreduction of *o*-chloroacetophenone to *(S)*-1-(2-chlorophenyl)ethanol. Water-immiscible organic solvents necessary to fully convert 300 mM substrate and the presence of 40 $g_{cell\ dry\ weight}$/L *E. coli* catalyst resulted in partial separation of organic and aqueous phase accompanied by an intermediate, accumulated 'crud' phase after centrifugation. Microscopic investigation of reaction mixtures revealed the formation of droplet-like, emulsified structures placed at the organic/aqueous phase boundary suggesting Pickering-like emulsions. Addition of 1.5 v/v reaction volumes of 1-propanol, isopropanol and ethanol to reaction mixtures containing 20 % v/v hexane caused crud phases to collapse. 90 % of isolated product was obtained when isopropanol was applied. The impact of 1-10 % isopropanol on the reaction and separation behavior manifested in decreased conversions and less extraction volumes required for complete crud phase destabilization. The droplet size distribution of reaction mixtures containing 20 % v/v hexane and isopropanol in increasing amounts faintly corresponded to the findings at the macroscopic scale. In addition, droplet sizes determined for 20 or 50 % v/v hexane/hexanol displayed a similar distribution. Cell damaging effects of 20-50 % v/v hexane or hexanol were evaluated by determining the protein release of lyophilized cells into the aqueous phase. Protein release of rehydrated cells was approximately 45 % of the total soluble protein assuming 50 % soluble protein of the total cell dry weight. 50 % v/v hexanol in reaction mixtures led to an increase to 55 %.

# 1. Introduction

A common strategy of overcoming low substrate solubility in whole-cell biocatalysis lies within the deployment of water-immiscible organic solvents. Moreover, by establishing two-phasic systems *in situ* substrate supply (ISSS) and product removal (ISPR) prevents reactant-based biocatalyst inactivation. In this study, the reduction of *o*-chloroacetophenone to *(S)*-1-(2-chlorophenyl)ethanol applying *Candida tenuis* xylose reductase (*Ct*XR) is serving as prime example in evaluating process constraints attributed to whole-cell bioreductions, such as cell-stabilized emulsions. These emulsions previously identified as Pickering-like emulsions (Leis et al., 2016) appear as cells positioned at the organic/aqueous interface stabilizing organic phase droplets (organic solvent, liquid substrate & product) thereby preventing them from coalescing. Despite favourable process conditions as increased mass transfer arising from emulsification, effective downstream processing is hindered by accumulation at the organic-aqueous phase boundary during extractive work-up finally leading to product loss. Thus, circumventing intermediate phase (= crud phase) formation will not solely shorten extraction time but also contribute to recover higher amounts of product. As previously shown by Leis (2016), altering the aqueous phase polarity of the reaction mixture by e.g. acidifying, alkalifying or increasing ionic strength, crud phases proved to be withstanding even harsh modifications. Hence, in order to weaken the interaction of cells and organic phase droplets, the effects of adding organic co-solvents capable of allowing for co-solvent molecules to be partitioned in both phases - organic and aqueous - will be studied.

## 2. Materials and methods

### 2.1. Chemicals and strains

Chloramphenicol, 1-hexanol (98 %), 1-butanol (99 %), *N*,*N*-dimethylformamide (99 %), acetonitrile (≥ 99.9 %), kanamycin, *o*-chloroacetophenone, polymyxin B sulfate and sodium formate were purchased at Sigma-Aldrich (Vienna, Austria). Ampicillin, D-xylose, hexane (≥ 99 %), $NAD^+$ (free acid, ≥ 97.5 %) and NADH disodium salt (≥ 98 %), methanol (≥ 99.9 %), 2-propanol (≥ 99.7 %), dimethyl sulfoxide (99.5 %), glycerol (98 %), acetone (≥ 99.5 %) were obtained from Roth (Karlsruhe, Germany). Ethanol (96 %) was from VWR Chemicals (Leuven, Belgium), 1-propanol (≥ 99.8 %) from Lab-Scan (Gliwice, Poland) and B-Per® Reagent (Bacterial Protein Extraction Reagent) from Thermo scientific (Waltham, MA USA). Pierce™ BCA Protein Assay Kit was from Thermo Fischer Scientific.

Other chemicals were from Sigma-Aldrich/Fluka or Roth, and were of the highest purity available. 15 and 50 mL tubes were obtained from Sarstedt (Wr. Neudorf, Austria), 1.5 mL tubes from Eppendorf (Wien, Austria) and 2 mL tubes (SafeSeal micro tubes, 2 mL, PP) from Eppendorf (Nümbrecht, Germany). Culture C tubes (16x100 mm, Teflon-faced cap) were from Wheaton (USA). The used strain was an *E. coli* Rosetta 2 co-expressing *Candida tenuis* xylose reductase and *Candida boidinii* formate dehydrogenase (Mädje et al., 2012).

### 2.2. Biomass production

Bioreactor cultivation was performed in a Biostat CT 6.9-Liter BioReactor (B. Braun Biotech International GmbH, Melsungen, Germany) with a working volume of 5 L, a vessel height to vessel diameter ratio of 2, equipped with a twin 6-blade disc turbine stirrer (stirrer diameter to vessel diameter ratio of 0.4). pH was maintained at 7.0 by automated addition of 1 M $H_3PO_4$ and 2 M KOH, temperature was kept at 37°C and 18°C (double jacket vessel). The inoculum ($OD_{600}$ 8) was prepared in two 1000 mL baffled shaken flasks using 250 mL of complex medium supplemented with 5.5 g/L glucose, 115 mg/L ampicillin, 50 mg/L kanamycin, 34 mg/L chloramphenicol. The bioreactor medium was a complex medium, supplemented with

22 g/L glucose, 115 mg/L ampicillin, 50 mg/L kanamycin, 34 mg/L chloramphenicol (Supporting Information, Table S1). Start $OD_{600}$ was 0.5, cultivation temperature 37°C, air saturation was kept at 45 % by an agitation and airflow cascade. At an $OD_{600}$ of 2.0, 1 mM IPTG and 115 mg/L ampicillin was added and the temperature was decreased to 18°C. After 24 h of cultivation, 115 mg/L ampicillin was again added. Cells were harvested after 48 h by centrifugation. Biomass was freeze-dried (Christ α 1-4 lyophilizer, Braun Biotech International) and stored at -18°C without activity loss for two years.

**2.3. Biotransformations**

*E. coli* biomass (40 gram cell dry weight per liter ($g_{CDW}$/L) of freeze dried or 164 gram cell wet weight per liter of fresh cells ($g_{cww}$/L)) were suspended in 100 mM potassium phosphate buffer (pH 6.2), supplemented with $NAD^+$ (0.5 mM), polymyxin B sulfate (36 µM) and sodium formate (350 mM). Cell suspensions were mixed at room temperature and 30 rpm on an end-over-end rotator (SB3 from Stuart) for 60 minutes to allow for cell permabilization and, in case of freeze dried cells, rehydration. The substrate *o*-chloroacetophenone was pre-dissolved in the respective co-solvent (50 or 20 % (v/v) hexane or hexanol) and added after cell permeabilization to the cell suspension. (Concentrations refer to total reaction volumes consisting of aqueous and organic phase) (Schmölzer et al., 2012). Bioreductions were performed either in 15 mL sterile polypropylene tubes from Sarstedt (length 112 mm, diameter 17 mm) in a total reaction volume of 10 ml or in 2 mL Eppendorf tubes in a total reaction volume of 1 mL. Tubes were incubated on an end-over-end rotator (SB3 from Stuart) at 30 rpm and room temperature for 24 h.

**2.4. Settling and centrifugation experiments**

Phase separation behavior of the obtained reaction mixtures was directly investigated in the used 15 ml, transparent tubes. The tubes were incubated at room temperature without further mixing and phase separation quality was photographically recorded after 1, 3, 5 and 24 hours. Then, tubes were centrifuged for 30 seconds, 10 minutes and 30 minutes at 4000 rpm (3220 g,

4°C) and photos were taken. Photos obtained from gravity settling and centrifugation experiments were visually analyzed with regard to phase volumes of the organic, aqueous, crud phase and the pellet. Samples were taken for light microscopic analysis.

*Organic modifiers.* The used solvents with their respective log*P* values in parenthesis were glycerol (-1.8), dimethyl sulfoxide (DMSO, -1.4), *N*,*N*-dimethylformamide (DMF, -0.83), methanol (-0.82), acetonitrile (-0.33), ethanol (-0.31), acetone (-0.042), 2-propanol (0.26), 1-propanol (0.34), 1-butanol (0.58), hexane (3.8) (10; 11). Modifiers were added to the reaction mixture after the bioreduction and prior to centrifugation. The effect of an increasing amount of modifier was studied by adding the solvent stepwise. After the addition of the solvent the mixture was centrifuged for 10 min (3220 g, 4°C), a photo of the tube was taken and the separated reaction mixture vigorously shaken until a homogeneous state was reached. The procedure was repeated until no more changes in phase separation upon addition of the solvent were observed.

**2.4.1. Forced phase separation**

Biotransformations (20 % v/v hexane) were performed as described prior (see 2.2) in a total reaction volume of 10 mL. After 24 h 4 mL of the reaction mixture were transferred into sterile glass tubes from Wheaton followed by adding 1.5 v/v reaction volumes of isopropanol (6 mL) and a short vortexing period. After initial spontaneous phase separation the mixtures were either left for gravity settling (72 h) or subjected to centrifugation. Centrifugal forces were increased stepwise while keeping centrifugation time (2 min) constant. Phase volume ratios were determined using Image J.

## 2.5. Light microscopy

Samples were analyzed directly after bioreduction before phase separation occurred, after 24 h of gravity settling, and after centrifugation at 4000 rpm (3220 g, 4°C) for 30 s, 10 min and 30 min. 5 µL of each sample were transferred onto an object plate and fixed with a cover glass (both from Carl Roth, Karlsruhe, Germany). Samples were investigated using a light microscope with 10-, 40- and 100-fold objective magnification and 5 or 10-fold ocular enlargement (Leica Microsystems DM LB2, Vienna, Austria). Photos were taken with an integrated camera (Leica Microsystems CDF350 FX, Vienna, Austria) for further droplet size and shape analysis. Droplet sizes were evaluated with the image processing software ImageJ (National Institutes of Health, Betheda, USA). Therefore, one picture per image enlargement and sample (generally 2 samples per reaction mixture) was analyzed.

*Droplet size distribution and average droplet size*. Numbers of analyzed droplets were >600 for reaction mixtures with 50 and 20 % v/v hexanol. 440 and 1100 (from two independent experiments) droplets were sized for reaction mixtures with 50 and 20 % v/v hexane, respectively. After aging and centrifugation of the reaction mixture with 50 % v/v hexanol 1100 and 300 droplets were analyzed, respectively. For reaction mixtures treated with isopropanol 720 droplets (1 % Isopropanol), 530 droplets (5 % Isopropanol) and 1400 droplets (10 % Isopropanol) were investigated.

## 2.6 Chiral HPLC analysis

Reaction mixtures were centrifuged for 30 minutes at 4000 rpm and 4 °C and samples of the separated organic and aqueous phases were taken. Aqueous samples were diluted 1:50 into potassium phosphate buffer, pH 6.2, 100 mM; the organic samples were diluted 1:50 into HPLC-grade ethanol (99 % absolute). HPLC analysis was performed as previously described (Schmölzer et al., 2012).

### 2.7. Protein and FDH release in the presence of organic solvents

Lyophilized cells (40 mg) were transferred into 2 mL Eppendorf tubes followed by addition of potassium phosphate buffer (100 mM, pH 6.2) up to a volume of 0.5 mL. The mixtures were placed on a thermomixer for 30 min, 25°C and 1400 rpm to allow for cell rehydration. 200 – 500 µL hexane/hexanol and 300 mM *o*-chloroacetophenone or *(S)*-1-(2-chlorophenylethanol) (optionally) were added. Reference mixtures were prepared without organic solvents. The total working volume was 1 mL. The mixtures were rotated (end-over-end rotator, 30 rpm, RT) for 1 h and centrifuged for 10 min at 13.2k rpm and 25°C. Resulting aqueous phases were isolated and subjected to protein and enzyme assays. Protein concentrations in the aqueous phase were diluted in potassium phosphate buffer and determined using Pierce™ BCA Protein Assay Kit.

### 2.8. Survival rate of the biocatalyst

40 mg cells were rehydrated for 30 min in 500 µL of potassium phosphate buffer, 100 mM, pH 6.2. Then the cells were diluted to 40 mg/mL in pure buffer or in buffer with 20 or 50 % v/v hexane or hexanol. The mixtures were incubated for 16 h. 200 µL of mixtures with a concentration of 40 mg/mL were plated on LB plates containing ampicillin, chloramphenicol and kanamycin. The plates were incubated at 37°C for 18 h prior to counting of surviving colonies.

### 2.9. Downstream processing of isopropanol-modified reaction mixtures

Reaction mixtures containing 20 % (v/v) hexane and 300 mM *o*-chloroacetophenone were distributed to 50 mL Sarstedt tubes to a final volume of 10 mL. Isopropanol was added with an excess of 2 (v/v) reaction volumes for crud phase disintegration. Therefore, the tubes were vortexed and centrifuged for 10 min (3220 g, 25°C) resulting in pelletized cells and the product-containing supernatant. The supernatant was transferred into a 100 mL round flask and evaporated under reduced pressure to fractionate the isopropanol-water azeotrope. *(S)*-1-(2-chlorophenyl)ethanol was separated from remaining water/cell debris by re-extraction into

ethyl acetate (20 mL; 2 v/v) in the presence of 0.5 g NaCl. The upper organic phase was subjected to a second evaporation step under reduced pressure.

## 3. Results

We have previously described the NADH-dependent reduction of *o*-chloroacetophenone to (*S*)-1-(2-chlorophenyl)ethanol, a chiral key intermediate for the synthesis of therapeutic relevant polo-like kinase 1 inhibitors (Sato et al, 2009), lysophosphatidic acid receptor agonists (Sato et al., 2012) and cannabinoid receptor 2 agonists (Bissantz et al., 2013). The used whole-cell biocatalyst was an *E. coli* co-expressing the catalytic reductase and a formate dehydrogenase for NADH recycling (Mädje et al., 2012). *In situ* extraction of hydrophobic substrates and products into a water-immiscible solvent has shown to intensify the reaction under the assumption of biocatalyst protection. A catalyst loading of 40 to 50 $g_{CDW}$/L recombinant *E. coli* and hexane 20 % v/v in the reaction mixture led to full conversion of 300 mM *o*-chloroacetophenone. Cells present in the reaction mixture acted as emulsifying agents and a homogenous, milk-like emulsion was obtained after the reaction. Product isolation was accomplished by threefold extraction with hexane. Each extraction step was followed by centrifugation to separate the organic phase. The costs for (*S*)-1-(2-chlorophenyl)ethanol isolation in a total yield of 86 % from a batch reduction of 23 g *o*-chloroacetophenone accounted for one third of the entire process costs (Eixelsberger et al., 2013). The accumulation of the product in the organic phase with a partition coefficient of 109 ($\frac{c_{org}}{c_{aqu}}$) (Leis et al., 2016) prompted investigations of the present reaction mixtures with regard to separation behavior.

### 3.1. Characterization of reaction mixtures

We have previously shown that reducing the percentage of the organic co-solvent during the whole-cell reduction from 50 to 20 % increased conversion. Bioreduction of 300 mM o-chloroacetophenone resulted in ~200 mM product when 50 % hexane was used and in full conversion (96 - 97 %) when 20 % hexane was used. Similarly, 50 % of hexanol as second phase led to a conversion of ~50 % and was increased to 70 % when 20 % of hexanol was used (2). In the present experiments reaction mixtures containing 20 % and 50 % (v/v) second phase were used in order to examine the effects of both, conversion and phase separation in the presence of organic modifiers.

#### 3.1.1. Gravity settling and centrifugation

We investigated the settling behavior of reaction mixtures containing 50 or 20 % v/v hexane or hexanol as *in situ* extractant (Figure 1). No organic phase separated after 24 h of gravity settling under these conditions. Approximately half of the aqueous phase separated in reaction mixtures containing hexane (Figures 1A,1B). <3 % v/v of the aqueous phase separated in reaction mixtures with 50 or 20 % v/v hexanol (Figures 1C,1D). Centrifugation (3220 g) of reaction mixtures with 50 % for only 30 s led already to the separation of 50 and 41 % v/v of hexane and hexanol, respectively. Further 9.5 min centrifugation of the reaction mixture with hexane increased the separated organic phase to 74 % v/v and finally to 77 % by another 50 min of centrifugation (Figure 1A). 49 % v/v of the organic phase separated from reaction mixtures containing 20 % v/v hexane after 60 min of centrifugation (Figure 1B). Hexanol separated generally slower compared to hexane. A total centrifugation time of 60 min led to 59 % v/v of hexanol from the reaction mixture containing 50 % v/v hexanol (Figure 1C). No organic phase separated during centrifugation in reaction mixtures with 20 % v/v hexanol (Figure 1D). The experiments were repeated with fresh cells. Lyophilized and fresh cells showed very similar separation behavior. No significant difference was observed (data not shown).

### 3.1.2. Spontaneous vs. forced phase separation

After adding isopropanol (1.5 v/v) to reaction mixtures containing 20 % v/v hexane spontaneous phase separation occurred after mixing leading to 48 – 67 % upper liquid phase and 33 – 52 % loosely contracted crud phase. Phase volume ratios continuously changed slowly ending up in a ratio of 70/30 after 24 h of gravity settling. No further phase alterations were observed even after 3 days of settling. Centrifugation at 10 g for 2 min was sufficient for a crud phase contraction of 16.5 % thereby forcing pelletation. Further centrifugation at 50 g (2 min) led to a contraction of 13 % with respect to the value obtained after 10 g for 2 min (see supporting infotmation, S1).

## 3.2 Characterization of lyophilized biocatalyst

### 3.2.1. Protein release from lyophilized biocatalyst

The protein release of rehydrated cells was approximately 45 % of the total soluble protein assuming 50 % soluble protein of the total cell dry weight. This percentage hardly changed when the aqueous phase was replaced by 20 or 50 % v/v hexane or 20 % hexanol. 50 % v/v hexanol in the mixture led to an increase to 55 %. FDH activity was 6.3 U/mL which is approximately 90 % of the total FDH activity in the lyophilized biomass. Presence of 20 % co-solvents decreased the FDH activity by approximately 20 % whereas 50 % v/v hexane or hexanol led to a reduction of ca. 40 %. Presence of substrate or product hardly changed protein release. Furthermore, FDH activities insignificantly decreased compared to reaction mixtures without substrate or product.

### 3.2.2. Survival rate of biocatalyst

The survival rate after lyophilization and rehydration was 11 colonies per milligram cell dry weight. The additional presence of 20 and 50 % hexane or hexanol resulted in complete sterilization of the biomass.

### 3.3. Light microscopy of emulsions

Microscopic analysis of reaction mixtures after 24 h of mixing showed that the major proportion of the organic phase was present as droplets in an oil-in-water emulsion. Droplets were covered and separated by single *E. coli* cells and cell aggregates (Figure 2A). Smallest droplets evaluable by light microscopic resolution were approximately in the size of the *E. coli* cells (~1 µm). Microscopic emulsion structures that showed larger organic phase inclusions (starting at approximately 70 µm) lost drop shape characteristics and were considered as bicontinuous structures (Figure 2B). Droplet size distribution of reaction mixtures with 20 and 50 % v/v hexanol or hexane was similar (Figure 2C, 2D). Most droplets were in the size range of ~1 to 5 µm. Large droplets with >50 µm diameter and bicontinuous emulsion structures were recorded for all reaction mixtures. However, samples with hexanol showed in general a higher tendency to form bicontinuous emulsion structures. Mean droplets sizes were 12.8 and 9.8 µm for 50 and 20 % v/v hexanol. Droplet sizes of reaction mixtures with 20 and 50 % v/v hexane showed mean droplet sizes of 10.1 to 10.6 µm. Droplet size differences with hexane were merely significant as the standard droplets size deviation was determined to 0.4 µm. Droplet size distribution was furthermore investigated during emulsion aging and centrifugation in reaction mixtures with 50 % v/v hexanol. After 24 h, droplet sizes were shifted towards larger droplets and after centrifugation (3220 g, 30 min) droplets sizes of 5 to 15 µm dominated (Figure 3). Average droplet sizes for reaction mixtures containing 20 % v/v hexane and isopropanol were 17.6, 21 and 7.7 µm for 1, 5 and 10 % v/v isopropanol present. In comparison to non-modified reaction mixtures, isopropanol contributes to the formation of disrupted droplet-structures.

### 3.4. Addition of solvents as emulsion modifiers

The solvents ethanol, 1-propanol, isopropanol, 1-butanol and hexane were added stepwise to a reaction mixture with 20 % v/v hexane as co-solvent after a reaction time of 24 h. The goal was to minimize the interfacial crud phase and thereby optimize product recovery.

Additionally, the impact of 1 – 10 % isopropanol on the reaction- and separation- behavior was investigated (Figure 6). Isopropanol decreases conversion by 0.4 % present at 1 % v/v whereas 10 % v/v cause a massive drop in conversion of 45 % accompanied by a complete crud phase destabilization at 0.8 v/v reaction volumes.

#### 3.4.1. Centrifugation

Changes in organic (= water-immiscible co-solvent) or upper liquid phases (= water-miscible co-solvent) and crud phase ratios upon addition of ethanol, 1-propanol, isopropanol, 1-butanol and hexane to reaction mixtures containing 20 % (v/v) hexane are depicted in Figure 4. As e.g. in the case of hexane or butanol excessive amounts of co-solvent had to be applied to display no or minor effects upon addition, all crud phase values were referenced to those obtained after 10 min of centrifugation without organic modifiers present (23.8 %; straight line) thereby avoiding distorted phase volume ratios and keeping data comparable. On the x-axis the actual percentage of organic modifier added is shown, while the y-axis displays the capability of the modifier to interact with both, organic and aqueous phase. Therefore, effective interactions result in high upper liquid phase ratios accompanied by low amounts of modifier added. Addition of hexane up to 80 % v/v shows no effect on the extent of the interfacial crud or the organic phase volume ratio. At this point, still 20% (v/v) of the total volume consist of pellet, aqueous phase and crud phase, with the latter being nearly unchanged compared to its initial volume. Butanol leads to an increase in the upper liquid phase accompanied by a crud phase swelling until it collapses to its initial value of approximately 23 % (v/v). Highly water-miscible co-solvents like isopropanol, 1-propanol and ethanol efficiently destroy the crud phase at 60 % (v/v) organic modifier present all

leading to one-phasic systems: Isopropanol continuously decreases the crud phase to the point it finally disappears ending up in 90 % (v/v) upper liquid phase and 10 % (v/v) pellet. 1-propanol extensively increases the crud phase volume until it finally breaks. Ethanol as well leads to a decrease in the crud phase starting from 30 % v/v. As ethanol participates in the aqueous phase to a higher extent, the final crud collapse at 60 % v/v accompanied by a massive increase in the upper phase is explicable by aqueous and organic phase combining to one phase at this point.

### 3.5. Product isolation

Downstream processing of isopropanol-modified reaction mixtures yielded 90 % of isolated product. Centrifugation temperature was increased to 25°C as there was no different behavior observable compared to 4°C at 3220 g. The extraction volume of isopropanol was increased from 1.5 to 2 (v/v) ensuring no product will be lost in the pellet.

## 4. Discussion

Multiphasic bioreductions require fine dispersion to increase interfacial areas and promote mass transfer. Cells that attach to the aqueous-organic interface get trapped and stabilize organic phase droplets leading to the formation of stable emulsions (Pickering emulsions). Simple geometric considerations suggest that spreading the biomass present in the reaction mixture (40 $g_{cdw}$/L) leads to a single cell layer with an area of ~300 m². Summing up drop surface areas of the 20 % v/v hexanol mixture leads to a similar value of 100 m². Assuming a monolayer of cells stabilizing organic droplets leads to a two-fold excess of *E. coli* cells. Excessive cells are found either in the aqueous phase or as cell aggregates attached to organic phase droplets. "Bridging" of droplets by a single cell layer (Horozov, 2006) and incomplete droplet coverage play minor roles and the obtained 100 m² drop surface area might represent the maximally stabilizable interface using 40 $g_{cdw}$/L. This notion is supported by the observation that excessive hexanol in the 50 % v/v mixture was present as a bicontinuous

structure that was easily separable by centrifugation. Larger droplets in reaction mixtures with 50 % v/v hexanol were not observed (Chevalier and Bolzinger, 2010).

*Effect of surface tension.* Leis et al. (2016) have previously investigated separation times of plain hexane-water and hexanol-water mixtures in a settling cell constructed for fast liquid-liquid separation (Henschke et al., 2002). A 45 % longer separation time of the hexane-water mixture (41 s) compared to the hexanol-water mixture was observed. The capability of hexanol to form hydrogen bonds is reflected by its lower liquid/water interfacial tension (6.8 mN/m, 25°C) compared to hexane (51.1 mN/m, 20°C). Hence, the energy necessary to increase the interface is higher when hexane is used, which explains the longer separation time in plain buffer.

However, separation willingness is reversed in the presence of biomass: Attachment of *E. coli* cells to surfaces mediated by hydrogen bonding and hydrophobic interactions (Zita and Hermansson, 1997) is reflected by a lower separation efficiency especially in terms of hexanol. The interaction of *E. coli* with hexane is solely hydrophobic mirroring higher organic phase recoveries compared to hexanol. Additionally, the ability of reaction mixtures with hexanol to form bicontinuous structures is again explicable by the high affinity of hexanol to the biomass and its lower interfacial tension (Tavacoli et al., 2015).

*Centrifugation experiments: 20 % v/v hexane and addition of modifiers.* Glonke et al. (2016) recently reported a full extraction of *(S)*-styrene oxide from a whole-cell biocatalytic system (E. *coli*) through catastrophic phase inversion applying bis(2-ethylhexyl)phthalate (BEHP) as extractive solvent. The emulsion was forced to switch from oil-in-water to water-in-oil by adding dispersed phase (organic phase) in a volumetric phase ratio of 4:1 organic:aqueous phase. In our experiments a similar approach was intended when hexane was added in excess amounts to reaction mixtures already containing 20% (v/v) hexane as second phase. Alas, no catastrophic phase inversion was observed even after the reaction mixture consisting of more

than 80 % (v/v) hexane. Here, hydrophobic interactions between cells and hexane seem to be stable and independent from the volume of the co-solvent deployed. Further, Furtado et al (2015) stated that 10 % v/v iso-butanol (logP 0.8) added to 30% (v/v) of hexadecane serving as second phase in 70% (v/v) of aqueous yeast suspension led to 96 % oil recovery by means of gravity settling, while 10 % (v/v) ethanol only resulted in 10 % recovery. With hexane being less hydrophobic compared to hexadecane, we applied 1-butanol instead of iso-butanol. With almost no change in crud phase volume but a slight increase of the upper liquid phase, 1-butanol turned out to be as less effective as hexane. After addition of ~ 80 % v/v 1-butanol the combined substrate and product concentration measured in the upper liquid phase (~ 94 % v/v) of the reaction mixture was 242.6 mM. This result clearly shows that emulsion destabilizing effects originating from butanol partitioning are only weakly present. These findings are also supported by the difference of only 14 % v/v regarding butanol added and increased upper liquid phase, indicating the naturally low miscibility of butanol and water. Ethanol, 1-propanol and isopropanol displaying higher water miscibility made crud phases collapse at 60 % v/v added modifier. Substrate and product concentrations determined in the upper liquid phase after the crud phases entirely pelletized widely differed, though. Isopropanol resulted in a total recovery of ~ 288 mM, while ethanol and 1-propanol only led to ~ 210 mM and ~ 170 mM, respectively.

*Impact of isopropanol present during the reaction.* Isopropanol displaying a logP value of 0.26 proved to be most suitable in destabilizing Pickering-like emulsions for crud-phase-free downstream processing. In addition, by continuously influencing emulsion stability in ongoing reactions the amount of isopropanol for extractive work up is reduced. Simultaneously, crud phase volumes decrease (Figure 6). These findings might be ascribed to a weakening in interfacial tension of hexane (and liquid substrate/product) droplets upon partition of isopropanol. As droplets grow smaller, cells are no longer capable of stabilizing

emulsified structures and are forced into the aqueous phase, theoretically. However, the macroscopic behavior of isopropanol modified reaction mixtures does not entirely correspond to the microscopic results: By comparing the droplet size distribution of reaction mixtures modified with 1 – 10 % v/v isopropanol, an increase in the number of droplets ranging from ≥ 1 and < 5µm and decreased numbers for ≥ 5 and < 15µm can be observed. The size distribution of reaction mixtures containing 20 % v/v hexane shows a high similarity to that obtained for 10 % v/v isopropanol present, suggesting no effect at all. Large quantities of isopropanol also give rise to cell rupture followed by cell debris being present in the upper liquid phase requiring further processing after the initial extractive work up. Conversion drops simultaneously to increased isopropanol present during the reaction. Data corroborate that the stability of isolated XR in the presence of 12.5 % v/v isopropanol in 50 mM potassium phosphate buffer (pH 7) is markedly affected by decreasing the half-life time $t_{1/2}$ from 10.7 d to 8.3 h (Kratzer R., unpublished results, 2005).

*Spontaneous vs. forced phase separation.* As gravity settling limits phase separation to approximately 70:30 upper liquid phase:crud phase, addtional energy input is required to overcome bacterial attachment to organic phase droplets. The centrifugal force necessary leading to bacterial desorption appears to be relatively low (< 10 g), suggesting that isopropanol largely accounts for destabilizing Pickering-like emulsions. Additionally, Wheaton tubes were preferred over Sarstedt tubes due to the less cone shaped bottom causing cells to settle more uniformly. In order to achieve the highest product recovery possible reaction mixtures were centrifuged at 3220 g for 10 min yielding 282 – 294 mM (94 – 98 %) product in the upper liquid phase.

*Significance for product isolation.* Leis et al. (2016) alkalified reaction mixtures containing 20 % v/v hexane to pH 13.5 prior to extractive work up. After three consecutive extraction/centrifugation steps deploying 1.2 v/v hexane in total the final evaporation step resulted in 87% isolated yield. With the intention to further increase the isolated yield, an alternative downstream strategy involving crud phase disintegration was developed. As already mentioned above, the newly developed method yielded 90 % of isolated product. Ethyl acetate had to be applied additionally to isopropanol in the extractive workup. Having in mind that both solvents can be recycled and no consecutive centrifugation steps are necessary, the time saving achieved justifies the slight increase of 3% isolated yield.

*Protein release from lyophilized biocatalyst.* As protein concentrations and FDH activities were measured after 1 h (Figure 5) ensuring proper enzyme activities, further reaction mixtures containing 20 % v/v hexane or hexanol were prepared to determine the protein release after 24 h (rotation, 30 rpm, RT) followed by 24 h of gravity settling (see supporting information, S2). By comparing the protein concentrations of reaction mixtures with 20 % v/v hexane or hexanol, a slight increase can be observed after 24 h, whereas protein release into the aqueous phase during the process of aging hardly changes.

Additionally, in the case of 50 % v/v hexanol and 300 mM of product present, the FDH activity is similar to reaction mixtures containing substrate, but protein concentration is significantly decreased indicating protein precipitation. This phenomenon is explicable by a higher solubility of product in hexanol: As emulsions form, a higher product concentration will be found in hexanol droplets with cells being attached to it. This inevitably leads to a more severe damage of the cell membrane by permeabilization of both, product and hexanol followed by increased protein release and precipitation at the organic/aqueous interface. Nevertheless, precipitated proteins are hardly involved in crud phase stabilization as it has to be assumed that proteins would further enrich in the crud phase, despite nearly 50 % of the

total protein already being released into the aqueous phase. Further, as reaction mixtures containing lyophilized cells or fresh cells tend to stabilize crud phases in a similar way, protein stabilization is unlikely due to fresh cells should not be showing protein release to this high extent.

## 5. Conclusion

Organic modifiers displaying partition coefficients suitable for the dissolution of both, organic and aqueous phase, turned out to be the solvents of choice to pelletize an emulsified intermediate phase. However, efficient crud phase disintegration only occurred when isopropanol was used yielding 90 % of isolated product. The droplet size distribution of reaction mixtures containing 20 % v/v hexane and isopropanol in increasing amounts do not fully correspond to the findings at the macroscopic scale, as elevated amounts of isopropanol significantly reduce the extraction volume for crud phases to collapse. In addition, droplet size distributions for 20 or 50 % v/v hexane/hexanol are barely congruent with phase volume ratios suggesting interactions not observable by light microscopic methods.

## Funding

This work was supported by the Austrian Science Fund (FWF; Elise Richter grant V191-B09 to R.K.) Funding to pay the Open Access publication charges for this article was provided by the Austrian Science Fund (FWF).

Bissantz C, Grether U, Kimbara A, Nettekoven M, Roever S, Rogers-Evans M. 2013. 1,2,3-Triazolo[4,5-d]pyrimidine derivatives as agonists of the cannabinoid receptor 2 agonists. WO 2013076182 A1

Chevalier Y, Bolzinger MA. 2013. Emulsions stabilized with solid nanoparticles: Pickering emulsions. Colloids Surf B 439, 23-34.

Collins J, Grund M, Brandenbusch C, Sadowski G, Schmid A, Bühler B. 2015. The dynamic influence of cells on the formation of stable emulsions in organic–aqueous biotransformations. J Ind Microbiol Biotechnol 42, 1011-1026.

Henschke M, Schlieper LH, Pfennig A. 2002. Determination of a coalescence parameter from batch-settling experiments. Chem Eng J 85, 369-378.

Krebs T, Ershov D, Schroen C, Boom RM. 2013. Coalescence and compression in centrifuged emulsions studied with in situ optical microscopy. Soft Matter 9, 4026-4035.

Leis D, Lauß B, Macher-Ambrosch R, Pfennig A, Nidetzky B, Kratzer R. 2016. Integration of bioreduction and product isolation: Highly hydrophobic co-solvents promote *in situ* substrate supply and extractive product isolation. J Biotechnol *in press*, http://dx.doi.org/10.1016/j.jbiotec.2016.11.021.

Mädje, K., Schmölzer, K., Kratzer, R., Nidetzky, B. 2012. Host cell and expression engineering for development of an *E. coli* ketoreductase catalyst: Enhancement of formate dehydrogenase activity for regeneration of NADH. Microb. Cell Fact, 11, 1-7.

Sato T, Sugimoto K, Inoue A, Okudaira S, Aoki J, Tokuyama H. 2012. Synthesis and biological evaluation of optically active Ki16425. Bioorg Med Chem Lett, 22, 4323-4326.

Sato Y, Onozaki Y, Sugimoto T, Kurihara H, Kamijo K, Kadowaki C, Tsujino T, Watanabe A, Otsuki S, Mitsuya M, Iida M, Haze K, Machida T, Nakatsuru Y, Komatani H,

Kotani H, Iwasawa Y. 2009. Imidazopyridine derivatives as potent and selective polo-like kinase (PLK) inhibitors. Bioorg Med Chem Lett 19, 4673-4678.

Schmölzer, K., Mädje, K., Kratzer, R., Nidetzky, B. Process engineering to overcome substrate and product toxicity in *E. coli* whole cell-catalyzed reduction of o-chloroacetophenone. Bioresour. Technol. 2012, 108, 216-223.

Tavacoli JW, Thijssen JHJ, Clegg PS. 2015. Bicontinuous emulsions stabilized by colloidal particles. In: Particle-stabilized emulsions and colloids. Eds. Ngai T, Bon SAF. pp. 131-144. The Royal Society of Chemistry, Cambridge, UK.

Zita A, Hermansson, M. 1997. Effects of bacterial cell surface structures and hydrophobicity on attachment to activated sludge flocs. Appl Environ Microbiol, 63, 1168-1170.

Glonke, S., Sadowski, G., Brandenbusch, C. 2016. Applied catastrophic phase inversion: a continuous non-centrifugal phase separation step in biphasic whole-cell biocatalysis. J Ind Microbiol Biotechnol, 43, 1527-1535.

Furtado GF, Picone CSF, Cuellar MC, Cunha RL. 2015. Breaking oil-in-water emulsions stabilized by yeast. Colloids Surf B 128, 568-576.

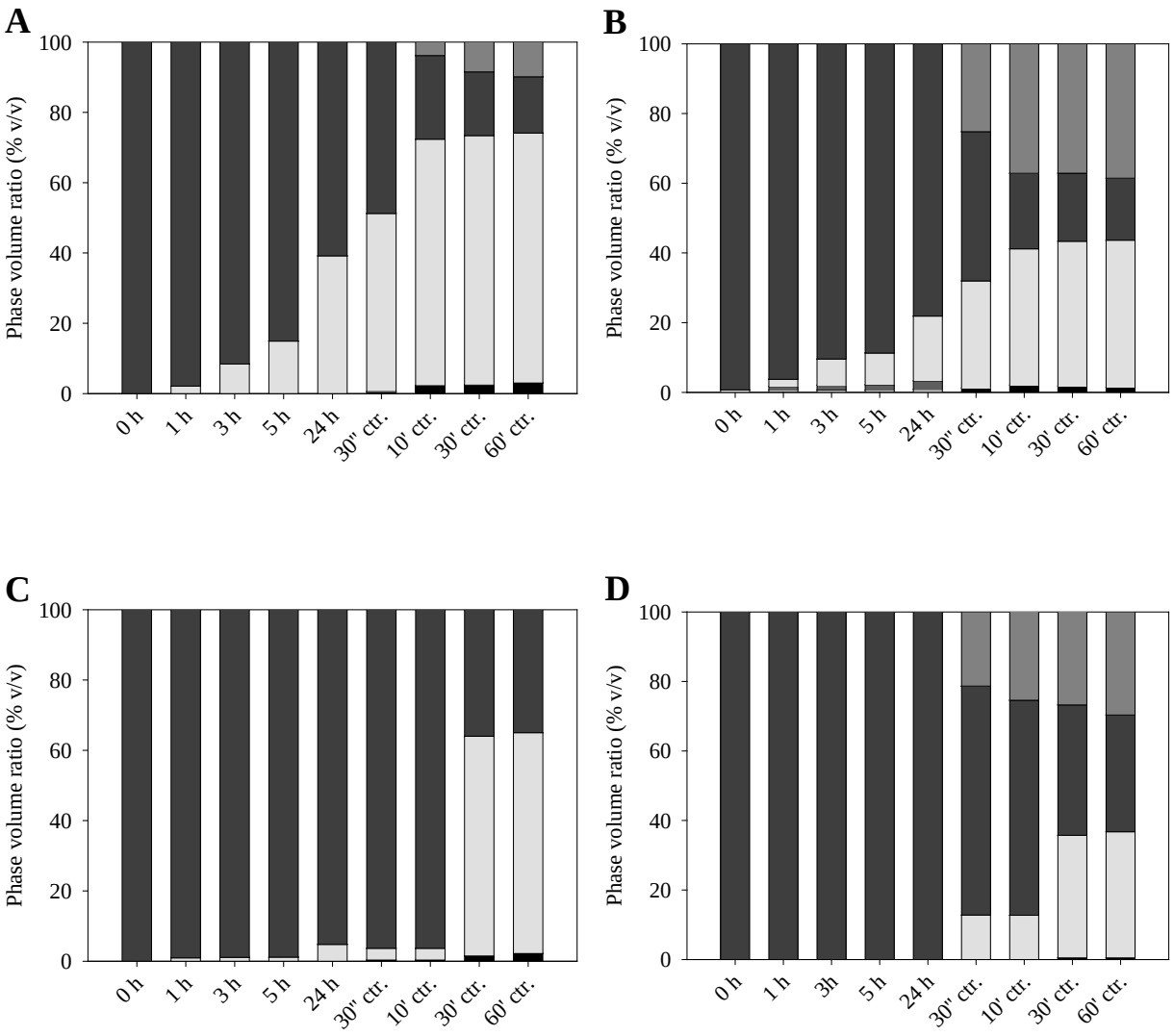


Figure 1. Phase-volume ratios obtained from settling of reaction mixtures. Phase separation during gravity settling (0-24 h) and centrifugation (3220 g; 30 s, 10-60 min). Grey bars indicate organic phases, light grey indicate aqueous phases and dark grey indicate pelleted biomass and crud phases. Reaction mixtures with 20 % v/v hexane (A) or hexanol (C) and with 50 % v/v hexane (B) or hexanol (D).

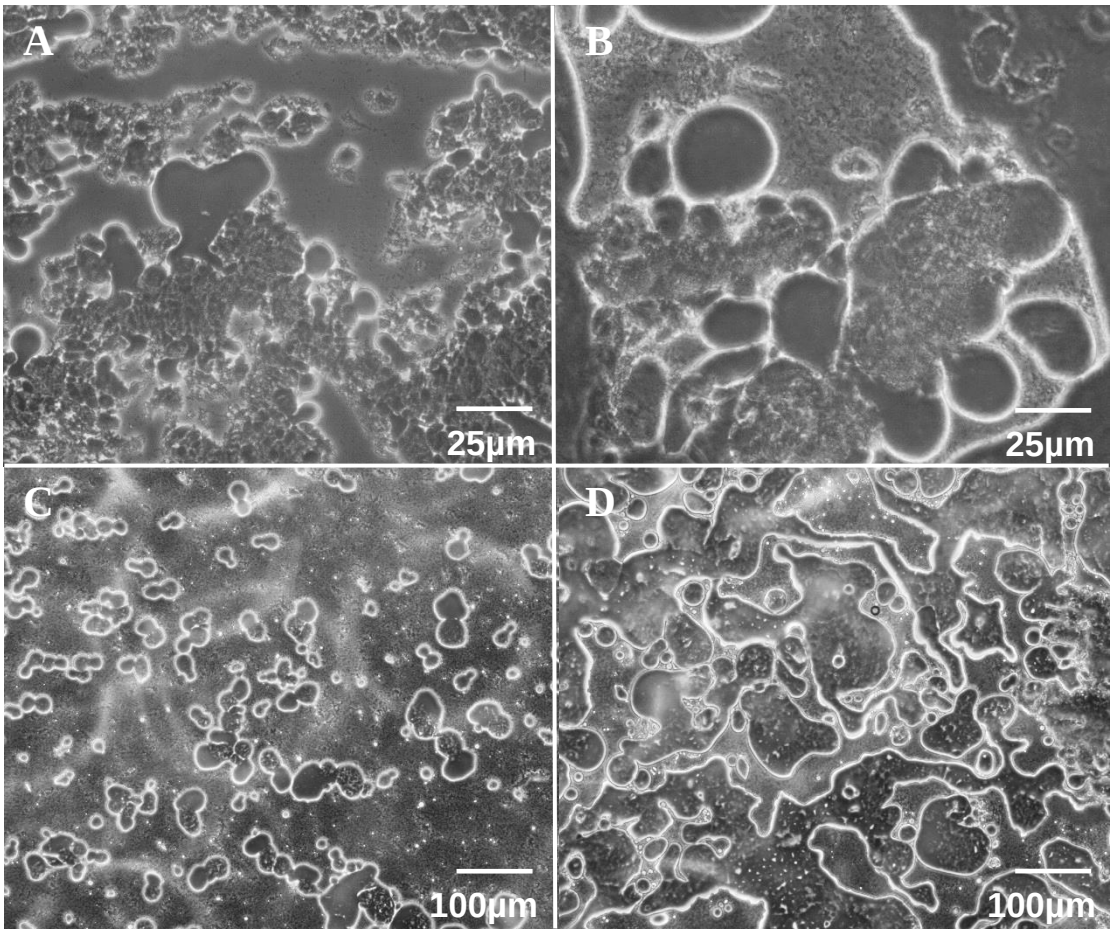


Figure 2. Reaction mixtures analyzed by light microscopy. Conditions were 20 % (A) and 50 % v/v hexane (B, magnification 400-fold); 20 % (C) and 50 % v/v hexanol (D, magnification 100-fold).

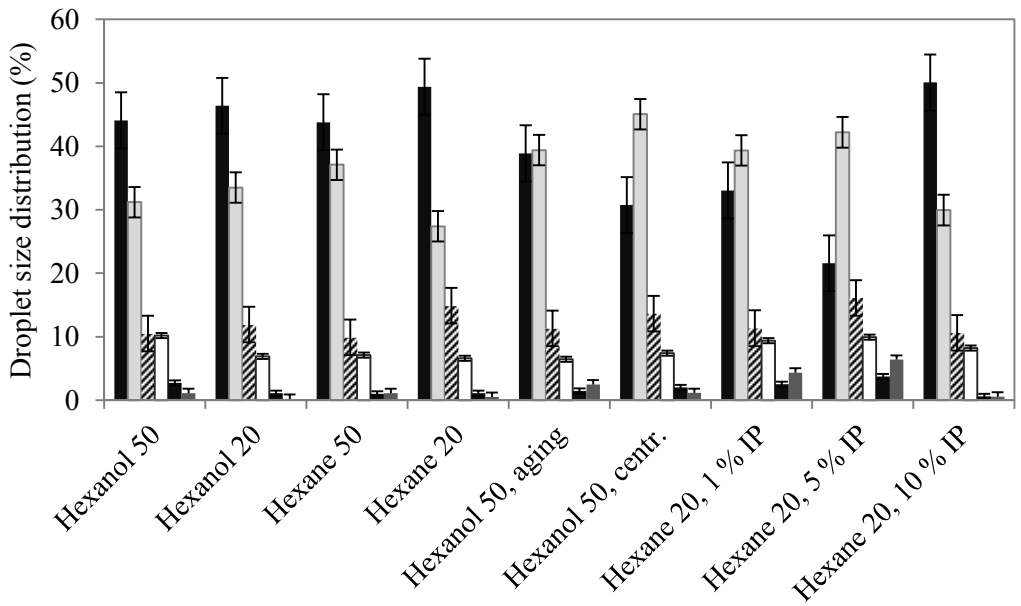


Figure 3. Droplet size distribution in two-phase, whole cell bioreaction mixtures. Droplet size ≥ 1 and < 5µm black bars, ≥ 5 and < 15µm light grey bars, ≥ 15 and < 25µm hatched bars, ≥ 25 and < 50 µm white bars, ≥ 50 and < 75 µm black bars, ≥ 75 µm dark grey bars. IP = isopropanol.

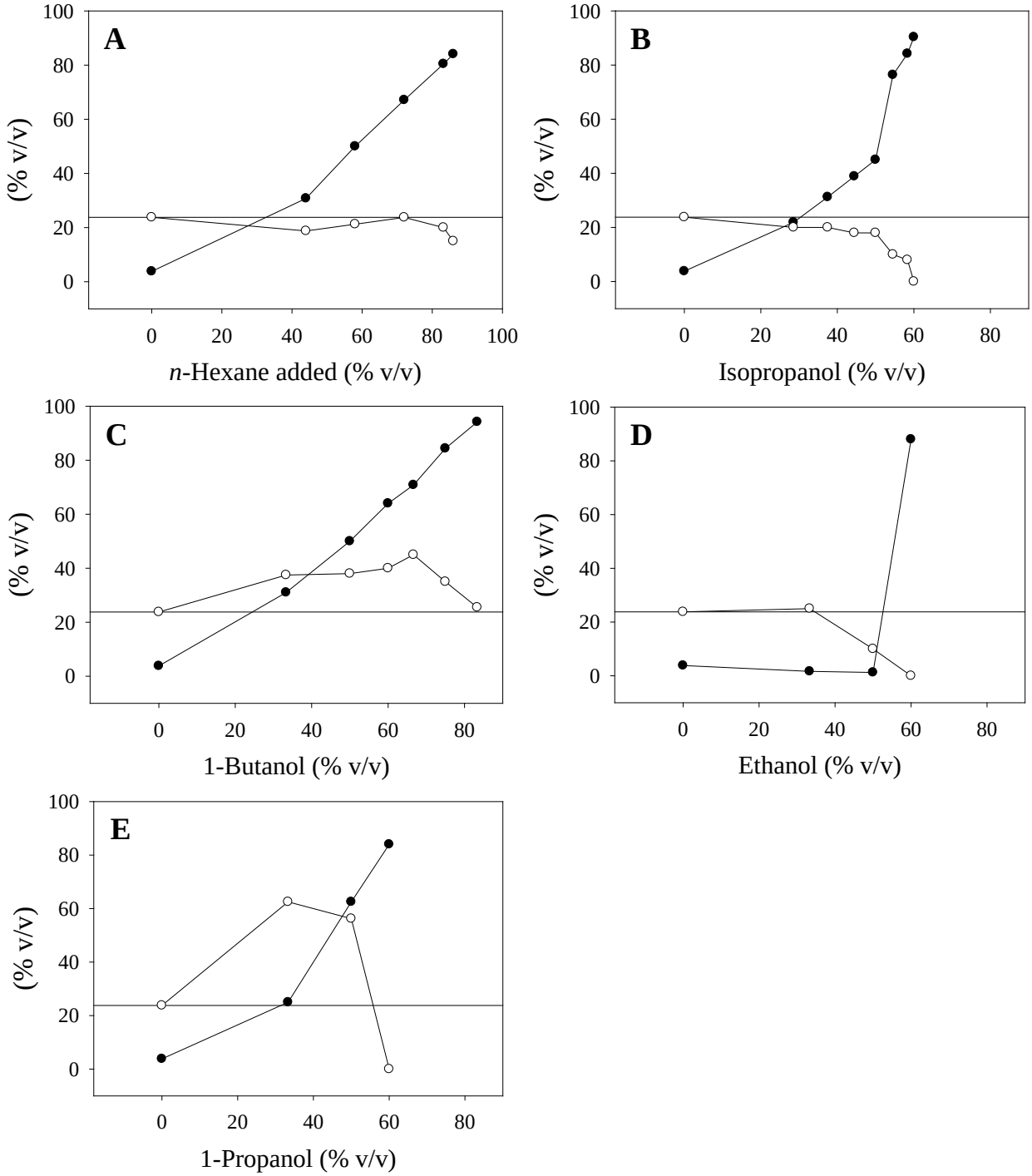


Figure 4. Effect of organic solvent addition on phase separation quality. Solvents were added stepwise to a reaction mixture with 20 % v/v hexane, phase separation was forced by centrifugation (3220 g, 10 min). Black dots show upper liquid phase; open circles show expansion or contraction of crud phases referenced to those obtained without organic modifiers (% v/v; straight line).

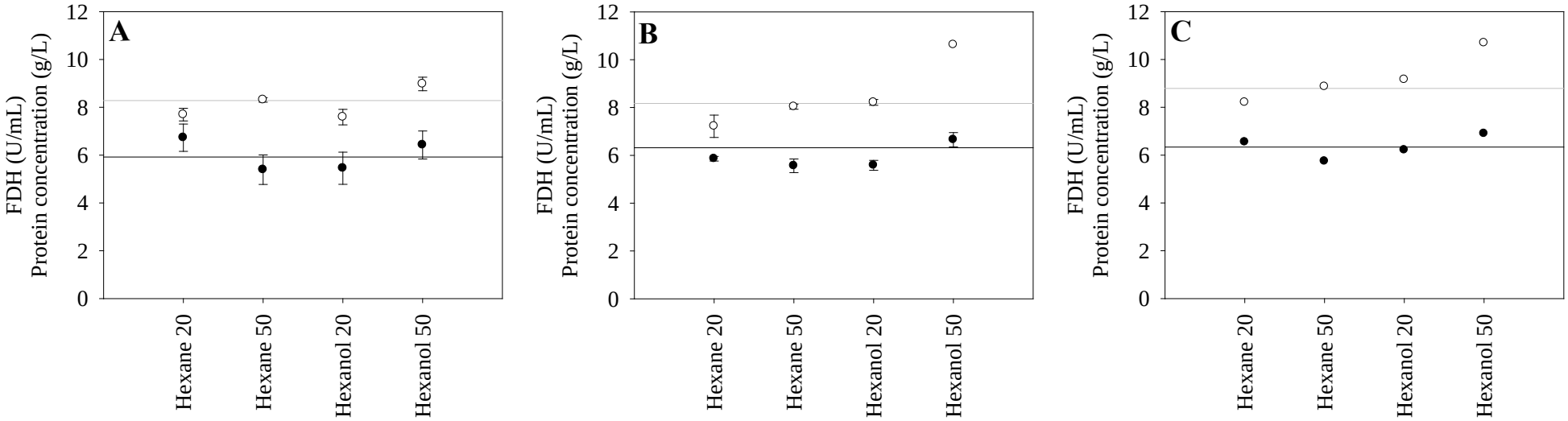


Figure 5. FDH activity and protein release in the presence of co-solvent with 300 mM of product (A), with 300 mM of substrate (B) or plain (C). Straight line (black): FDH activity (reference); straight line (grey): protein concentration (reference); open circles: protein concentration with organic solvent present; black dots: FDH activity with organic solvent present.

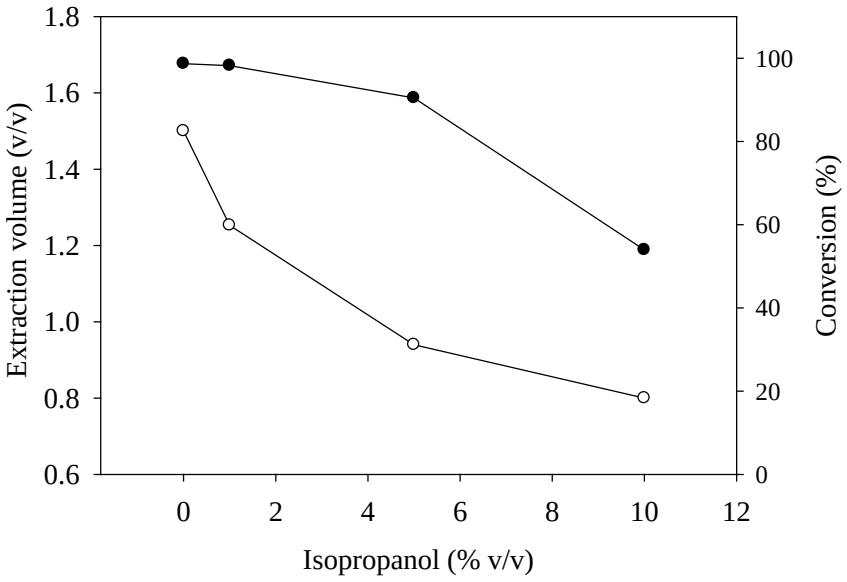


Figure 6. Effect of isopropanol added to the reaction mixture (0, 1, 5, 10 % v/v) on conversion (black dots). Requirement for further isopropanol addition after the reaction to achieve complete phase separation (open circles).

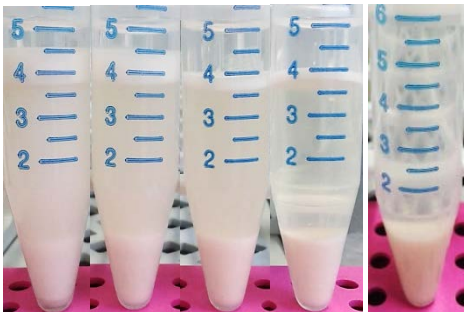

Figure 7. Reaction mixture (hexane 20 % v/v) with increasing amounts of isopropanol. First tube without isopropanol, next tubes with 1, 5, 10 % v/v isopropanol, last tube with 60 % v/v isopropanol.

# Supporting Information

# Separation behavior and microstructure of *E. coli* stabilized Pickering emulsions derived from two-phasic whole cell bioreductions

Bernhard Lauss[1], Christian Rapp[1], Dorothea Leis, Bernd Nidetzky*, Regina Kratzer*

Institute of Biotechnology and Biochemical Engineering, Graz University of Technology, Petersgasse 12/I, 8010 Graz/Austria

Content

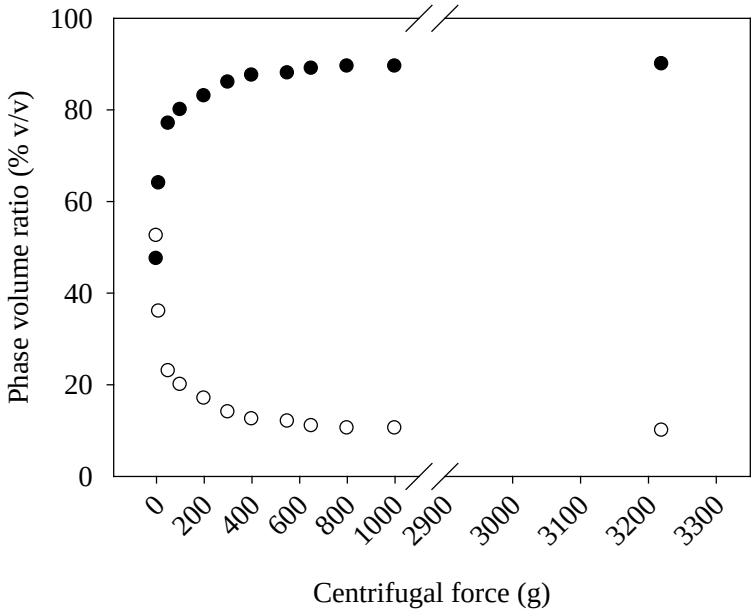


Figure S1. Forced phase separation of reaction mixtures (20% v/v hexane) with added isopropanol (1.5 v/v). Upper liquid phase (black dots) and crud phase compaction (circles) while increasing centrifugal force.

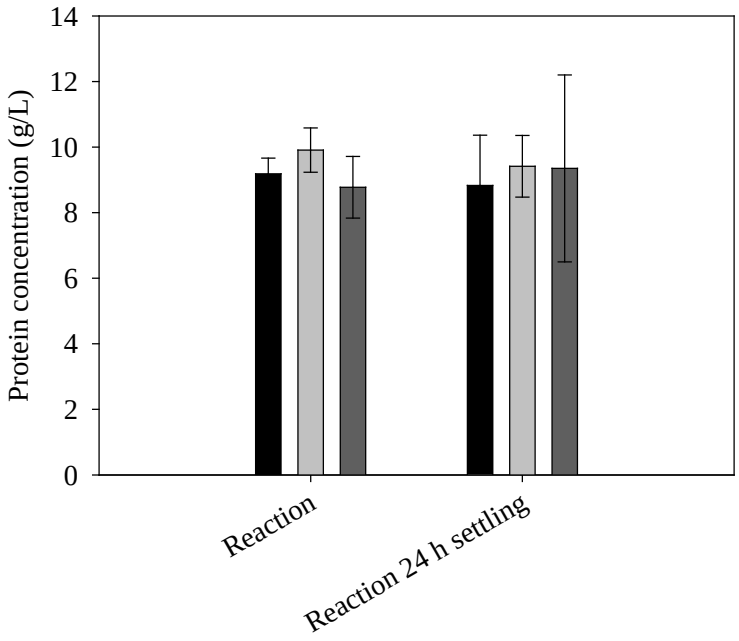


Figure S2. Protein release of reaction mixtures with 20% v/v co-solvent after the reaction and after 24h of additional settling. Black bars show reaction mixtures with hexane, light grey bars reaction mixtures with hexanol, dark grey bars reaction mixtures with hexane but without substrate.

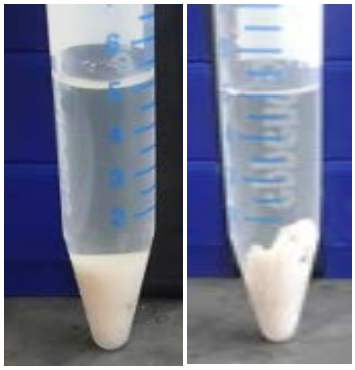

Figure S3. Pelletized crud phase of reaction mixtures (20% hexane) after addition of 60% v/v 1-propanol (A) or ethanol (B).

# Appendix

## Bioreductive dynamic kinetic resolution of *rac*-2-phenylpropanal


### Abstract

A bioreductive dynamic kinetic resolution (DKR) of *rac*-2-phenylpropanal to *(S)*-2-phenylpropanol was successfully established by applying an *E. coli* whole-cell catalyst. Full conversion of 1 M substrate accompanied by an enantiomeric excess >93% was achieved by keeping substrate/cell ($g_{substrate}/g_{cdw}$) ratios at 3.4. Biotransformations were carried out without adding organic solvents. Increased $NAD^+$ concentrations elevated conversions by overcoming mass transfer limitations in viscous reaction mixtures attributed to high catalyst and substrate loadings. Reduction and racemization rates were tremendously affected in the presence of whole-cell catalysts manifesting in e.e. values tending to be higher in whole-cell compared to cell-free biotransformations. Cell membranes were thought to function as substrate sink thereby largely controlling enzyme/substrate accessibility and reduction rates indirectly. Unbalanced substrate/catalyst ratios led to inactivation of both, cell-free and whole-cell catalyst.

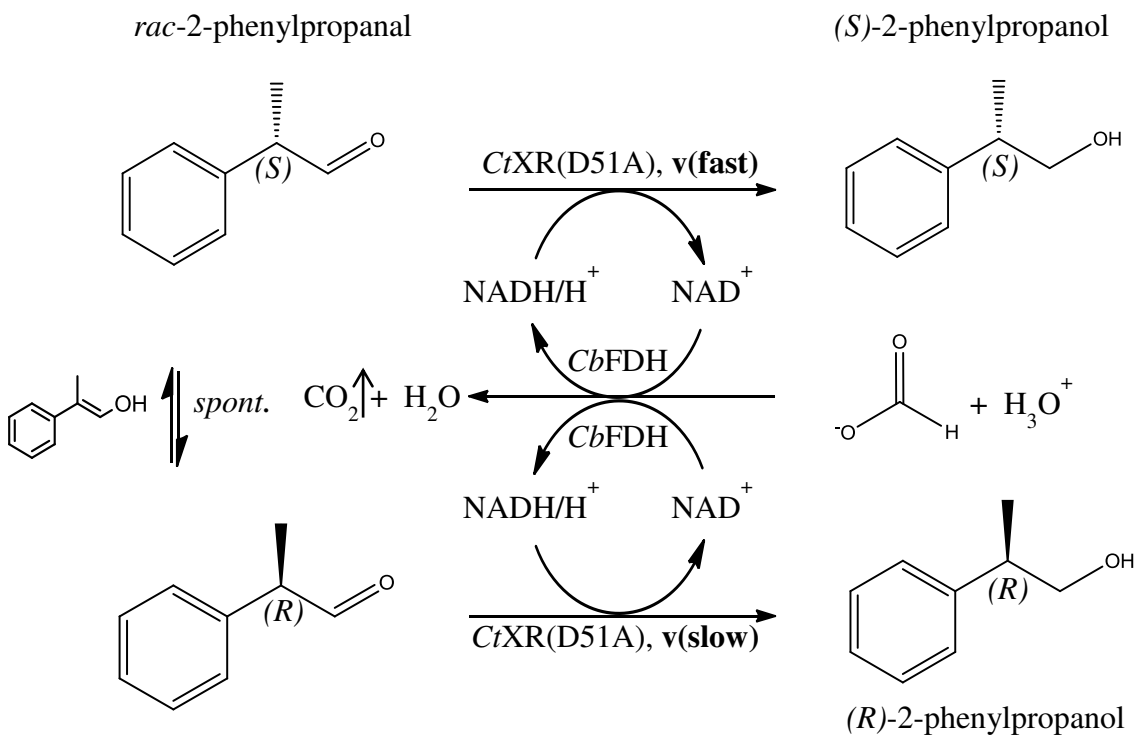


**Figure 1: Reaction scheme:** Whole-cell bioreduction of *rac*-2-phenylpropanal.

## 1. Introduction

A close liaison of low yields and moderate enantiomeric excess constituted the driving force of heading towards a more effective and alternative route to profen-precursor synthesis[1]. Profens comprise enantiomerically pure 2-arylpropionic acid derivatives known to be valuable as non-steroidal anti-inflammatory drugs, where especially the *(S)*-enantiomer is biologically active[2,3]. Here, the bioreductive dynamic kinetic resolution (DKR) of *rac*-2-phenylpropanal to *(S)*-2-phenylpropanol serves as starting point and model aiding in evaluating the use of similar precursors under emulsified conditions far beyond the intrinsic substrate solubility in aqueous solution. Therefore, a cofactor recycling system was established by co-expressing *Candida tenuis* xylose reductase (*Ct*XR) D51A mutant and *Candida boidinii* formate dehydrogenase (*Cb*FDH) in E. *coli* Rosetta 2. Cells are functioning as sink for substrate/product thereby influencing both, solubility and accessibility, launching

biotransformations without organic co-solvents. The spontaneous racemization of substrate molecules in aqueous solution via keto-enol tautomerism enables a dynamic approach, where theoretical considerations suggest 100 % yield[4].

## 2. Materials & methods

### 2.1. Chemicals and strains

2-phenylpropanal (Aldrich, 98 %), (+/-)-2-phenylpropanol (Aldrich, 97%), (*R)*-2-phenylpropanol (Fluka, ≥99.0 %), (*S)*-2-phenylpropanal (Accela, 95 %), (*R)*-2-phenylpropanal (Accela, 95 %), acetic acid ethyl ester (Roth, ≥99.9%) *n*-hexane (Roth, ≥99), acetophenone (Aldrich, 99 %), (+/-)-1-phenylethanol (Fluka, ≥98 %), (2-Hydroxypropyl)-β-cyclodextrin (Carbosynth), NADH-disodium salt (Roth, ≥98 %), NAD (Roth, ≈98 %), D(+)-xylose (Roth, ≥98.5 %), sodium formate (Sigma, ≥99 %), B-PER© cell lysis buffer (Thermo Scientific), yeast extract (Roth), polypropylene glycol (Aldrich), potassium hydroxide (Merck, p.a.), glucose (Sigma, Ultra), $K_2HPO_4$ (Roth, ≥99 %), $KH_2PO_4$ (Roth, ≥99 %), IPTG (Carbosynth), kanamycin (Roth), chloramphenicol (Fluka), ampicillin (Roth, ≥99.5 %), phosphorous acid (Roth, 85%), ethanol (AustrAlco, 99.9 %), acetonitrile (Roth, ≥99).

Tubes (15 & 50 mL) were received from Sarstedt (Wr. Neudorf, Austria), 1.5 & 2 mL reaction tubes from Eppendorf (Wien, Austria).

An *E. Coli* Rosetta2 strain co-expressing *Ct*XR D51A and *Cb*FDH was applied. The *Ct*XR D51A variant was previously described (Kratzer et al., 2006)[5].

### 2.2. Preparation of electrocompetent cells and bacterial transformation

*E. Coli* Rosetta2 cells were transformed with pET11a C.t. XR_D51A and pRSF _CbFDH following the instructions for rapid preparation of electrocompetent *Escherichia coli* and *Vibrio cholerae.*[6]

### 2.3. Shake flask cultivation

E. coli strains were grown in 1000 mL baffled shake flasks containing 200 mL of LB media supplemented with ampicillin (115 mg/L), kanamycin (50 mg/L) and chloramphenicol (34 mg/L). Cultures were shaken at 130 rpm and 37°C in a Certomat® BS-1 incubator (Sartorius) and cooled (~ 15 min at 4°C) to 25°C after reaching an optical density of 0.9 – 1.2. Protein production was induced by 250 µM isopropyl-β-D-thiogalactopyranoside (IPTG) accompanied by adding ampicillin (115 mg/L). After 20 h of cultivation, cells were harvested by centrifugation (Sorvall RC-5B). The biomass was frozen at -20°C, lyophilized (Christ α 1-4 lyophilizer from Braun Biotech International) and stored at -20°C.

### 2.4. Enzyme activity measurement

Xylose reductase and formate dehydrogenase activities were measured photometrically (Beckman Coulter DU 800® spectrophotometer) by observing oxidation or reduction rates of NADH/$NAD^+$ at 340 nm and 25°C for 5 minutes. 1 µmol of NADH formed or consumed per minute equals one unit of enzyme activity. Soluble enzyme activities were determined by weighing out lyophilized cells (10 mg) followed by re-hydration (30 min) in 1 mL potassium phosphate buffer (100 mM, pH 6.2) at 25°C and 1400 rpm on a thermomixer (Eppendorf thermomixer comfort). Cells then were centrifuged for 10 min at 13.2 k rpm. The resulting supernatant was isolated, properly diluted (buffer) and 10 µL subjected to enzyme activity measurements. B-PER© cell lysis reagent was used for insoluble protein extraction by adding 2 mL to pelletized cells, vortexing (2 min) and centrifugation (10 min, 13.2 k rpm). Determined activities for soluble and insoluble fractions were added up. For assaying *Ct*XR (D51A) activity 1 M D-xylose and 300 µM NADH were applied. *Cb*FDH-assay was carried out using 200 mM sodium formate and 2 mM $NAD^+$. Both assays were performed in 100 mM potassium phosphate buffer (pH 6.2) and started by adding NADH or $NAD^+$. Non-specific background oxidation/reduction was taken into account by measuring blank activities.

## 2.5. Biotransformations

### 2.5.1. Whole-cell biotransformation

Lyophilized cells were re-hydrated in potassium phosphate buffer (100 mM, pH 6.2, re-hydration volume ≤ 50 % v/v) in the presence of $NAD^+$ (3-14 mM) and sodium formate (50 mM excess on [substrate]) using 2 mL Eppendorf tubes. The tubes were placed on a thermomixer for 30 min at 25°C and 1400 rpm. In case of HBC-aided conversions, cyclodextrins were weighed out separately in Eppendorf tubes followed by adding *rac*-2-phenylpropanal and 50 µL buffer. Tubes were vortexed vigorously for complexation of substrate and HBC. Afterwards, re-hydrated cells were combined with HBC/substrate complexes and filled up to a total working volume of 1 mL. Alternatively, substrate was added directly to the re-hydrated cells if no HBC was applied. Eppendorf tubes were sealed with parafilm and vortexed until emulsification was reached. The mixtures were reacted for 24 – 48 h at RT using an end-over-end rotator (30rpm) placed under the fume-hood. All samples were prepared in duplicates or triplicates.

### 2.5.2. Cell-free biotransformation

Lyophilized cells (40 mg) were re-hydrated for 30 min in 1 mL potassium phosphate buffer (100 mM, pH 6.2) at 1400 rpm and 25°C on a thermomixer followed by centrifugation (13.2k rpm; 10 min; 25°C). The supernatant was isolated and either applied directly or diluted 1/2, 1/4 or 1/10 corresponding to the activity of 40, 20, 10 or 4 $g_{cdw}$/L. *rac-2*-phenylpropanal (100 mM), sodium formate (150 mM), HBC, and $NAD^+$ (6 mM) were added afterwards. All mixtures were adjusted to 1 mL and placed on an end-over-end rotator (30 rpm) for 24 h.

### 2.5.3. Visualization of substrate-racemization

The initial enantiomeric excess of pure *(S)*- or *(R)*-2-phenylpropanal was determined by quickly transferring 2 µL of one enantiomer into 500 µL dried ethyl acetate. The samples

were subjected to GC analysis. Rate of racemization was evaluated by transferring 18 µL of pure aldehyde (130 mM) into 100 mM potassium phosphate buffer (1 mL, pH 6.2). Samples were mixed at 400 rpm and extracted with dried ethyl acetate (500 µL) followed by chiral GC-FID analysis.

## 2.6. Analytical methods

### 2.6.1. Sample preparation

For HPLC and GC analyses, ethyl acetate (1 mL) was added to 1 mL of a reaction performed in 2 mL Eppendorf tubes. The tubes were vortexed followed by transferring the mixture into 15 mL Sarstedt tubes. Tubes were filled up to 10 mL with ethyl acetate, vortexed and centrifuged for 15 min, 25°C and 3220 g for extraction. The resulting organic phase was separated and transferred into new 15 mL Sarstedt tubes, which were again filled up to 10 mL. Final dilutions in ethyl acetate contained 5 mM substrate/product. The enantiomeric excess (e.e.) was calculated by:

$$e.e.(\%) = \left(\frac{mM\ Enantiomer\ 1 - mM\ Enantiomer\ 2}{mM\ Enantiomer\ 1 + mM\ Enantiomer\ 2}\right) * 100$$

For NMR analysis, substrate/product present in ethyl acetate after extraction was transferred into round-flasks and evaporated under reduced pressure. The isolated substrate/product was directly diluted in deuterated methanol or DMSO-$d_6$ (20 µL substrate/product + 680 µL solvent).

### 2.6.2. Chiral HPLC analysis

HPLC analysis was performed using a Merck-Hitachi LaChrom HPLC system equipped with a Merck L-7490 RI detector, an L-7400 UV-detector, a reversed phase Chiralpak® AD-RH column (Daicel) and a thermo-stated column oven (40 °C). The mobile phase used contained 25 % acetonitrile in dd$H_2O$. A flowrate of 30 mL/min was applied. HPLC standards were

prepared deploying racemic product in a range of 0.1, 0.5, 1, 5, 10 mM. Peak areas at corresponding retention times were used to calculate concentrations.

### 2.6.3. Chiral GC-FID analysis

GC analysis was performed using an Agilent 7890A GC with FID detection at the Institute of Organic and Bioorganic Chemistry, University of Graz, Heinrichstraße 28/II, 8010 Graz, Austria. Carrier gas: $H_2$. Column: Macherey-Nagel Hydrodex®-β-TBDAc (length: 25 m; inner diameter: 0.25 mm). Method: Injection volume: 5 µL; inlet temperature: 230°C; split ratio: 50:1; flow: 1 mL/min. Detector temperature: 250°C.

**Table 1:** GC-FID temperature program. Isocratic section for rac-2-phenylpropanal and gradient for 2-phenylpropanol separation.

| Rate (°C/min) | Value (°C) | Hold time (min) |
|---|---|---|
| | 110 | 10 |
| 2 | 123 | 3 |
| 10 | 200 | 1 |
| | | Run time: 28.2 min |

### 2.6.4. GC-MS analysis

GC-MS analysis was performed using a 7890B GC system and a 5977A MS device from Agilent Technologies at the Institute of Environmental Biotechnology, Graz University of Technology, Petersgasse 12/I, 8010 Graz, Austria. Carrier gas: He. Column: HP-5 (length: 30 m; inner diameter: 0.25 mm). Method: Injection volume: 1 µL; inlet temperature: 250°C; split ratio: 50:1; flow: 1 mL/min.

**Table 2:** GC-MS temperature program.

| Rate (°C/min) | Value (°C) | Hold time (min) |
|---|---|---|
| | 100 | 5 |
| 20 | 320 | 11 |
| | | Run time: 16 min |

### 2.6.5. NMR analysis

$^1$H-NMR spectra of isolated substrate/product from biotransformations (50 or 80 % conversion) were recorded using a 300 MHz Bruker NMR unit (300 MHz for $^1$H and) at 300 K. Chemical shifts (δ) are depicted in ppm relative to the resonance of the solvent (MeOD or DMSO-$d_6$).

# 3. Results

## 3.1. Whole-cell vs cell-free biotransformation: 100 mM *rac*-2-phenylpropanal

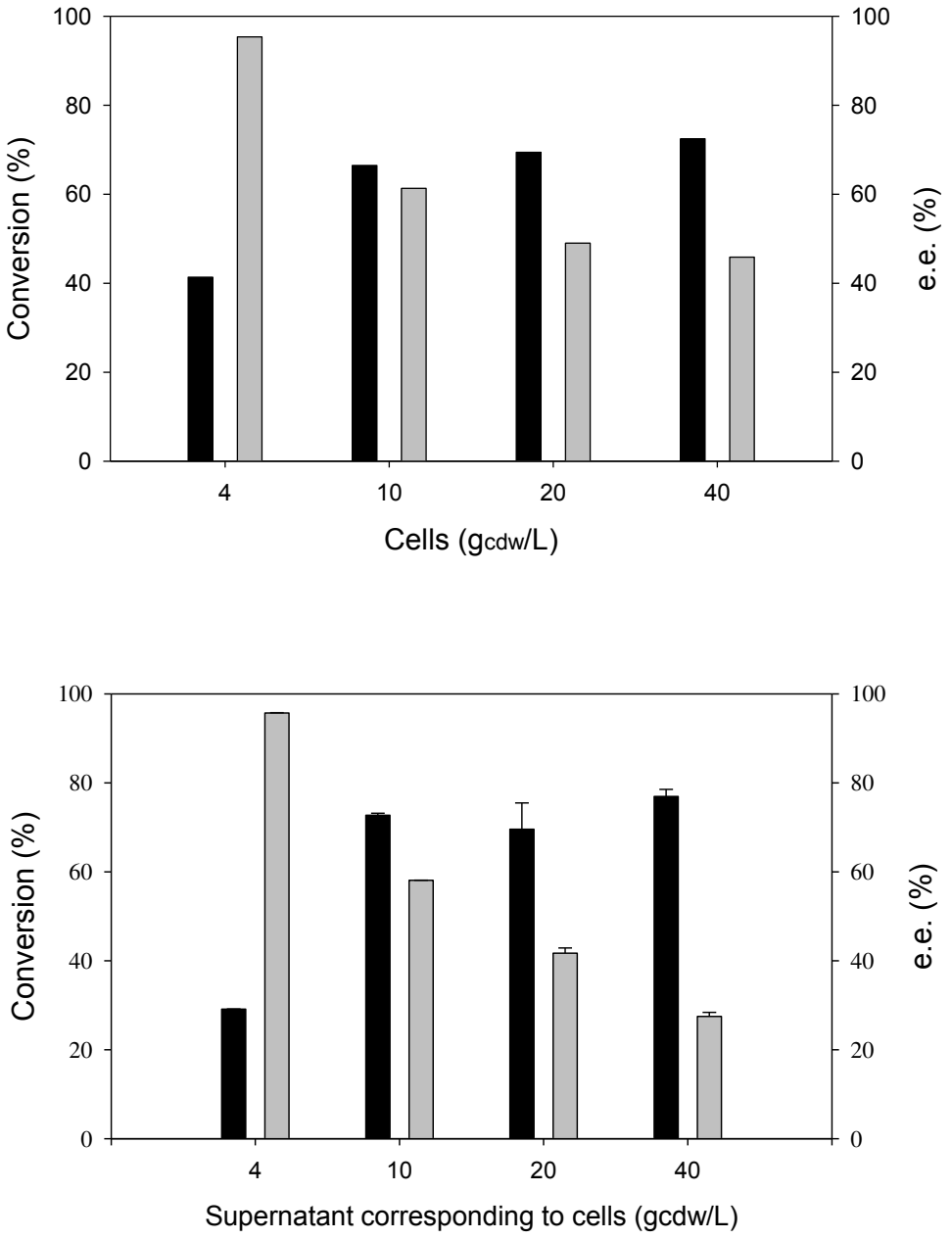


**Figure 2: Top: Whole-cell conversion. Bottom: Cell-free conversion.** Reaction conditions: 100 mM *rac*-2-phenylpropanal, 6 mM $NAD^+$, 150 mM sodium formate, 24h. Specific activity: 2000 U/gcdw (XR D51A), 60 U/gcdw (FDH). Black bars: Conversion (%). Grey bars: Corresponding e.e. values (%).

**Table 3: Results corresponding to Figure 2:** Data are based on HPLC analysis. Conversions directly correspond to product recoveries. HBC = (2-Hydroxypropyl)-β-cyclodextrin.

| **Cell-free** (gcdw/L) | **Cells** (gcdw/L) | **rac-2-phenylpropanal** (mM) | **HBC** (g/L) | **Reaction time** (h) | **$NAD^+$** (mM) | **Conversion** (%) | **e.e. *(S)*-2-phenylpropanol** (%) |
|---|---|---|---|---|---|---|---|
| 4 | | 100 | - | 24 | 6 | 29.1 | 95.7 |
| 10 | | 100 | - | 24 | 6 | 72.7 | 58.1 |
| 10 | | 100 | 50 | 24 | 6 | 66.4 | 48.6 |
| 20 | | 100 | - | 24 | 6 | 69.6 | 41.7 |
| 40 | | 100 | - | 24 | 6 | 76.9 | 27.5 |
| | 4 | 100 | - | 24 | 6 | 41.3 | 95.3 |
| | 10 | 100 | - | 24 | 6 | 66.5 | 61.3 |
| | 10 | 100 | 50 | 24 | 6 | 66.0 | 59.2 |
| | 20 | 100 | - | 24 | 6 | 69.4 | 49.0 |
| | 40 | 100 | - | 24 | 6 | 72.4 | 45.8 |

As can be seen in Table 3, e.e. values tend to decrease at elevated catalyst concentrations starting at > 95 % and ending at 27.5 % for cell-free and 45.8 % for whole-cell biotransformations. Addition of 50 g/L HBC to reaction mixtures containing 10 $g_{cdw}$/L lyophilized cells or the supernatant thereof only improved conversion and enantiomeric excess of the cell-free approach. Full conversion of 100 mM substrate could not be reached despite applying high catalyst loadings of 40 $g_{cdw}$/L.

## 3.2. Whole-cell biotransformation: 1 M *rac*-2-phenylpropanal & increased $NAD^+$ concentration

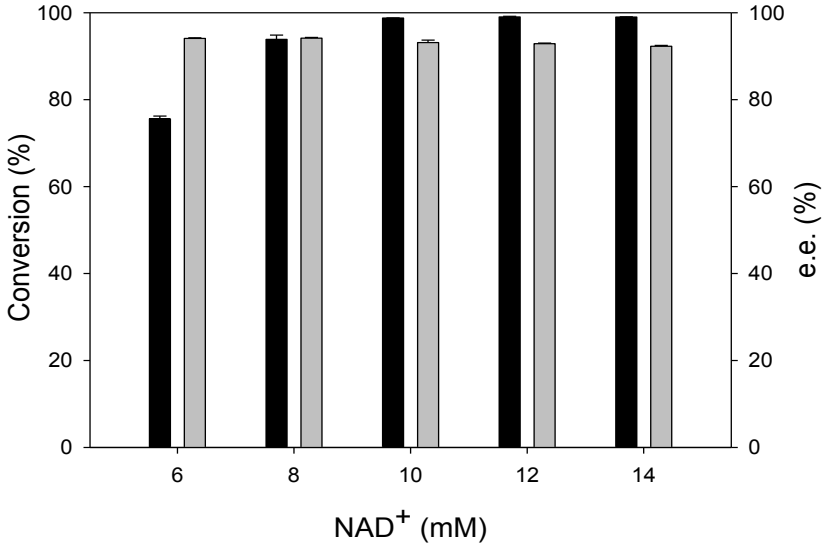


**Figure 3: Whole-cell conversion (1 M):** Reaction conditions: 1 M *rac*-2-phenylpropanal, 40 gcdw/L lyophilized cells, 6-14 mM $NAD^+$, 1.05 M sodium formate, 48h. Specific activity: 2000 U/gcdw (XR D51A), 60 U/gcdw (FDH). Black bars: Conversion. Grey bars: Corresponding e.e. values.

**Table 4: Results corresponding to Figure 3:** Conversion data are based on standard curves for racemic substrate and product using GC-MS. Calculation: P/(S+P). e.e.values are taken from HPLC analysis. Product recoveries correspond to GC-MS results.

| **Cells** (gcdw/L) | **rac-2-phenylpropanal** (M) | **Product Recovery** (mM) | **Reaction time** (h) | **$NAD^+$** (mM) | **Conversion** (%) | **e.e. *(S)*-2-phenylpropanol** (%) |
|---|---|---|---|---|---|---|
| 40 | 1 | 645.6 | 48 | 6 | 75.6 | 94.1 |
| 40 | 1 | 732.2 | 48 | 8 | 93.9 | 94.1 |
| 40 | 1 | 842.8 | 48 | 10 | 98.8 | 93.1 |
| 40 | 1 | 839.3 | 48 | 12 | 99.0 | 92.9 |
| 40 | 1 | 765.1 | 48 | 14 | 99.0 | 92.3 |

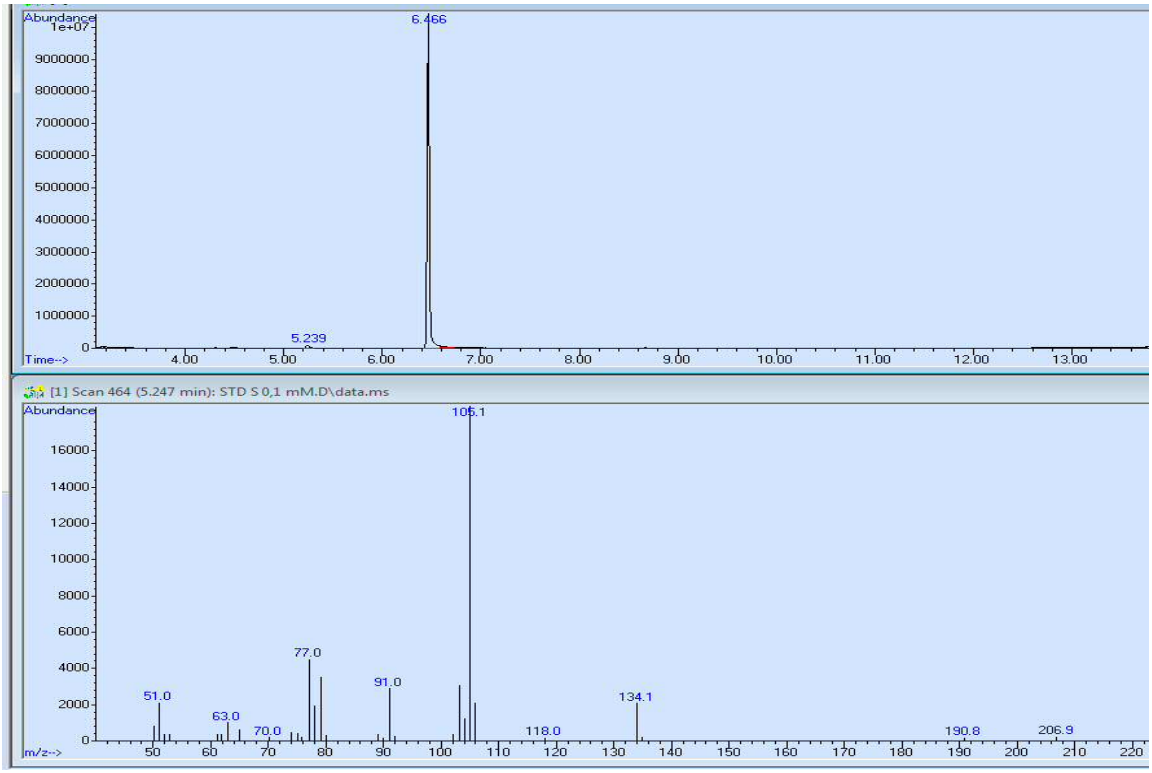


**Figure 4:** GC-MS results for 1 M conversion (10 mM $NAD^+$): Top: Retention time: *rac*-2-phenylpropanal = 5.24 min, *rac*-2-phenylpropanol = 6.5 min. Bottom: Mass spectrum of *rac*-2-phenylpropanal.

Table 4 reveals that $NAD^+$ constitutes a major limiting factor, as catalyst loadings were kept constant at 40 $g_{cdw}$/L lyophilized cells. While a concentration of 6 mM $NAD^+$ resulted in 75.6 % conversion pushing e.e. values up to 94.1 %, 12 mM $NAD^+$ yielded 99 % conversion concomitantly decreasing e.e. values to 92.9 %. Additional reaction mixtures were prepared without $NAD^+$ to evaluate substrate recovery, which was found to be 847.3 mM *rac*-2-phenylpropanal in average. Reaction mixtures containing 8 mM $NAD^+$ were further evaporated under reduced pressure to check for conversion consistency of isolate and reaction sample. Both approaches resulted in conversions of 93.9 %. The specific activities (soluble and insoluble fraction) of the whole-cell catalyst applied were calculated to 2000 U/$g_{cdw}$ (XR D51A) and 60 U/$g_{cdw}$ (FDH) thereby vastly exceeding those of the catalyst used in section 3.3.

## 3.3. Whole-cell biotransformation: 1 M *rac*-2-phenylpropanal & increased HBC concentration

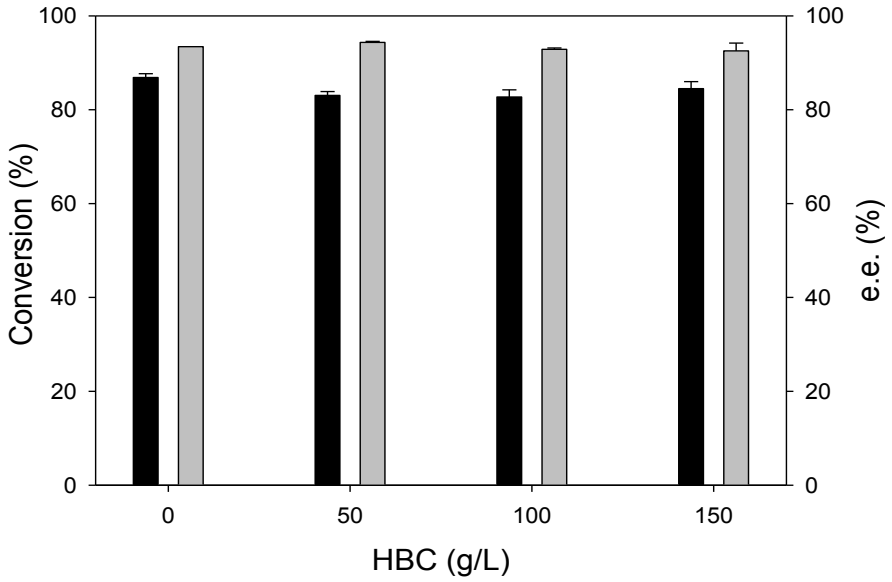


**Figure 5: Whole-cell conversion (1 M):** Reaction conditions: 1 M *rac*-2-phenylpropanal, 40 gcdw/L lyophilized cells, 6 mM $NAD^+$, 1.05 M sodium formate, 0-150 g/L HBC, 48h. Specific activity: 1105 U/gcdw (XR D51A), 37 U/gcdw (FDH). Black bars: Conversion. Grey bars: Corresponding e.e. values.

**Table 5: Results corresponding to Figure 5:** Conversion data are based on standard curves for racemic substrate and product using chiral GC-FID. Calculation: P/(S+P). e.e.values are taken from HPLC analysis. Product recoveries correspond to HPLC results. HBC = (2-Hydroxypropyl)-β-cyclodextrin.

| **Cells** (gcdw/L) | **rac-2-phenylpropanal** (M) | **HBC** (g/L) | **Product Recovery** (mM) | **Reaction time** (h) | **$NAD^+$** (mM) | **Conversion** (%) | **e.e. *(S)*-2-phenylpropanol** (%) |
|---|---|---|---|---|---|---|---|
| 40 | 1 | 0 | 690.5 | 48 | 6 | 86.9 | 93.4 |
| 40 | 1 | 50 | 633.9 | 48 | 6 | 83.1 | 94.3 |
| 40 | 1 | 100 | 597.9 | 48 | 6 | 82.7 | 92.9 |
| 40 | 1 | 150 | 592.0 | 48 | 6 | 84.5 | 92.5 |

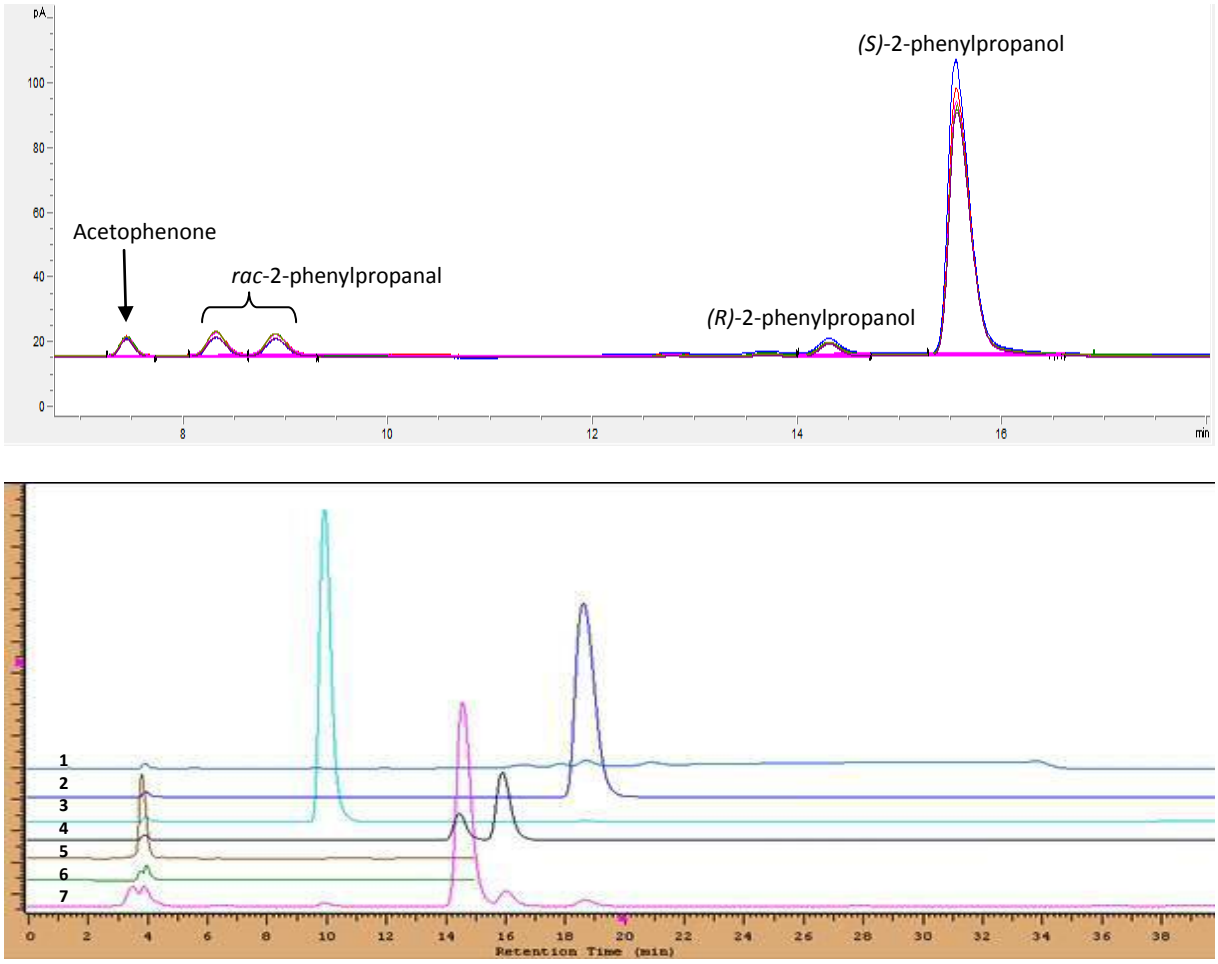


**Figure 6: Chiral GC-FID and HPLC results for 1 M conversions with increased HBC**: Top: GC-FID results including substrate, product and acetophenone (by-product). Bottom: HPLC result for one 1 M reaction including peak-descriptions: 1 = *rac*-2-phenylpropanal, 2 = acetophenone, 3 = 1-phenylethanol, 4 = *rac*-2-phenylpropanol, 5 = $NAD^+$ in buffer, 6 = potassium phosphate buffer, 7 = reaction sample (1M).

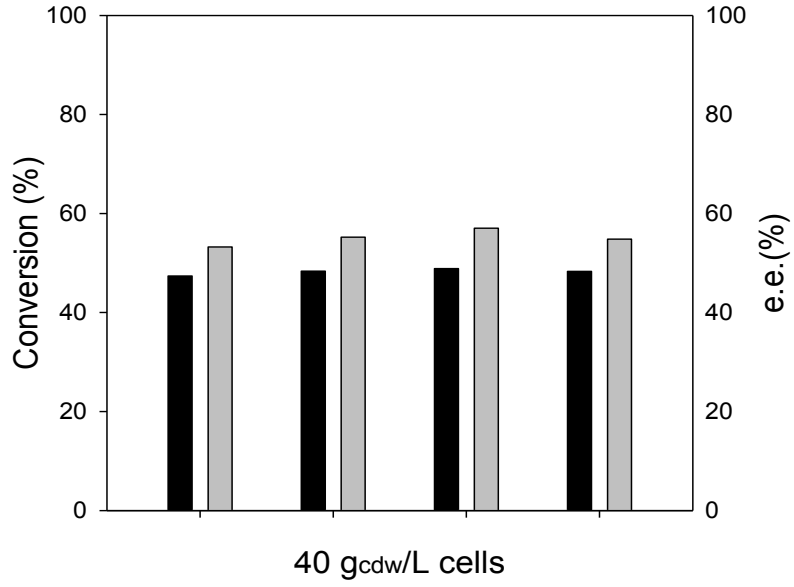


**Figure 7: Influence of lower catalyst activity on five identical reactions: Whole-cell conversion (1 M):** Reaction conditions: 1 M *rac*-2-phenylpropanal, 40 gcdw/L lyophilized cells, 6 mM $NAD^+$, 1.05 M sodium formate, 48h. Specific activity: 1105 U/gcdw (XR D51A), 37 U/gcdw (FDH). Black bars: Conversion. Grey bars: Corresponding e.e. values.

**Table 6: Results corresponding to Figure 7:** Conversion data are based on standard curves for racemic substrate and product using chiral GC-FID. Calculation: P/(S+P). e.e.values are taken from HPLC analysis. Product recoveries correspond to HPLC results.

| **Cells** (gcdw/L) | **rac-2-phenylpropanal** (M) | **Product Recovery** (mM) | **Reaction time** (h) | **$NAD^+$** (mM) | **Conversion** (%) | **e.e. *(S)*-2-phenylpropanol** (%) |
|---|---|---|---|---|---|---|
| 40 | 1 | 433.5 | 48 | 6 | 47.4 | 53.3 |
| 40 | 1 | 387.5 | 48 | 6 | 48.4 | 55.2 |
| 40 | 1 | 417.8 | 48 | 6 | 48.9 | 57.0 |
| 40 | 1 | 437.1 | 48 | 6 | 48.3 | 54.8 |

Table 5 displays the influence of 50-150 g/L HBC on reaction mixtures containing 1 M substrate and 40 $g_{cdw}$/L lyophilized cells. Compared to the reference mixture (86.9 % conversion, e.e. = 93.4 %) not involving cyclodextrins, no major positive effects on conversion or enantiomeric excess arose, except for 50 g/L HBC faintly increasing e.e. values up to 94.3 %. Figure 6 displays the corresponding GC and HPLC chromatograms including both product and substrate enantiomers as well as by-products (acetophenone, 1-phenylethanol). After 48 h of reaction time, 2-phenylpropanal remained racemic clearly indicating keto-enol tautomerization. The activities for the whole-cell catalyst used in these experiments were determined to 1105 U/$g_{cdw}$ (XR D51A) and 37 U/$g_{cdw}$ (FDH). Further reactions were carried out deploying the same catalyst resulting in a high degree of variation (Table 6) regarding conversion (< 50 %) and e.e. values (53 - 57 %). These findings suggest that lower XR and FDH activities tremendously limit reproducibility.

## 3.4. Whole-cell biotransformation: 1 M *rac*-2-phenylpropanal & decreased cell concentration

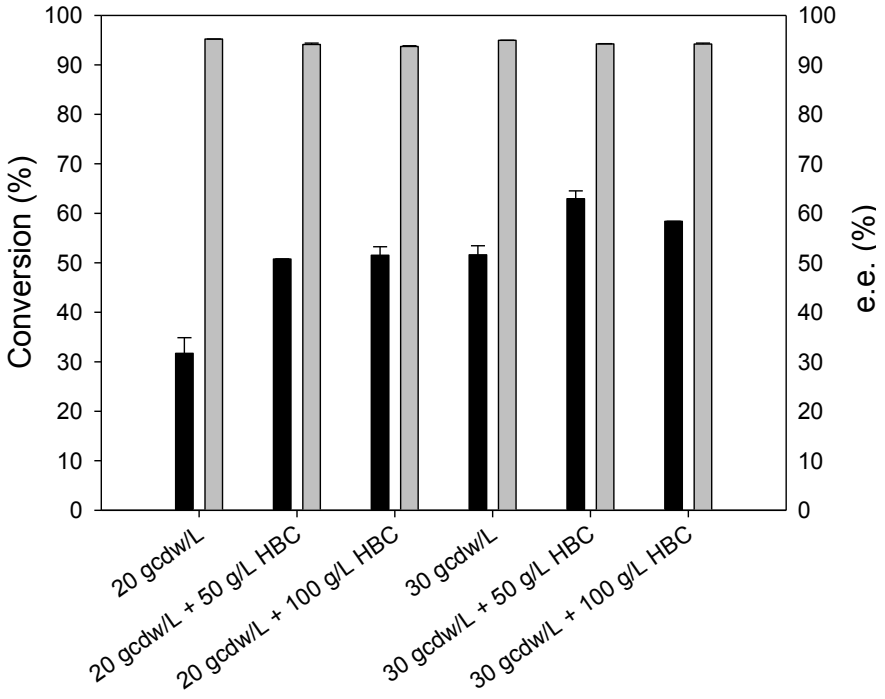


**Figure 8: Whole-cell conversion (1 M):** Reaction conditions: 1 M *rac*-2-phenylpropanal, 20-30 gcdw/L lyophilized cells, 3 mM $NAD^+$, 0-100 g/L HBC, 1.05 M sodium formate, 48h. Specific activity: 2000 U/gcdw (XR D51A), 60 U/gcdw (FDH). Black bars: Conversion. Grey bars: Corresponding e.e. values.

**Table 7: Results corresponding to Figure 8:** Conversion data are based on standard curves for racemic product using chiral HPLC and average product recoveries (~85 %). Calculation: P/(P recovered/100). e.e.values are taken from HPLC analysis. Product recoveries correspond to HPLC results. HBC = (2-Hydroxypropyl)-β-cyclodextrin.

| **Cells** (gcdw/L) | **rac-2-phenylpropanal** (M) | **HBC** (g/L) | **Product Recovery** (mM) | **Reaction time** (h) | **$NAD^+$** (mM) | **Conversion** (%) | **e.e. *(S)*-2-phenylpropanol** (%) |
|---|---|---|---|---|---|---|---|
| 20 | 1 | 0 | 269.1 | 48 | 3 | 31.7 | 95.2 |
| 20 | 1 | 50 | 432.0 | 48 | 3 | 50.8 | 94.1 |
| 20 | 1 | 100 | 428.7 | 48 | 3 | 51.5 | 93.7 |
| 30 | 1 | 0 | 424.9 | 48 | 3 | 51.6 | 95.0 |
| 30 | 1 | 50 | 495.9 | 48 | 3 | 62.9 | 94.2 |
| 30 | 1 | 100 | 455.3 | 48 | 3 | 58.4 | 94.2 |

Table 7 displays outcomes at reduced catalyst loadings and addition of HBC on 1 M substrate. For 20 $g_{cdw}$/L, conversions increased at elevated HBC concentrations from 31.7 to 51.5 %, although no significant differences were observable compared to the results obtained upon adding 50 or 100 g/L HBC. The enantiomeric excess diminished from 95.2 to 93.7 %. Similar trends occured at 30 $g_{cdw}$/L yielding 51.6 % conversion and e.e. values of 95 %, while the presence of HBC slightly increased conversions but lowered e.e. values to 94.2 %

### 3.5. Whole-cell biotransformation: *rac*-2-phenylpropanal – fed batch

**Table 8:** Fed batch: Reaction conditions: 50 µL *rac*-2-phenylpropanal were fed three times after 0, 2 and 4 h. The reaction was carried out for 48 h. Specific activity: 2000 U/gcdw (XR D51A), 60 U/gcdw (FDH). Conversion data are based on standard curves for racemic substrate and product using GC-MS. Calculation: P/(S+P). e.e.values are taken HPLC analysis. Product recoveries correspond to HPLC results.

| **Cells** (gcdw/L) | **rac-2-phenylpropanal** (mM) | **HBC** (g/L) | **Product Recovery** (mM) | **Reaction time** (h) | **$NAD^+$** (mM) | **Conversion** (%) | **e.e. *(S)*-2-phenylpropanol** (%) |
|---|---|---|---|---|---|---|---|
| 30 | 955 | 50 | 609.9 | 48 | 6 | 72.7 | 93.9 |
| 40 | 955 | - | 679.3 | 48 | 6 | 80.0 | 94.0 |

Aiming at enhancing racemization rates and preventing fast catalyst inactivation, a fed batch reaction was carried out by adding 50 µL *rac*-2-phenylpropanal (~ 955 mM) after 0, 2 and 4 h. The reaction was stopped after 48 h. The first approach involved 30 $g_{cdw}$/L lyophilized cells and 50 g/L HBC resulting in 72.2 % conversion and an enantiomeric excess of 93.9 %. The second reaction was performed just applying 40 $g_{cdw}$/L lyophilized cells yielding 80 % conversion and an e.e. value of 94 %. Comparing these outcomes to the corresponding batch reactions, an improvement of ~ 10 % (62.9 to 72.2 %) in terms of conversion was achieved for 30 $g_{cdw}$/L lyophilized cells, while e.e. values did not alter significantly. For 40 $g_{cdw}$/L catalyst loadings no noteworthy alterations occurred in comparison to 75 - 87% conversion and e.e. values between 93.4 - 94.1 % for batch reactions.

## 3.6. Whole-cell biotransformation: 2 M *rac*-2-phenylpropanal

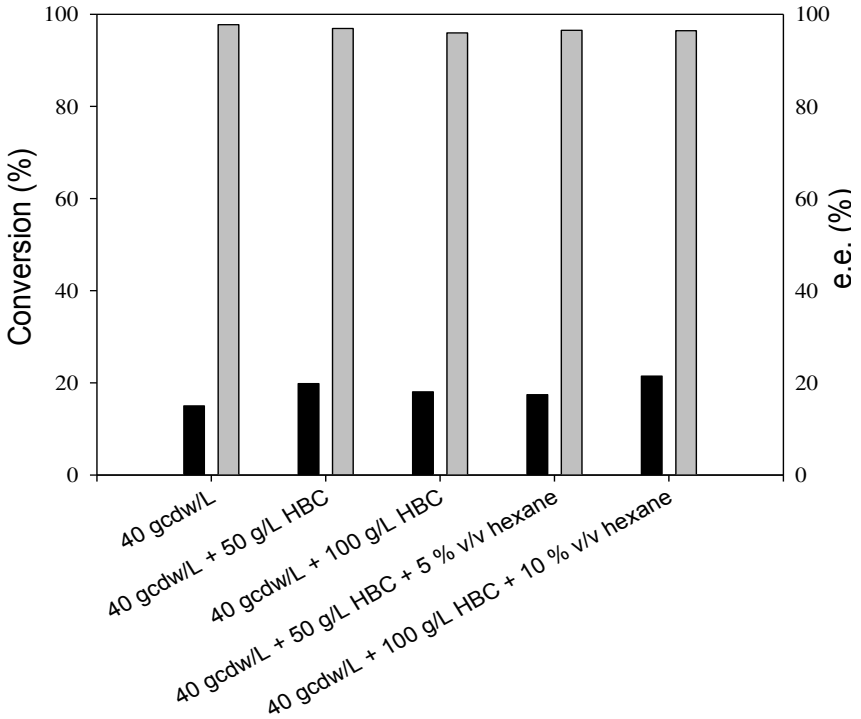


**Figure 9: Whole-cell conversion (2 M):** Reaction conditions: 2 M *rac*-2-phenylpropanal, 40 gcdw/L lyophilized cells, 6 mM $NAD^+$, 50-100 g/L HBC, 5-10 % v/v *n*-hexane, 2.05 M sodium formate, 48h. Specific activity:
1105 U/gcdw (XR D51A), 37 U/gcdw (FDH). Black bars: Conversion. Grey bars: Corresponding e.e. values.

**Table 9: Results corresponding to Figure 9:** Conversion data are based on standard curves for racemic substrate and product using chiral GC-FID. Calculation: P/(S+P). e.e.values are taken from HPLC analysis. Product recoveries correspond to GC-FID results. HBC = (2-Hydroxypropyl)-β-cyclodextrin.

| **Cells** (gcdw/L) | **rac-2-phenylpropanal** (M) | ***n*-hexane** (% v/v) | **HBC** (g/L) | **Product Recovery** (mM) | **Reaction time** (h) | **$NAD^+$** (mM) | **Conversion** (%) | **e.e. *(S)*-2-phenylpropanol** (%) |
|---|---|---|---|---|---|---|---|---|
| 40 | 2 | | - | 264.6 | 48 | 6 | 15.0 | 95.3 |
| 40 | 2 | | 50 | 293.4 | 48 | 6 | 19.8 | 93.3 |
| 40 | 2 | | 100 | 297.9 | 48 | 6 | 18.0 | 92.0 |
| 40 | 2 | 5 | 50 | 253.1 | 48 | 6 | 17.4 | 93.0 |
| 40 | 2 | 10 | 100 | 320.2 | 48 | 6 | 21.5 | 92.6 |

Table 9 displays the results obtained for 2 M substrate loading and 40 $g_{cdw}$/L whole-cell catalyst. Additionally, 50 - 100 g/L HBC and 5 - 10 % v/v hexane were added. Specific activities were 1105 U/$g_{cdw}$ (XR D51A) and 37 U/$g_{cdw}$ (FDH). Best outcomes were achieved deploying 100 g/L HBC and 10 % v/v hexane yielding 21.5 % conversion accompanied by an enantiomeric excess of 92.6 %. The unmodified mixture yielded 15 % conversion and e.e. value of 95.3 %.

### 3.7. Visualization of racemization

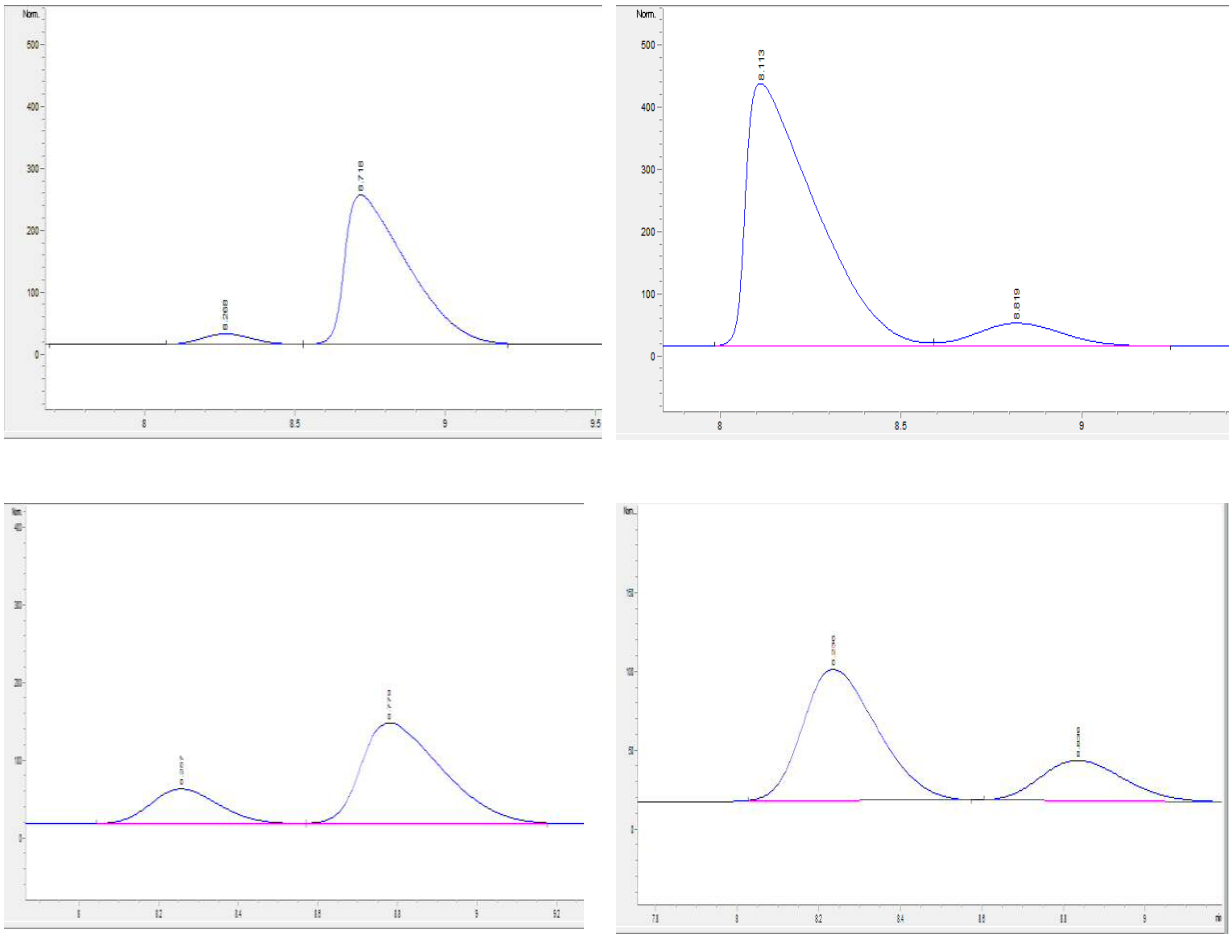

**Figure 10: Racemization of 2-phenylpropanal**. Initial e.e. values after dilution in ethyl acetate: Top left, *(S)*-enantiomeric aldehyde; Top right, *(R)*-enantiomeric aldehyde. Racemization after 24h in potassium phosphate buffer (100 mM, pH 6.2): Bottom left, (*S*)-enantiomeric aldehyde. Bottom right, *(R)*-enantiomeric aldehyde.

**Table 10: Results for the racemization of 2-phenylpropanal.** The enantiomeric excess was calculated using GC area values.

| Component | Initial e.e. (%) | e.e. after 24h (%) |
|---|---|---|
| *(S)*-2-phenylpropanal | 80.3 | 55.6 |
| *(R)*-2-phenylpropanal | 89.3 | 49.3 |

In order to assure racemization of 2-phenylpropanal and to exclude severe GC interference on e.e. values upon injection at elevated temperatures, quasi-enantiomerically pure samples were investigated. The initial e.e. values obtained immediately after dilution in ethyl acetate were determined to 80.3 % for *(S)*-2-phenylpropanal and 89.3 % for *(R)*-2-phenylpropanal. In accordance with the data given by the manufacturer, both enantiomers should display e.e. values of 95 %. As storage time over several months might have decreased the enantiomeric excess, the impact on racemization attributed to GC injection seems negligible. After transferring 130 mM of both enantiomers into potassium phosphate buffer (100 mM, pH 6.2) followed by 24 h of incubation, e.e. values decreased to 55.6 and 49.3 % for *(S)*- and *(R)*-aldehyde, respectively. These findings clearly support racemization in aqueous solution.

### 3.8. NMR analysis

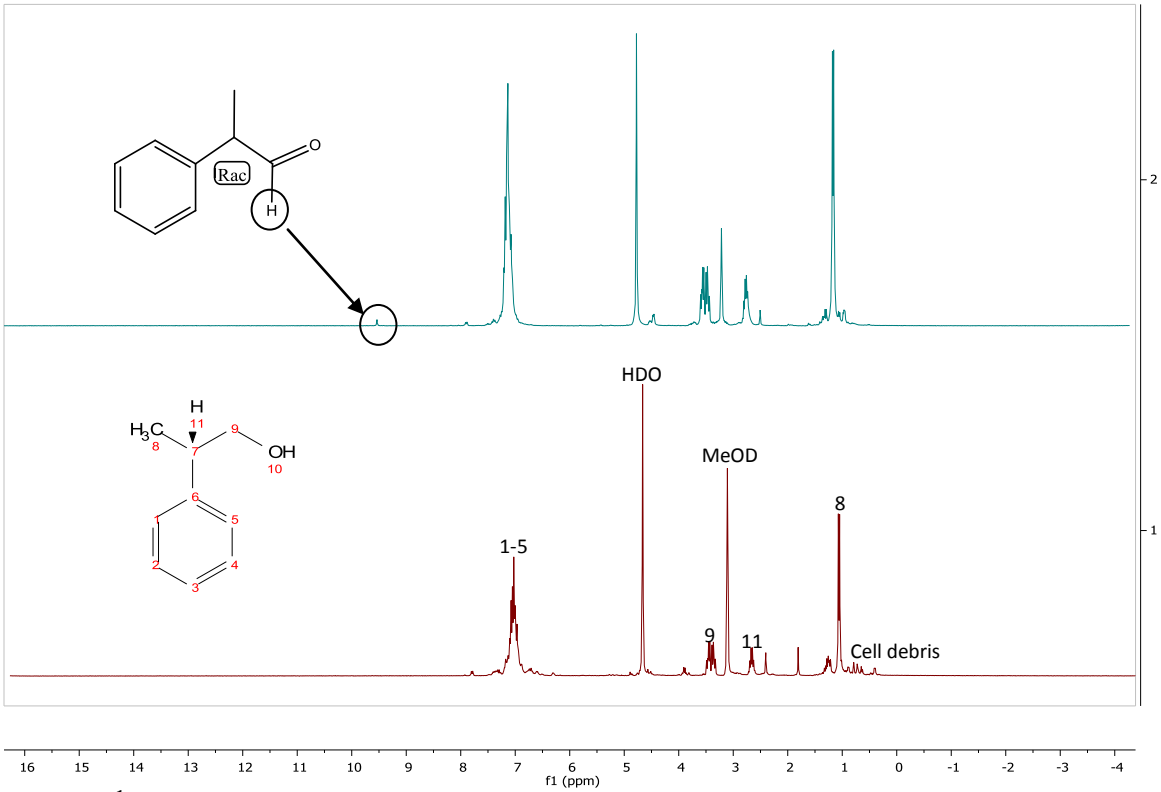


**Figure 11: $^{1}$H-spectra of two independent biotransformations (1 M):** Solvent MeOD. Top: Spectrum of isolated product/substrate of a reaction with 80 % conversion recorded immediately after work-up. Bottom: Spectrum of isolated product/substrate of a reaction with 50 % conversion recorded several hours after work-up. Ethyl acetate related signals at 1.75, and 3.9 ppm; acetophenone related signal at 2.45 ppm.

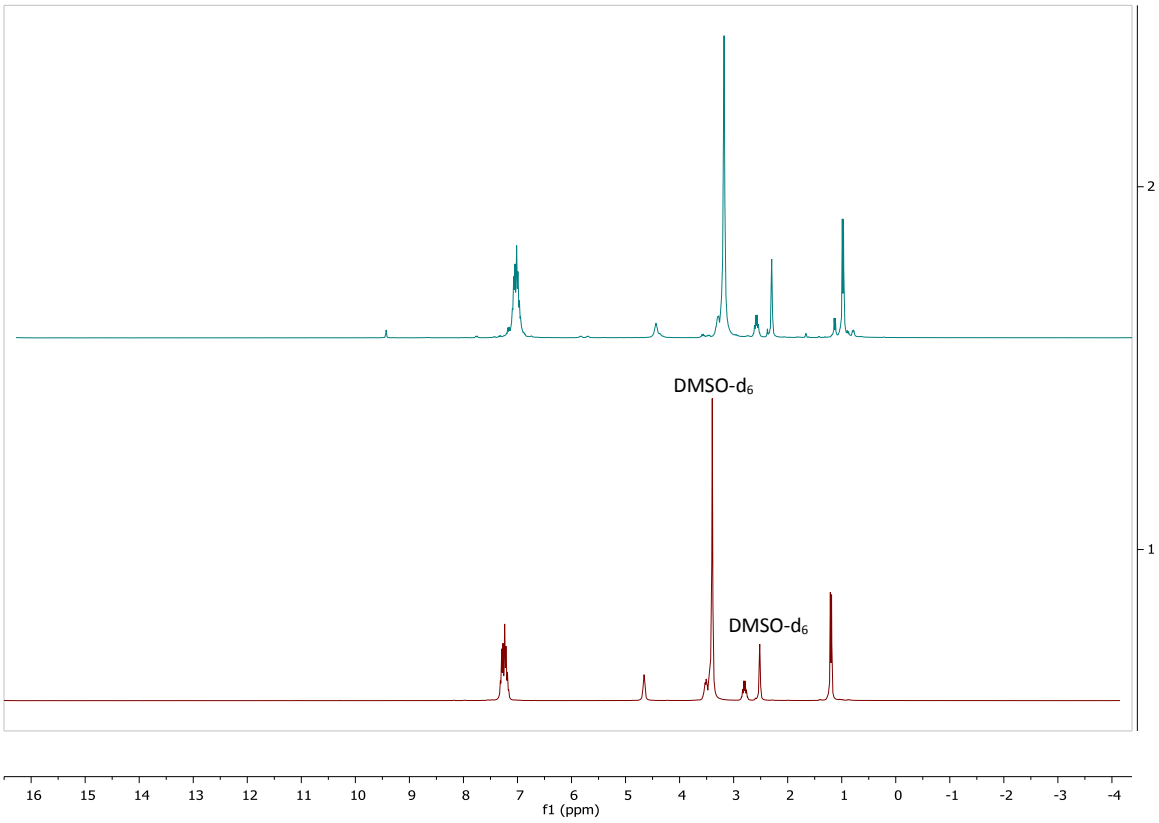


**Figure 12: $^{1}$H-spectra in DMSO-d$_6$:** Top: Spectrum of isolated product/substrate of a reaction with 80 % conversion. Bottom: Spectrum of isolated product of a reference reaction mixture only containing product. Spectra were recorded immediately after work-up. For peak description compare to Figure **11**.

# 4. Discussion

*Constraints in shake flask cultivation:*

The optical density prior to cooling and induction tremendously influences the performance of the biocatalyst: An $OD_{600}$ ~ 1 nearly doubles *Ct*XR (D51A) and FDH activities to 2000 and 60 U/$g_{cdw}$, respectively, whereas $OD_{600}$ ~ 0.9 or 1.2 lead to 1105 and 37 U/$g_{cdw}$. One major downside to lower activities not only manifests in lower conversions but also in higher variations regarding the enantiomeric excess, where a drop of ~ 35 % might possibly occur under identical reaction conditions (compare Figure 7 & first bar of Figure 5). Apart from variations occurring in shake flask cultivations when co-expressing enzymes, this phenomenon might be explicable by a limited NADH availability further slowing down the

reduction rate accompanied by substrate mediated enzyme distortion leading to altered substrate specificity (1 M substrate ~ 14 % v/v).

*By-products:*

Acetophenone (< 7%) formed by oxygen-catalyzed degradation of *rac*-2-phenylpropanal and the enzymatic reduction thereof to 1-phenylethanol (< 1%) constitute two minor by-products[4] in the reaction described above inevitably leading to substrate loss (Figure 6). One further aspect to consider concerning substrate racemization includes a second chemical equilibrium between *rac*-2-phenylpropanal and its corresponding hydrates (Figure 13).[7] Despite *(S)*-2-phenylpropionic acid is not produced by *Ct*XR (D51A), it has to be assumed that this equilibrium is fully reversible and driven by the consumption of mainly *(S)*-2-phenylpropanal. Moreover, a tight pH control appears to be negligible, as a shift from 6.2 to max. ~ 7.5 occurring in the course of the reaction seems to not heavily influence racemization and hydrate formation. Full conversion of 1 M substrate accompanied by e.e. values exceeding 90 % strongly corroborate this supposition (Figure 3).

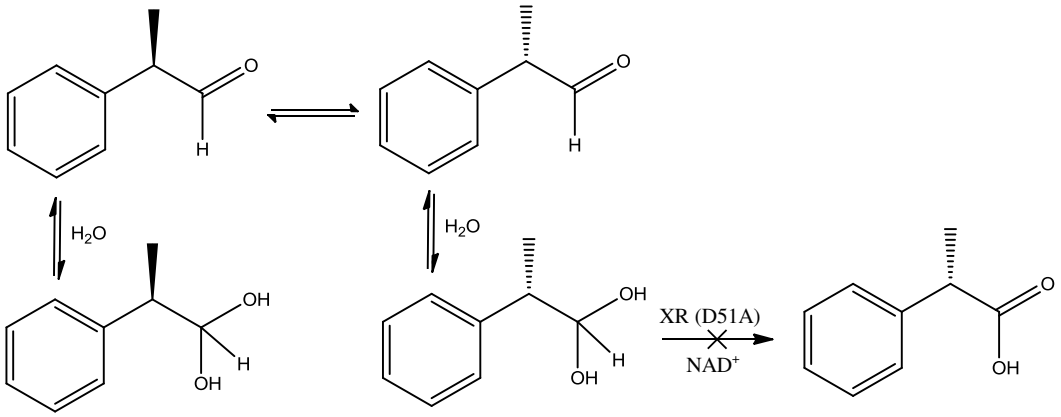


**Figure 13: Formation of substrate-hydrates.** No oxidation of *rac*-2-phenylpropane-1,1-diol by *Ct*XR (D51A).

*$^{1}$H-NMR:*

MeOD-spectra (Figure 11): No aldehyde-proton peak was detectable for a biotransformation ending at ~ 50 % conversion measured several hours after extractive work-up. Amongst others, proton exchange, tautomerization of *rac*-2-phenylpropanal to the enol-intermediate and formation of hydrates might have caused the aldehydic proton signal at 9.5 ppm to disappear (see Post Appendix for predicted NMR spectra). This assumption is based on e.g. the peak appearing at 1.75 ppm which might not necessarily be solely ethyl acetate related, but also indicating the presence of the enol-intermediate (methyl-group). Peaks at and around 1.25 ppm might correspond to the formation hydrates. As the lower spectrum in comparison to the upper one was recorded with major time delay, the time frame for hydration and tautomerization to happen is extended and becoming more likely.

DMSO-$d_6$-spectra (Figure 12): In order to avoid substrate instability, aprotic solvents are first choice when investigating 2-phenylpropanal or 2-phenylpropanol. Unfortunately, one solvent peak at 3.4 ppm overlaps with (-$CH_2$-) from substrate and product. Further, possible formation of hydrates can be observed in the upper spectrum (1.25 ppm). As these spectra were recorded with minor delay, the hydration might have happened during biotransformation as well.

*Product recovery:*

A strongly emulsified reaction mixture inexorably causes constraints in product extraction, but intensifies cell-substrate interaction. As ~ 840 mM could be recovered maximally, one has to take into account that also substrate degradation to acetophenone and hydration contribute to product loss. Evaporation of substrate/product in the course of the reaction appears to be negligible at 1 M substrate loading, as ~ 0.5 % of the total weight of the reaction mixture are lost over 48 h. Hydrate formation and vapour pressures of 0.4 hPa for *rac*-2-phenylpropanal and 0.04 hPa for *rac*-2-phenylpropanol confirm these findings.

*Whole-cell vs cell-free biotransformation (100 mM):*

The results obtained for whole-cell and cell-free biotransformations display similar trends in terms of conversion and enantiomeric excess: Low catalyst concentrations cause higher e.e. values and faster catalyst inactivation mirrored by lower conversions. However, one main difference lies within the enantiomeric excess dropping slower with increased whole-cell catalyst concentrations, while conversions are comparable to cell-free experiments, except for $4 g_{cdw}$/L. An assumption based on the intrinsic solubility of *rac*-2-phenylpropanal (~ 10 mM) being exceeded by a factor of 10 suggests, that both enantiomers will be present as oil-in-water emulsion. As can be seen in Figure 10, racemization of both enantiomerically (almost) pure substrate-aldehydes proceeds quite moderate under emulsified conditions (40 % after 24 h for *(R)*-2-phenylpropanal) and will further slow down the less water is available. This can be easily deduced from the all-in-all good storage stability of the enantiomerically pure substrate-aldehydes applied in this experiment. In average, the racemization rate for both enantiomers can be calculated to 32.35 % / 24 h applying 130 mM. Assuming no significant change in racemization for 100 mM substrate, the resulting rate equals 0.02 mM / min (32.35 mM / 24 h). Further considering FDH as rate limiting thereby determining the reduction rate of *Ct*XR (D51A), following conclusions can be drawn:

**Table 11: Ratio of reduction and racemization rates based on the volumetric activity of FDH.**
Average racemization rate = 0.02 mM/min. FDH activities are based on enzyme activity measurements resulting in 44 U/gcdw for the soluble fraction.

| FDH (mM/min) | Catalyst ($g_{cdw}$/L) | Reduction rate/ racemization rate |
|---|---|---|
| 1.76 | 40 | 78.3 |
| 0.88 | 20 | 39.2 |
| 0.44 | 10 | 19.6 |
| 0.18 | 4 | 7.8 |

Results from Table 11 suggest, that even the lowest catalyst concentration exceeds the racemization rate ~ 8-fold, not enabling a dynamic approach. An enantiomeric excess > 95 % for biotransformations using 4 $g_{cdw}$/L cells or supernatant (=soluble fraction) accompanied by low conversions of 41 and 29 %, respectively, only corroborates catalyst inactivation. No

clear statements can be made for substrate racemization under these conditions, as 50 % conversion could not be reached. For experiments applying 40 $g_{cdw}$/L, e.e.values of 27.5 % (supernatant) and 45.8 % (cells) with similar conversions of 76.9 % (supernatant) and 72.4 % (cells) were obtained. By taking into account that the reduction rate exceeds the racemization rate 78-fold, only low e.e. values can be expected, while conversions should be beyond 50 %. Based on the assumption that an oil-in-water emulsion is formed, both enantiomers have to cross the organic/aqueous interface for fast racemization in aqueous solution. As the reduction rate of *Ct*XR (D51A) for *(S)*-2-phenylpropanal prevails, the *(R)*-aldehyde will be left emulsified. In the case of cell-free conversions, a higher catalyst loading delays full enzyme inactivation (e.g. allosteric inactivation) leading to a fast consumption of mainly the *(S)*-aldehyde in the beginning. While the racemization of the *(R)*-aldehyde only sufficiently proceeds in aqueous solution, the data gathered suggest, that the reduction rate is higher than the racemization rate mainly caused by high catalyst loadings. In consequence, the *(R)*-aldehyde is reduced and the e.e. value drops. By comparing these findings to the results obtained in whole-cell biotransformations, one major advantage arises from the presence of cell membranes functioning as substrate sink thereby protecting enzymes from fast inactivation (see final section). Substrate droplets attach to and dissolve in cell membranes[8]. This results in limited substrate accessibility for enzymes present inside/outside of the whole-cell catalyst (enzyme leakage) and therefore indirectly decreases the reduction rate, which in consequence enables a larger time frame for racemization and increased e.e. values. Unfortunately, if low substrate concentrations are applied accompanied by high cell concentrations, more substrate will be irreversibly lost in membranes.

*Whole-cell biotransformation (1-2 M):*

As outstanding e.e. values were obtained for 100 mM biotransformations applying 4 $g_{cdw}$/L whole-cell catalyst including higher conversions (compared to cell-free reactions), substrate/cell ($g_{substrate}/g_{cdw}$) ratios might be used instead of reduction and racemization rates to get insights into the outcome of reactions (Table 12):

**Table 12: Comparison of 0.1, 1 and 2 M reactions:** TON = Turnover number; 1 M substrate = 136.6 g

| **Cells** (gcdw/L) | **Substrate** (M) | **$NAD^+$** (mM) | **e.e.** (%) | **Conversion** (%) | **$V_{substrate}/V_{water}$** | **TON** (gproduct/gcdw) | **Substrate/cells** (gsubstrate/gcdw) |
|---|---|---|---|---|---|---|---|
| 4 | 0.1 | 6 | 95.3 | 41.3 | 0.014 | 1.4 | 3.4 |
| 10 | 0.1 | 6 | 61.3 | 66.5 | 0.014 | 0.9 | 1.4 |
| 20 | 0.1 | 6 | 49.0 | 69.4 | 0.014 | 0.5 | 0.7 |
| 40 | 0.1 | 6 | 45.8 | 72.4 | 0.014 | 0.2 | 0.3 |
| 40 | 1 | 6 | 93.4 | 86.9 | 0.158 | 3 | 3.4 |
| 40 | 1 | 10 | 93.1 | 98.8 | 0.158 | 3.4 | 3.4 |
| 40 | 2 | 6 | 95.3 | 15 | 0.376 | 1.0 | 6.8 |
| 30 | 1 | 3 | 95 | 51.6 | 0.014 | 2.3 | 4.6 |
| 20 | 1 | 3 | 95.2 | 31.7 | 0.014 | 2.2 | 6.8 |

As can be seen in Table 12, a ratio $\geq$ 3.4 $g_{substrate}/g_{cdw}$ gives rise to high e.e. values > 90 % for 0.1, 1 and 2 M whole-cell biotransformations. Substrate/cell ratios < 3.4 result in low e.e. values, but increased conversions. A ratio of 3.4, kept by increasing substrate and cells by a factor of 10, results in high conversions and high e.e. values. As the water content decreases, increased conversions might also be explicable by less hydrates being formed causing more aldehyde to be available for reduction. By taking into account rather mild mixing conditions (30 rpm), a fine dispersion of ~ 14 % substrate (organic phase) cannot be expected. The partition of substrate molecules will be either shifted towards the organic phase or the hydrophobic cell membrane, with the latter being dominant, as racemization will proceed to slowly in the organic phase.

An increased $NAD^+$ concentration largely contributes to overcome mass transfer limitations primarily caused by the elevated viscosity at high catalyst and substrate loadings (Figure 3) which is mirrored by full conversions (~99 %) at 10 - 14 mM $NAD^+$. A downside to these

findings is represented by a slight drop in the enantiomeric excess from 94 to 92 % due to NADH will be readily available for substrate reduction.

The addition of (2-Hydroxypropyl)-β-cyclodextrins (HBC) as enzyme stabilizing agents[9] only affects lower catalyst loadings (Figure 5, Figure 8). This can be ascribed to the increased viscosity of the reaction mixture at e.g. 40 $g_{cdw}$/L preventing efficient interaction between exposed hydrophobic amino acids and HBC necessary for enzyme stabilization. The enantiomeric excess faintly drops in the presence of HBC, which might be due to complexation of substrate molecules and cyclodextrins[10] thereby creating a non-favourable environment for racemization (hydrophobic cavity). Nonetheless, e.e. values in average exceeding those of biotransformations with higher catalyst loadings can be obtained.

Enzyme inactivation dominates at 2 M (~ 27 % v/v) substrate concentration (Figure 9). Neither HBC nor hexane partially serving as substrate/product sink are capable of pushing conversions far beyond 20 %. Additionally, e.e. values decrease in the presence of both, HBC or hexane.

*Remarks on applying free enzymes:*

Only few reports on successfully established reductive DKRs using *rac*-2-phenylpropanal exist. For example, 75 % conversion accompanied by an enantiomeric excess of 99 % were achieved exclusively applying horse liver alcohol dehydrogenase (HLADH), 0.5 mM substrate and 1 mM NADH at a pH of 7.5 after 5 h of reaction time[2]. 89 % conversion and an enantiomeric excess of 95 % resulted after 24 h. For oxidative DKRs, a screening of 70 ADHs was performed yielding only 9 that were capable of producing the desired acid[7]. Sufficient $NAD^+$ supply was shown to be a major driving force for improved selectivity and high reactivity of the substrate[7] was thought to be major a reason for low conversions. In accordance to the studies performed here, this statement seems to be supportable as considerable interactions of e.g. 100 mM substrate and cell-free extract were observed,

manifesting in the reaction mixture turning from transparent to white immediately after adding substrate. Following that, formation of Schiff bases with exposed amino groups might lead to allosteric inactivation besides inactivation by precipitation during the reaction. On the other hand, addition of excess amounts of $NAD^+$ only resulted in higher conversions for 1 M reactions while e.e. values decreased.

*Interfacial catalysis and influence of cell membrane:*

In order to unravel variations in enantiomeric excess and conversions manifesting in whole-cell biotransformations, the concept of interfacial catalysis might be introduced. The whole-cell catalyst applied displays a high permeability, which was proven firstly in the reduction of *o*-chloroacetophenone and secondly in the DKR of rac-2-phenylpropanal solely deploying the supernatant for cell-free conversions. In consequence, enzyme leakage into the reaction medium is highly likely to occur. As XR is capable of withstanding the presence of e.g. 50 % v/v hexane without losing activity suggesting that a hydrophobic environment is partially preferred, one assumption involves interfacial catalysis at the boundary of emulsified substrate droplets and the aqueous phase. This postulation might be joined with the Two-film theory: The mass transfer rate = $k_La(C_i-C_d)$, with $C_i$ being the interfacial concentration (~10 mM, max.solubility of *rac*-2-phenylpropanal), $C_d$ representing the dissolved concentration of *rac*-2-phenylpropanal in the aqueous bulk phase and $k_L$ depicting the liquid mass transfer coefficient combined with the droplet surface area a. Two major scenarios can be drawn:

**100 mM substrate, 40 $g_{cdw}$/L:** At lower substrate concentrations, a finer dispersion of droplets would be expected causing the surface area to be increased. The probability of substrate droplets to spread over and dissolve in cell membranes would be largely increased, especially at elevated whole-cell catalyst loadings and low substrate concentrations. Therefore, biotransformation is thought to take place in the aqueous bulk phase, cytosol or

periplasma to a higher extent rather than at the organic/aqueous interface (see Figure 14 & 15). In consequence, strong enzyme precipitation at the organic/aqueous interface would be prevented as well as interfacial catalysis due to cell membranes functioning as sink for small substrate droplets. Further, decreased droplet sizes would result in thinner aqueous liquid films causing $k_L$ values to be lower. The transfer of single substrate molecules from substrate droplets into the aqueous phase would be enhanced followed by racemization in the aqueous phase. Hence, the reduction rate of leaked enzymes would be increased compared to those precipitated at the organic/aqueous interface. Reactions occurring in the aqueous bulk phase would therefore show a diminished enantiomeric excess owing to the racemization rate being slower than the reduction rate at high catalyst and low substrate loadings accompanied by high conversions. As mentioned before, cell membranes functioning as sink for substrate (and product) molecules are also highly likely to enhance substrate inaccessibility at high membrane/substrate ratios. The biotransformations carried out and described in section 3.1. result in higher e.e. values for whole-cell compared to cell-free conversions. This now could be ascribed to the higher reduction rate for the *(S)*-aldehyde leading to an excess of *(R)*-aldehyde droplets slowly dissolving in cell membranes and making them harder accessible – in contrast to cell-free conversions.

**1 M substrate, 40 $g_{cdw}$/L:** Increased droplet sizes would be observed at higher substrate concentrations. A lesser extent of substrate molecules would be found dissolved in cell membranes leading to an increased number of organic droplets favouring enzyme precipitation at the organic/aqueous interface. Further, (re-)formation of substrate droplets might be triggered as higher substrate loadings are thought to destroy cell membranes to a higher degree thereby counteracting substrate loss. Hence, interfacial catalysis is assumed to take place more likely constituting the major driving force of the reaction. As mass transfer would be hampered by thicker aqueous liquid films and a decreased surface area, substrate conversions occuring in the cytosol, aqueous bulk phase and the periplasma play minor roles,

as well as allosteric inactivation. In the course of interfacial precipitation, enzymes might be continuously inactivated which therefore decreases the reduction rate. In consequence, the racemization rate at the interface would be faster than the reduction rate leading to an increased enantiomeric excess. As mentioned prior, substrate supply is maximized at the interface resulting in high conversions. As can be seen, even at high substrate concentrations no organic solvents are needed as cell membranes are fulfilling the task of increasing substrate solubility and carrying out a protective function.

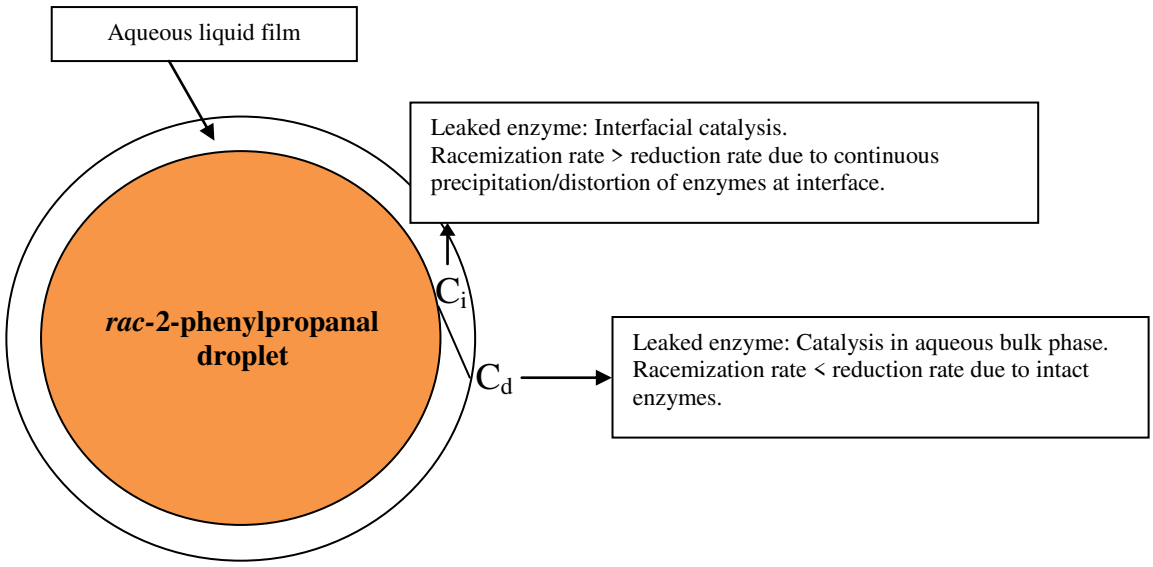


**Figure 14: Depiction of interfacial catalysis.**

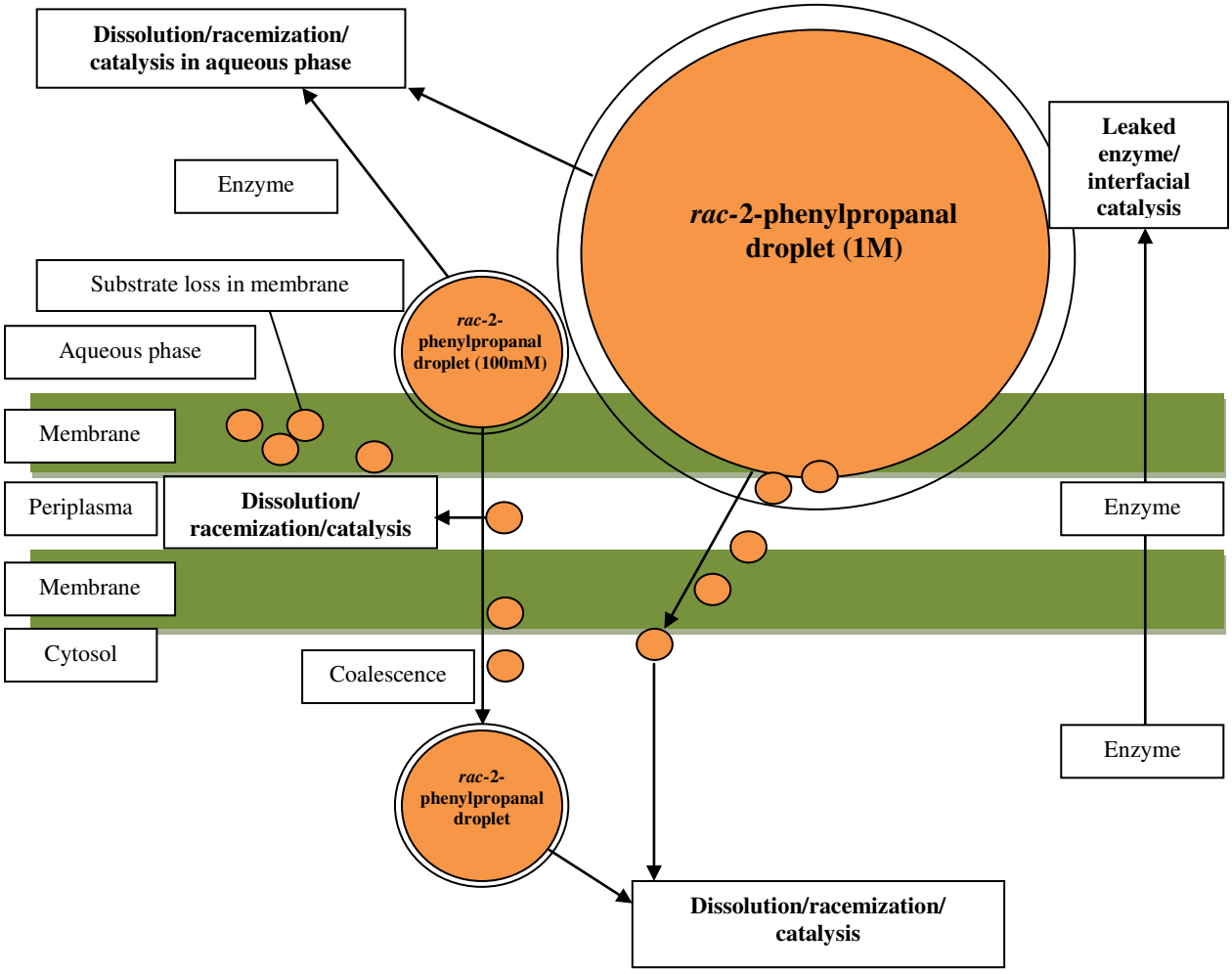


**Figure 15: Visual comparison of 100 mM and 1 M whole-cell biotransformations.**

## 5. Conclusion

Increased $NAD^+$ concentrations elevate conversions by overcoming mass transfer limitations in viscous reaction mixtures attributed to high catalyst and substrate loadings. Simultaneously, the enantiomeric excess decreases. Reduction and racemization rates are highly influenced in the presence of whole-cell catalysts: e.e. values tend to be higher in whole-cell biotransformations due to cell membranes functioning as substrate sink thereby largely controlling enzyme/substrate accessibility and reduction rates indirectly. The inactivation of cell-free or whole-cell catalyst by substrate/product is mirrored by low conversions accompanied by strong emulsification. Full conversion of 1 M *rac*-2-phenylpropanal

concomitantly reaching e.e. values > 93 % can be achieved by keeping substrate/cell ($g_{substrate}/g_{cdw}$) ratios at 3.4.

## 6. Literature


1. Kourist, R., Domínguez de María, P. & Miyamoto, K. Biocatalytic strategies for the asymmetric synthesis of profens – recent trends and developments. *Green Chem.* **13,** 2607 (2011).

2. Galletti, P. *et al.* Chemoenzymatic synthesis of (2S)-2-arylpropanols through a dynamic kinetic resolution of 2-arylpropanals with alcohol dehydrogenases. *Org. Biomol. Chem.* **8,** 4117–23 (2010).

3. Pietruszka, J. & Schölzel, M. Ene reductase-catalysed synthesis of (R)-profen derivatives. *Adv. Synth. Catal.* **354,** 751–756 (2012).

4. Fuchs, C. S. *et al.* Dynamic kinetic resolution of 2-phenylpropanal derivatives to yield β-chiral primary amines via bioamination. *Adv. Synth. Catal.* **356,** 2257–2265 (2014).

5. Kratzer, R., Leitgeb, S., Wilson, D. K. & Nidetzky, B. Probing the substrate binding site of Candida tenuis xylose reductase (AKR2B5) with site-directed mutagenesis. *Biochem. J.* **393,** 51–58 (2006).

6. Gonzales, M. F., Brooks, T., Pukatzki, S. U. & Provenzano, D. Rapid Protocol for Preparation of Electrocompetent Escherichia coli and Vibrio cholerae. 6–11 (2013). doi:10.3791/50684

7. Könst, P. *et al.* Enantioselective oxidation of aldehydes catalyzed by alcohol dehydrogenase. *Angew. Chemie - Int. Ed.* **51,** 9914–9917 (2012).

8. Hua, F. & Wang, H. Q. Uptake and trans-membrane transport of petroleum hydrocarbons by microorganisms. *Biotechnol. Biotechnol. Equip.* **28,** 165–175 (2014).

9. Serno, T., Geidobler, R. & Winter, G. Protein stabilization by cyclodextrins in the liquid and dried state. *Adv. Drug Deliv. Rev.* **63,** 1086–1106 (2011).

10. Del Valle, E. M. M. Cyclodextrins and their uses: A review. *Process Biochem.* **39,** 1033–1046 (2004).

# 7. Post Appendix: $^{1}$H-NMR predictions

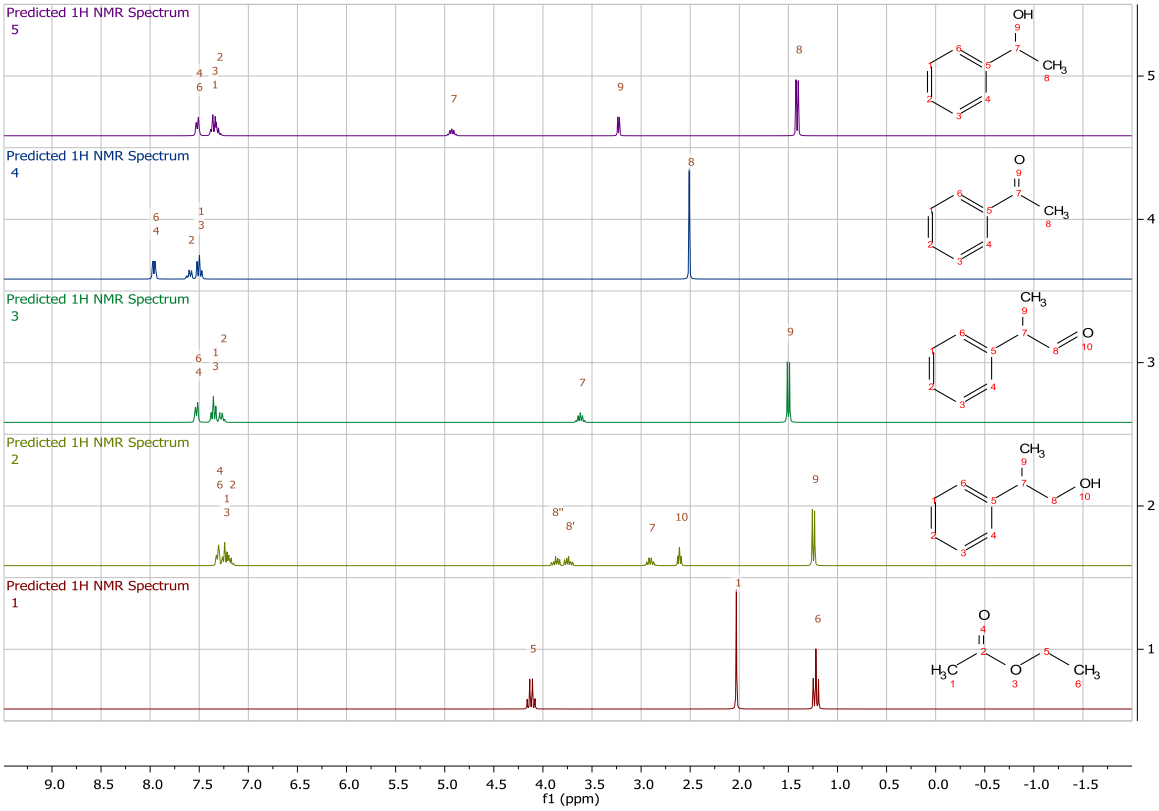

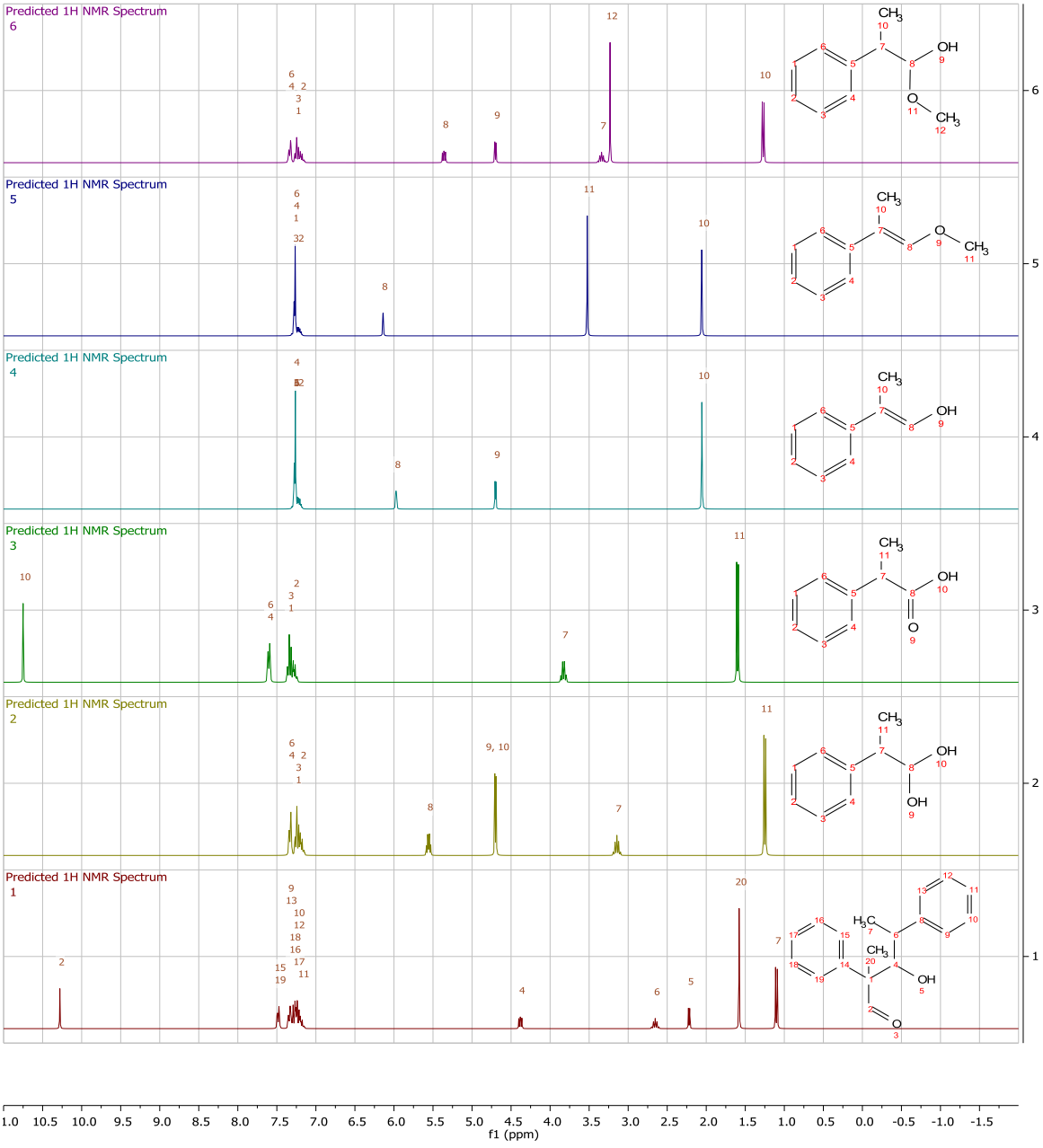
Predicted 1H NMR Spectrum
6
Predicted 1H NMR Spectrum
5
Predicted 1H NMR Spectrum
4
Predicted 1H NMR Spectrum
3
Predicted 1H NMR Spectrum
2
Predicted 1H NMR Spectrum
1
f1 (ppm)